Osmosensitivity and Vacuole Biogenesis in Yeast

Harwood, Eleanor Claire

Osmosensitivity and Vacuole Biogenesis in Yeast

Eleanor Claire Harwood

Thesis submitted for the degree of Doctor of Philosophy

Department of Biological Sciences
University of Durham

September 1996

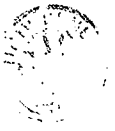

Osmosensitivity and Vacuole Biogenesis in Yeast

Eleanor Claire Harwood

Abstract

A collection of salt-sensitive vacuolar (*ssv*) *Saccharomyces cerevisiae* mutants were selected for analysis in an attempt to reveal components of the osmosensing signal transduction pathway. A previous screen of these mutants had been used to select those with an impaired glycerol response to salt stress. In this study the glycerol-3-phosphate dehydrogenase activity was measured in all the strains which showed reduced glycerol accumulation to demonstrate a corresponding low enzyme activity which could be caused by lack of signalling through the high osmolarity glycerol (HOG) response pathway. However, enzyme activity was found to be impaired in only one of the strains tested. This demonstrated that the measurement of glycerol accumulation is not a particularly useful screening method for defects in the HOG pathway.

The activity of the promoter of *CTT1*, another stress-responsive gene, was measured in selected *ssv* strains using a *lacZ* reporter gene attached to the *CTT1* promoter stress response element. This gave further information about the stress-responsiveness in the strains tested. *CTT1* promoter activity did not correlate with GPDH activity in all of the strains tested. As *CTT1* is subject to control by more than one type of stress the results imply that in at least one of the strains another stress response may be impaired.

The *VAC1* homologue (*VAC1H*) on chromosome XIV was characterised as a candidate for one of the *SSV* genes, *SSV17*. Although it was demonstrated not to be *SSV17*, a role for *VAC1H* in vacuolar protein sorting was discovered. The Δ*vac1h* strain also displayed class E vacuolar morphology. Sequence analysis and complementation experiments demonstrated that *VAC1H* is identical to *VPS27*.

ACKNOWLEDGEMENTS

First I would like to thank my supervisor, Dr Martin Watson, who has always been there when I have needed help but has not interfered when I have not! He has been one of that rare breed of good supervisors. My thanks also to BBSRC (formerly SERC) for funding this research.

There are so many other people to thank it will be impossible to name them all. In particular all the past members of labs 24 and 6, especially Caroline Hartley, Bert Pöpping and Elaine Broomfield, for humour - even hilarity - and, more seriously, for assistance in the lab and scientific discussion. Thanks too for the expert technical assistance of Terry Gibbons who keeps the department going, never mind the lab. I would also like to thank Michelle Metcalfe for sharing experimental ups and downs, cups of tea and gossip. I have also appreciated all the other friendships I have made in the department which have made it an enjoyable place to work and socialise.

For outstanding support during the writing up stages I am extremely grateful to Peter Slee, Keith Seacroft and the corporate communications team. Also during the writing up stages and during the tail end of the lab work, I have been warmly welcomed into the home of Jeff Dean and Annette Morris and I thank them for making the last few months happy ones.

Finally I would like to thank Mum, Dad and Adrian. The understanding, love, humour and friendship I have received from them has helped make it all possible.

CONTENTS

Figures

DECLARATION

No part of this thesis has previously been submitted for any other degree in this or any other university. All work was performed by the author, except where otherwise stated.

Eleanor Claire Harwood

Statement of Copyright

ABBREVIATIONS

BCIP	Bromochloroindolyl phosphate
bp	Base pair
BSA	Bovine serum albumin
CPY	Carboxypeptidase Y
dH_2O	distilled water
DHAP	Dihydroxyacetone phosphate
dNTP	deoxynucleotide triphosphate
DPAP A	Dipeptidyl aminopeptidase A
DPAP B	Dipeptidyl aminopeptidase B
EDTA	Ethylenediaminetetraacetic acid
ER	endoplasmic reticulum
EtOH	Ethanol
GPDH	Glycerol-3-phosphate dehydrogenase
HOG	High osmolarity glycerol response
NADH	Nicotinamide adenine dinucleotide
NBT	Nitro blue tetrazolium
PrA	Proteinase A
ssv	salt-sensitive vacuolar
TE	10mM Tris.HCl pH 8.0, 1mM EDTA buffer
Tris	Tris-(hydroxymethyl)-methylamine-[2-amino-2-(hydroxymethyl)-propane-1,3-diol (tris)]
X-Gal	5-bromo-4-chloro-3-indolyl-β-D-galactoside
YMM	Yeast minimal medium

CHAPTER 1

INTRODUCTION

1.1 General Introduction

Eukaryotes have several complex control mechanisms that allow growth in a range of physiological conditions. In the study of these mechanisms, yeasts, such as *Saccharomyces cerevisiae*, are valuable research tools. They are simple eukaryotes which are relatively easy to manipulate genetically and biochemically. The understanding of molecular processes in yeast cells may hold the key to answering more complicated biological questions of higher organisms.

1.2. Osmohomeostasis

When a cell culture of *Saccharomyces cerevisiae* is transferred into high osmotic strength medium (1.4M NaCl) there is a drop in cell viability which is less severe if the cells are pre-treated in 0.7M NaCl (Blomberg and Adler, 1989). Adaptation to osmotic stress is associated with an accumulation of glycerol as a compatible osmolyte. During osmotic conditioning with 0.7M NaCl the rate of formation of glycerol is increased (Blomberg and Adler, 1989). The activities of glycerol-3-phosphate dehydrogenase (GPDH) and phosphofructokinase are elevated in cells subjected to osmotic stress (Edgley and Brown, 1983) allowing a shift in the metabolic flux to favour glycerol production. The glycerol accumulation in response to osmotic stress will be discussed in more detail in section 1.3.2.

Before yeast cells can adjust their intracellular glycerol levels they must first recognise a change in extracellular osmolarity and initiate signals that cause the cell to respond to that change. Signal transduction in response to salt stress occurs through the High Osmolarity Glycerol response pathway (Brewster *et al.*, 1993) and other less well defined pathways. The HOG pathway enhances intracellular glycerol concentration by increasing the transcription of GPDH (Albertyn *et al.*, 1994).

To maintain osmohomeostasis, yeast must also be able to respond to a decrease in extracellular osmolarity. Mutants of the PKC1 (protein kinase C1, or C-kinase) pathway have previously been described as having a cell lysis defect which can be stabilised by a high osmolarity medium (Lee and Levin, 1992; Levin and Bartlett-Heubusch, 1992; Paravicini *et al.*, 1992) suggesting a role for the pathway in cell integrity. There is now

evidence that the PKC1 pathway is involved in recognising decreases in extracellular osmolarity (Davenport *et al.*, 1995) and thus acts as a second osmosensing signal transduction pathway. The role of the HOG pathway and the PKC1 pathway in maintaining osmohomeostasis will be discussed more fully in section 1.3.

An important function in osmohomeostasis is removing toxic ions such as Na^+ from the cytoplasm. A gene with enhanced activity during salt stress is the *ENA1* gene (Marquez and Serrano, 1996). *ENA1* is the first gene of a tandem array encoding ion transporters of the P-type ATPase family (Haro *et al.*, 1991; Garciadeblas *et al.*, 1993). Ena1p can function as either a Li^+ or a Na^+ transporter and is particularly important for excluding Na^+ ions during salt stress. Although the *ENA* genes are partially functionally redundant, the *Δena1* mutation confers osmosensitivity suggesting a particular role for the *ENA1* gene in recovery from osmotic shock. Signalling through the HOG pathway enhances *ENA1* transcription at 0.3M NaCl but at higher salt concentrations, e.g. 0.8M, *ENA1* transcription can be enhanced even in the absence of functional Hog1p (Marquez and Serrano, 1996). The phosphatase calcineurin was found to be necessary for this HOG-independent response. The phosphatases Ppz1p and Ppz2p also have an effect on salt exclusion (Posas *et al.*, 1995). The *Δppz1* mutation increases tolerance to Na^+ and Li^+ ions and the expression of *ENA1* is enhanced in *Δppz1 Δppz2* mutant cells. Thus Ppz1p and Ppz2p limit salt exclusion through effects on *ENA1*.

One approach to the study of osmohomeostasis is the investigation of genes which, when overexpressed, confer a greater osmotolerance to a strain. It was using this approach that the *HAL* genes (for halotolerance) were characterised. *HAL1* is induced by osmotic stress and the *Δhal1* strain has a reduced salt tolerance (Gaxiola *et al.*, 1992). Overexpression of *HAL1* increases K^+ accumulation suggesting that Hal1p may interact with the K^+ transport machinery. *HAL3* is also involved in ion transport but its effects are specific for Na^+ and Li^+ (Ferrando *et al.*, 1995). *HAL3* overexpression results in increased expression of *ENA1* and, conversely, *ENA1* overexpression can suppress the osmosensitivity of *Δhal3*. The exact roles of Hal1p and Hal3p in ion homeostasis have yet to be elucidated. *HAL2* is apparently unrelated to *HAL1* and *HAL3* as it encodes an inositol phosphatase with a role in methionine biosynthesis (Glaser *et al.*, 1993). The ability of this gene, when overexpressed, to confer a greater osmotolerance suggests that the methionine biosynthetic machinery may be particularly sensitive to fluctuations in osmolarity. Supplementing the growth media with methionine can have the same growth effect as overexpression of *HAL2* for salt-stressed yeast.

A mutant strain has now been described which has an enhanced salt tolerance (Gaxiola *et al.*, 1996). The study of this strain underlines again the importance of intracellular

cation concentrations to osmohomeostasis. This strain has half as much Na^+ and 60% more K^+ than its 'wild-type' parental strain and thus a greatly reduced Na^+/K^+ ratio. This improves its osmotolerance as it withstands concentrations of 2M NaCl.

A role for actin in osmohomeostasis was proposed after the discovery that increasing the osmotic strength of the medium decreased the temperature sensitivity of a collection of actin mutants (Novick and Botstein, 1985). On exposure to high osmotic stress, the actin cytoskeleton undergoes a rapid and reversible disassembly (Chowdhury *et al.*, 1992). This disassembly is most obvious in cells with small buds or in cells about to bud and occurs within the first minute of an increase in extracellular osmolarity. Reassembly of the cytoskeleton during recovery from osmotic shock was found to require an actin binding protein, Rah3p (Chowdhury *et al.*, 1992).

Many mutations causing defects in vacuolar protein sorting also cause osmosensitivity (Banta *et al.*, 1988; Latterich, 1992). The initial response to increased osmolarity may involve a flow of solute from the vacuole (as suggested by Mager and Varela (1993)). The vacuole may also play a role in osmohomeostasis by reducing the cytoplasmic Na^+ concentration via the Na^+/H^+ antiporter (as discussed by Haro *et al.*, (1993)). Vacuole function and osmohomeostasis will be discussed more fully in section 1.4.

Some of the reactions in osmohomeostasis may form part of a general stress response. For example the cytoplasmic catalase T gene (*CTT1*) is under the control of many stress response pathways, including the HOG pathway, which act through an upstream activation sequence named STRE (for stress response element) (Marchler *et al.*, 1993; Schuller *et al.*, 1994). Induction of certain heat shock genes has also been observed during salt stress (e.g. Hsp12p;Hirayama *et al.*, 1995; Varela *et al.*, 1992). Ubiquitin metabolism may play a role during salt stress as part of a general stress response.

The ubiquitination pathway is important for stress-induced proteolysis (see Hilt and Wolf, 1992 for a review). The polyubiquitin gene, *UBI4*, is positively regulated by heat stress and is essential for resistance to high temperature and nitrogen starvation (Finley *et al.*, 1987). In such conditions it is likely that *UBI4* provides a valuable pool of ubiquitin to allow a rapid turnover of proteins - either to remove heat-damaged proteins or to provide a means for altered metabolism. The nature of the ubiquitin-ubiquitin linkage is important to the stress response as mutations that disrupt a particular type of link are no longer able to survive heat and canavanine stress (Arnason and Ellison, 1994). Although a role for ubiquitin processing in response to osmotic stress is not well characterised, the *DOA4* gene, which encodes one of many ubiquitin-processing enzymes (Papa and Hochstrasser, 1993) was isolated through its ability to complement a mutation conferring salt-sensitivity (Latterich, 1992; R. Baker, personal

communication). The *DOA4* gene has since been implicated in the co-ordination of DNA replication to produce one copy of the genome per cell cycle (Singer *et al.*, 1996). The effects of *doa4* deletion seem to be two-fold. The temperature-sensitivity of a *doa4* strain can be rescued by overexpression of *UBI4* showing the importance of Doa4p in maintaining a free ubiquitin pool. However, the effects on DNA replication are not suppressed by *UBI4* overexpression indicating a separate role for Doa4p. Singer *et al* (1996) did not examine the effects of overexpression of *UBI4* on the salt-sensitivity of the Δ*doa4* strain so it is not yet known if it is the need for a free ubiquitin pool during stress conditions that links osmohomeostasis to the ubiquitin pathway.

The involvement of all of the above cell processes in osmohomeostasis underlines the complexity of the osmostress response. Osmosensitivity can be indicative of a defect in one of many processes, not restricted to osmosensing signal transduction or glycerol accumulation. The transcription levels of many proteins can be altered with salt stress (see (Mager and Varela, 1993) for a review) and the study of genes with enhanced or depressed activities in changing osmotic conditions will lead to a greater understanding of osmohomeostasis.

1.3. The High Osmolarity Glycerol (HOG) Response Pathway

1.3.1. Osmosensing signal transduction

An increase in intracellular glycerol concentration in response to an increase in extracellular osmolarity requires signalling through the High Osmolarity Glycerol (HOG) response pathway (Brewster *et al.*, 1993). Two components of the pathway, *HOG1* and *HOG4*, were identified by complementation cloning of osmosensitive mutants which showed a reduced glycerol accumulation after addition of salt (Brewster *et al.*, 1993). Sequence analysis revealed that *HOG1* is a member of the MAP (mitogen-activated protein) kinase (MAPK) family with significant sequence homology to the pheromone response pathway gene, *FUS3* (Elion *et al.*, 1990). It was discovered that *HOG4* is identical to *PBS2* and is related to MAP kinase kinases (Boguslawski and Polazzi, 1987). A linear kinase cascade was proposed based on the observation that Hog1p is tyrosine-phosphorylated in response to salt stress and that this phosphorylation requires functional Pbs2p (Brewster *et al.*, 1993).

When the HOG pathway was first described (Brewster *et al.*, 1993), little was known about other components of the pathway. The discovery of an upstream regulator came through the study of tyrosine phosphatases (Maeda *et al.*, 1994). Maeda *et al* (1994) studied mutants that require *PTP2* tyrosine phosphatase for survival. One gene

identified in their study was identical to the previously described *SLN1* gene (Ota and Varshavsky, 1993). *SLN1* has homology to bacterial two-component regulators that are involved in a variety of cellular processes, including osmoregulation (see Bourret, 1991 for a review). Sln1p consists of a histidine kinase domain and a potential extracellular sensor domain. Maeda *et al.* (1994) demonstrated that *SLN1* is an upstream regulator of the HOG pathway by using recessive mutations of *hog1* or *pbs2* to suppress Δ*sln1* lethality. This implies that the deletion of *SLN1* causes inappropriate signalling through the HOG pathway, and therefore that *SLN1* is a negative regulator of the HOG pathway. It is likely that the requirement for overexpression of *PTP2* to suppress the Δ*sln1* mutation is for dephosphoryation of the inappropriately activated Hog1p and thus down-regulation of the response.

The study of recessive suppressors of the Δ*sln1* mutation led to the identification of *SSK1* (for suppressor of sensor kinase). Ssk1p has homology to the receiver domain of bacterial response regulator molecules. Expression of *SSK1* in the absence of *SLN1* induces tyrosine phosphorylation of Hog1p. Ssk1p is probably unphosphorylated in Δ*sln1* cells suggesting unphosphorylated Ssk1p is the active form (Maeda *et al.*, 1994). Although *SSK1* clearly has a role in the HOG signal transduction pathway, the Δ*ssk1* mutation does not itself confer osmosensitivity. This implies that other receptors for osmotic stress also feed into the HOG pathway.

In a separate report, Maeda *et al.* (1995) describe another *ssk* gene, *SSK2*, which has homology to MAPK kinase kinases. Ssk2p is not solely responsible for activation of the HOG pathway and a related gene, *SSK22* was isolated by DNA hybridisation techniques. Deletion of the N-terminal non-catalytic domain of either *SSK2* or *SSK22* (leading to their constitutive activation) results in tyrosine phosphorylation of Hog1p in a Pbs2p-dependent manner. Such N-terminal deletions are lethal, with lethality rescued by deletions in either *PBS2* or *HOG1* but not *SSK1*. Two-hybrid analysis revealed that both Ssk2p and Ssk22p can interact with Ssk1p. On the basis of this evidence it was suggested that Ssk2p and Ssk22p act between Ssk1p and Pbs2p in the signal transduction pathway.

Ssk2p and Ssk22p are not however the only means of inducing tyrosine phosphorylation of Hog1p and Δ*ssk2* Δ*ssk22* double mutants are not osmosensitive (Maeda *et al.*, 1995). A search for a mutagenized gene that would confer osmosensitivity in a Δ*ssk2* Δ*ssk22* strain led to identification of *SHO1* (for synthetic, high-osmolarity sensitive). Sequence analysis of *SHO1* suggests that it encodes four transmembrane segments and an SH3-domain. SH3-domains have been described as important for protein interactions in a variety of processes (see Cohen *et al.*, 1995 for a review). Two-hybrid analysis showed that the SH3-domain of Sho1p can interact with

the proline-rich domain of Pbs2p. This interaction does not appear to require Ssk2p or Ssk22p suggesting Pbs2p can receive signals from two different branches of the HOG pathway (Maeda *et al.*, 1995). A model for osmosensing signal transduction based on a scheme proposed by Maeda *et al.* (1995) is shown in figure 1.1.

Although the HOG pathway is required for the induction of various genes involved in the osmostress response, for example *GPD1* (Albertyn *et al.*, 1994) and *CTT1* (Schuller *et al.*, 1994), the downstream targets of Hog1p which mediate this induction have yet to be discovered.

The HOG pathway is one of several MAP kinase pathways described for the yeast *Saccharomyces cerevisiae* (see Herskowitz, 1995 for a review). These pathways all have a central core of kinases which act in a cascade to transduce a signal. The MAP kinase itself is phosphorylated by MAP kinase kinase (MAPKK, also known as ERK kinase, or MEK) which is phosphorylated by MAPKK kinase (MAPKKK, also known as MERK, or MEKK).

The pheromone signalling pathway is a particularly well-characterised MAP kinase pathway in *Saccharomyces cerevisiae*. The pheromone binds to its receptor and consequently activates a trimeric G protein which causes a series of phosphorylation events (Zhou *et al.*, 1993). Ste11p (a MAPKKK homologue) phosphorylates, and thereby activates, Ste7p (a MAPKK homologue; Teague *et al.*, 1986) which in turn phosphorylates the MAPK homologues, Fus3p and Kss1p (Errede *et al.*, 1993; Neiman and Herskowitz, 1994). Fus3p activation and the cellular response to pheromone require Ste11p- and Ste7p-dependent phosphorylation of Fus3p on both threonine and tyrosine residues (Gartner *et al.*, 1992). Fus3p phosphorylates many components involved in the mating response, including Far1p (which results in cell cycle arrest) and the transcription factor Ste12p (Elion *et al.*, 1993).

Ste11p, Ste7p and Fus3p (or Kss1p) are brought into contact with each other by Ste5p (Choi *et al.*, 1994; Marcus *et al.*, 1994; Printen and Sprague, 1994) which acts as a scaffold for protein interaction. It is possible that Ste5p regulates the actions of the kinases it interacts with to prevent inappropriate signalling through the pathway and inappropriate cross-reactions with other MAP kinase cascades (Printen and Sprague, 1994). This would explain the observation that purified Ste11p is constitutively active *in vitro* and yet *in vivo* is apparently only involved in signalling in response to pheromone (Neiman and Herskowitz, 1994). However, mutational activation of Ste5p can constitutively activate the pheromone response pathway but cannot suppress mutations in *STE7*, *STE11*, *FUS3* or *KSS1* suggesting that Ste5p also acts upstream of Ste11p in the cascade (Hasson *et al.*, 1994).

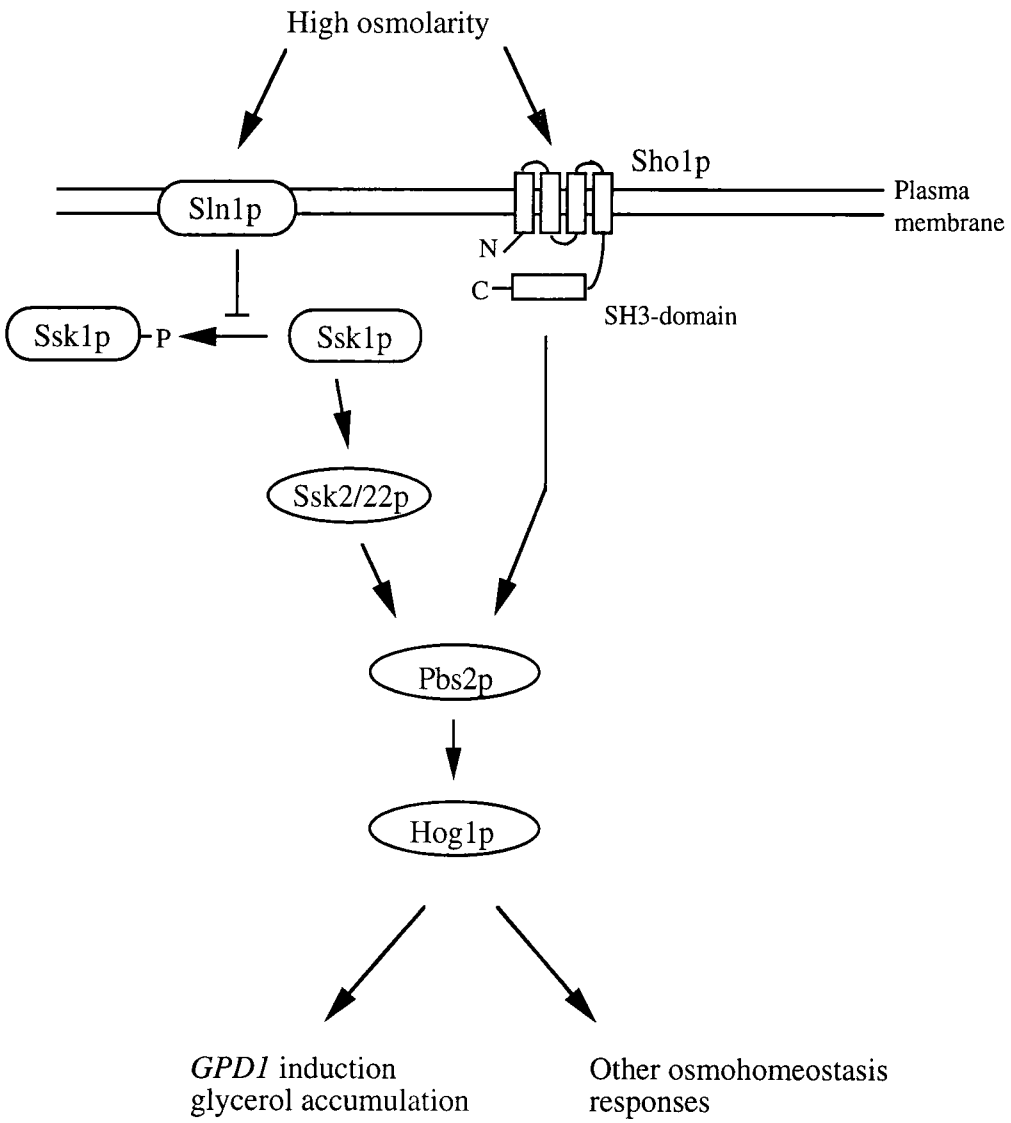

Figure 1.1 The HOG pathway

Increasing osmolarity causes tyrosine phosphorylation of Hog1p by Pbs2p. Pbs2p activation requires either phosphorylation by the Ssk2/22p kinases or interaction with the SH3-domain of Sho1p. Ssk2/22p is itself activated by unphosphorylated Ssk1p. Ssk1p is phosphorylated by Sln1p in the absence of osmotic stress.

Other MAP kinase pathways include the PKC1 pathway. As mentioned in section 1.2, this pathway is involved in cell integrity and growth. Mutations in components of the PKC1 pathway lead to a cell lysis defect which is recovered by adding osmotic stabilisers to the medium (Lee and Levin, 1992; Levin and Bartlett-Heubusch, 1992; Paravicini *et al.*, 1992). Pkc1p regulates β-glucanase activity linking the PKC1 pathway directly with cell wall maintenance (Shimizu *et al.*, 1994). The PKC1 pathway has also been discovered to be an osmosensing signal transduction pathway but in contrast to the HOG pathway it responds to a *decrease* in extracellular osmolarity (Davenport *et al.*, 1995).

MAPK, MAPKK and MAPKKK homologues in the PKC1 pathway were identified by their ability, when mutationally activated or present in multicopy, to overcome the requirement for *PKC1*. *BCK1* encodes a MAPKKK homologue with 45% identity to Ste11p (Lee and Levin, 1992). The functionally redundant Mkk1p and Mkk2p kinases act downstream of Bck1p. *MKK1* and *MKK2* are highly homologous to each other and also share homology with the MAPKK homologue *STE7* (Irie *et al.*, 1993). The MAP kinase homologue, Mpk1p, was found to be the previously identified Slt2p and Δ*mpk1* confers the cell lysis defect characteristic of mutations in other components of the pathway (Lee *et al.*, 1993). Genetic evidence confirms that the order of activity in the pathway is Pkc1p -> Bck1p -> Mkk1p/Mkk2p -> Mpk1p (Irie *et al.*, 1993; Watanabe *et al.*, 1995).

The two phosphatases Ppz1p and Ppz2p are required for the maintenance of cell size and integrity in response to hypo-osmotic stress (Hughes *et al.*, 1993) and mutations in *PPZ1* and *PPZ2* confer a cell lysis defect with similarities to defects in the PKC1 pathway. Overexpression of *PPZ1* or *PPZ2* can suppress *mpk1* deletion (Lee *et al.*, 1993) suggesting a direct relationship between the phosphatases and the PKC1 pathway. The Msg5p phosphatase can also interact with the PKC1 pathway as overexpression of *MSG5* can suppress the growth defect of a constitutively active *MKK1* allele (Watanabe *et al.*, 1995). How the dephosphorylation by Ppz1/2p or Msg5p can act co-operatively with, or even by-pass the need for, the phosphorylation events of the PKC1 pathway is not yet known.

Two downstream targets of Mpk1p, the DNA-binding proteins Nhp6Ap and Nhp6Bp, have been identified by their ability to act as high copy suppressors of the Δ*mkk1* mutation (Costigan *et al.*, 1994). There is no evidence for a direct interaction between Mpk1p and Nhp6p suggesting more components of the pathway are yet to be revealed. Δ*nhp6A/B* strains display very similar but less severe phenotypes compared to the Δ*mpk1* mutant (Costigan *et al.*, 1994) which implies that activated Mpk1p may also elicit Nhp6p-independent functions. The DNA binding protein Rlm1p may be involved

in such Nhp6p-independent functions as mutations in *RLM1* can suppress a constitutively active *MKK1* allele (Watanabe *et al.*, 1995). As was the case for the *Δnhp6* strain, *Δrlm1* confers similar but less severe growth phenotypes than *Δbck1* or *Δmpk1*.

Figure 1.2 shows the pattern of components of these signal transduction pathways in relation to a basic MAP kinase model.

1.3.2. Glycerol accumulation

Cytoplasmic GPDH activity is elevated during salt stress (Andre *et al.*, 1991; Blomberg and Adler, 1989) and recovery from salt stress requires protein synthesis (Albertyn *et al.*, 1994a; Blomberg and Adler, 1989). The transcription of the gene *GPD1*, encoding cytoplasmic GPDH, is increased in response to salt stress in a Hog1p-dependent manner and *Δgpd1* cells are osmosensitive (Albertyn *et al.*, 1994). *Δgpd1* cells show some residual glycerol accumulation and a second gene, *GPD2*, encoding an isoenzyme of cytoplasmic GPDH has been identified (Eriksson *et al.*, 1995). *GPD2* is not induced by salt stress and *Δgpd2* does not confer osmosensitivity.

GPDH uses the substrate dihydroxyacetone phosphate (DHAP) to produce glycerol-3-phosphate which is then converted to glycerol (Gancedo *et al.*, 1968). This reaction is in contrast to the glycerol utilisation pathway that occurs in mitochondria. The mitochondrial glycerol-3-phosphate dehydrogenase, encoded by *GUT2*, was identified by the study of mutants unable to grow on glycerol as the major carbon source (Sprague and Cronan, 1977). The *GUT2* gene contains a mitochondrial pre-sequence and a potential FAD-binding site (Ronnow and Kielland-Brandt, 1993) whereas the cytoplasmic GPDH has a specificity for NADH (Albertyn *et al.*, 1992; Gancedo *et al.*, 1968). The highest levels of glycerol accumulation in response to salt stress were observed in a *gut2* strain (Albertyn *et al.*, 1994a). Intracellular glycerol concentration is therefore dependent on the relative activities of glycerol metabolism and glycerol utilisation and the availability of substrates. A scheme for glycerol metabolism is shown in figure 1.3.

For some time it was considered that the conversion of glycerol-3-phosphate to glycerol was catalysed by a non-specific phosphatase (e.g. Gancedo *et al.*, 1968). However Norbeck *et al.* (1996) have recently reported the identification of two isoenzymes of glycerol-3-phosphatase. The expression of one of the corresponding genes, *GPP2*, is regulated by the HOG pathway. The osmotic induction of Gpp2p again implies the importance of glycerol accumulation to yeast in the response to osmotic stress.

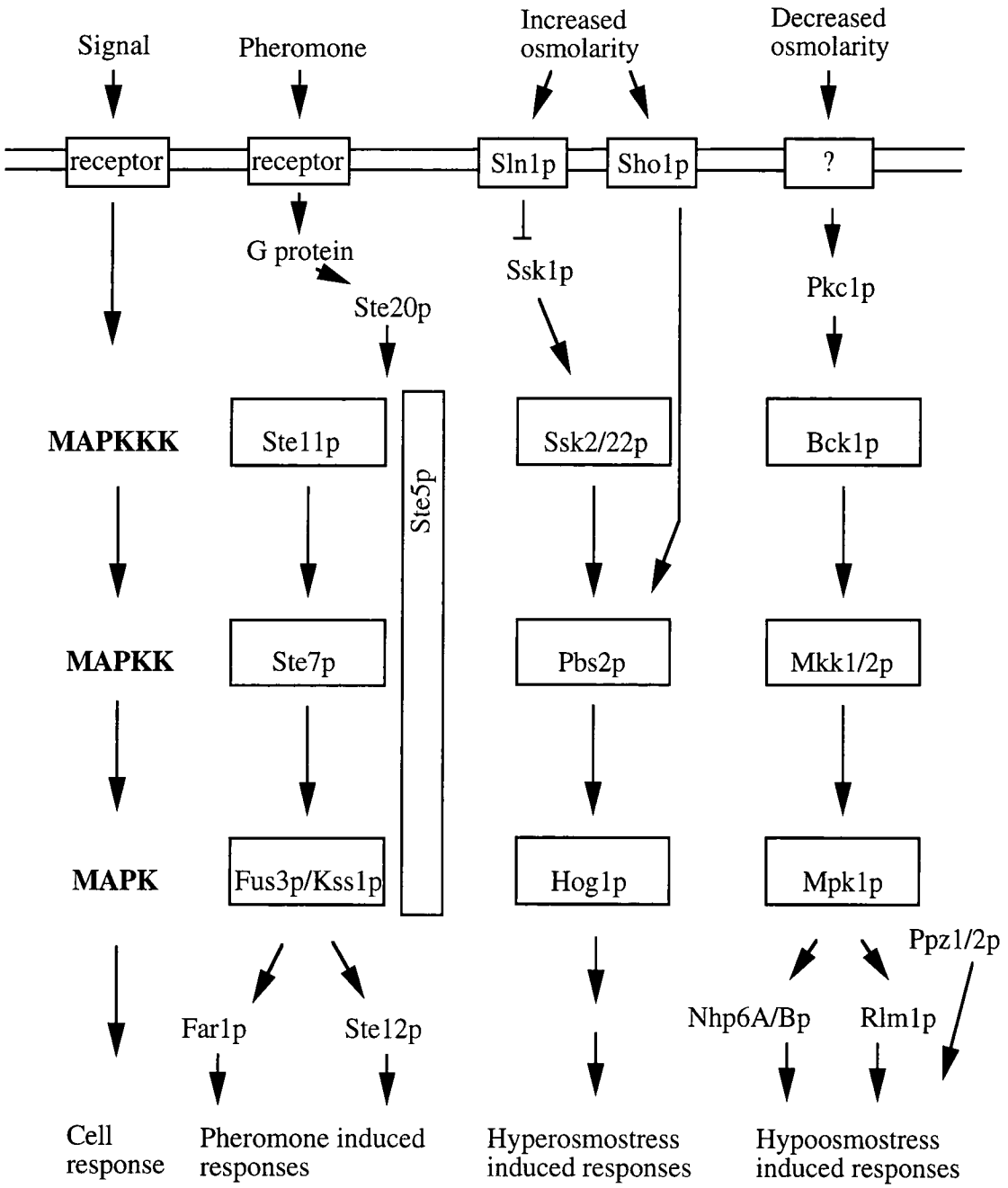

Figure 1.2. MAP kinase cascades in *Saccharomyces cerevisiae*

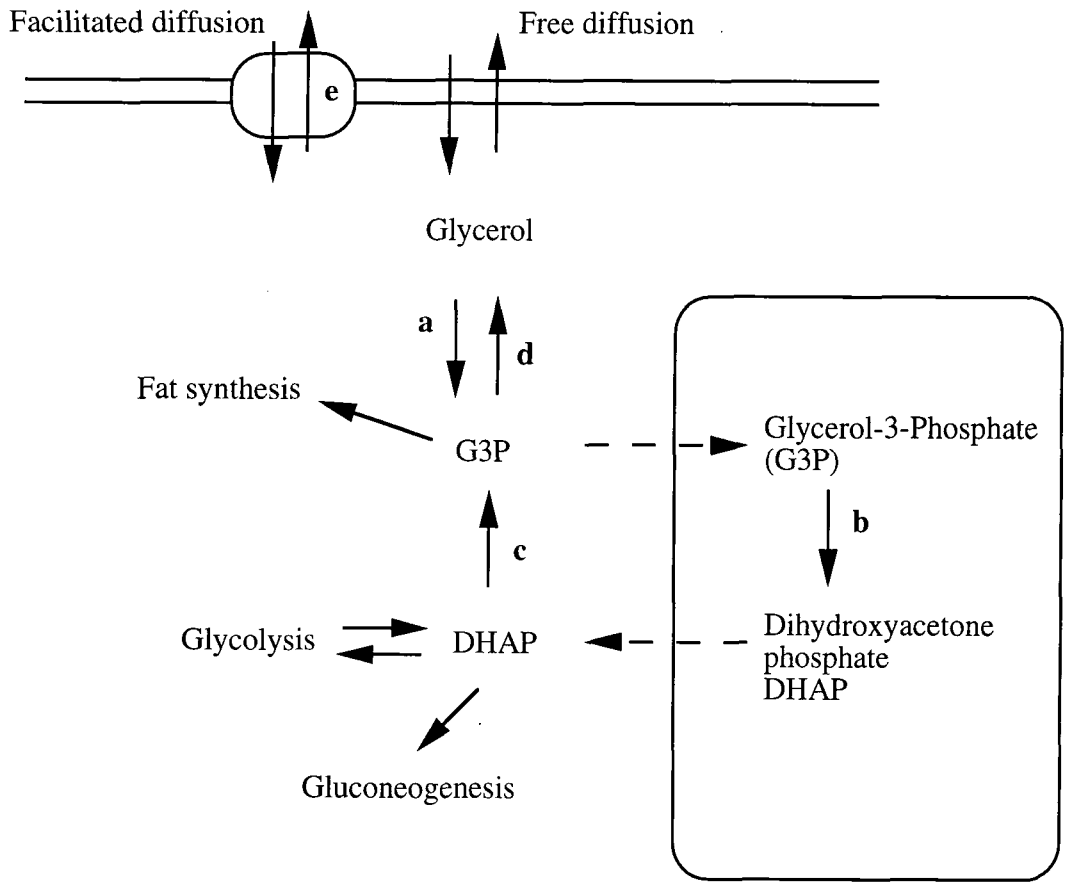

Figure 1.3. A scheme for glycerol metabolism in *S. cerevisiae*

The enzymes involved in glycerol metabolism:

Reaction	Enzyme	Gene	Notes
a	Glycerol kinase	*GUT1*	
b	Glycerol 3-phosphate dehydrogenase	*GUT2*	mitochondrial; FAD-dependent
c	Glycerol 3-phosphate dehydrogenase	*GPD1* / *GPD2*	osmostress-inducible (*GPD1* only); NADH-dependent
d	Glycerol-3-phosphate phosphatase	*GPP1* / *GPP2*	osmostress-inducible (*GPP2* only)
e	Glycerol channel	*FPS1*	inactive during osmostress

Glycerol accumulation is also affected by the rate at which glycerol can be lost to the extracellular medium. Although glycerol is able to diffuse across the membrane, facilitated diffusion by a glycerol channel, Fps1p, has also been described (Luyten *et al.*, 1995). In the absence of osmotic stress, Δ*fps1* mutants have higher intracellular and lower extracellular glycerol concentrations than the equivalent 'wild-type' strain. However, the glycerol accumulation during stress is not significantly different for the Δ*fps1* strain and kinetics of diffusion suggest that the Fps1p channel is inactive during osmotic stress. The inactivation of facilitated diffusion through Fps1p during osmotic stress is independent of Hog1p activity (Luyten *et al.*, 1995).

The metabolic shift to produce glycerol in osmotically stressed cells may be aided by the elevated activities of genes encoding proteins involved in the uptake of glucose. The study of hyperosmolarity responsive (*HOR*) genes showed enhanced transcription of glucokinase (Glk1p) and hexose transporter (Hxt1p) with osmotic stress (Hirayama *et al.*, 1995).

1.3.3. Interactions between the HOG pathway and other cell processes

Elevating intracellular glycerol is not the sole outcome of high-osmolarity signal transduction. As mentioned before, the HOG pathway enhances the transcription of the *ENA1* gene involved in sodium exclusion (Marquez and Serrano, 1996) in addition to the glycerol synthesis genes *GPD1* (Albertyn *et al.*, 1994) and *GPP2* (Norbeck *et al.*, 1996). The HOG pathway can also enhance the transcription of genes known to be responsive to oxidative stress (Krems *et al.*, 1995), heat shock (Varela *et al.*, 1992), and nutrient starvation (Marchler *et al.*, 1993). This suggests that some gene products may be involved in a general stress response.

The precise mechanism by which active Hog1p brings about enhanced transcription of stress responsive genes is not yet known. The induction of the *CTT1* gene in response to salt stress is mediated via the STRE which is also required for the action of other stresses (Schuller *et al.*, 1994). The transcription factor(s) which can bind to this element have not yet been described so it is not yet known whether there are a) several transcription factors, each responding to a different kind of stress; or b) one transcription factor that responds to several stresses. The *GPD1* gene does not appear to have an upstream STRE of the same nature as *CTT1*. Therefore a model could be proposed where there is both a general transcription factor which responds to a variety of stresses (and exerts action through the STRE) and a specific transcription factor which responds only to the HOG pathway. There is evidence that MAP kinases can be

found in both the nucleus and the cytoplasm (Chen *et al.*, 1992) and it is possible that Hog1p enters the nucleus and phosphorylates certain transcription factors in response to salt stress.

The HOG pathway also plays a role in bud site selection (Brewster and Gustin, 1994). In cells subjected to osmotic stress there is a temporary growth arrest and rapid dissociation of the actin cytoskeleton (Chowdhury *et al.*, 1992). On recovery from osmotic shock the actin cables reassemble and bud growth resumes in the same location. However, Δ*hog1* cells fail to resume bud growth at the same site and instead initiate a new bud site (Brewster and Gustin, 1994). Thus it would appear that the HOG pathway is required for retention of spatial information when the actin cytoskeleton disassembles. Both disassembly of the cytoskeleton and tyrosine phosphorylation of Hog1p occur within one minute of application of salt stress (Brewster and Gustin, 1994; Chowdhury *et al.*, 1992). The independence of the actin response from Hog1p raises the intriguing possibility that actin may interact with upstream components of the osmosensing signal transduction pathway. There are other possible causes for the actin response that cannot be ruled out however. For example, the immediate solute loss due to changes in osmolarity may cause a mechanical response which triggers reorganisation of the cytoskeleton. Temperature stress and changes in carbon source can cause a similar actin disassembly (Chowdhury *et al.*, 1992) but in these conditions Hog1p is not required to redirect growth to the original bud site. It is clear that the HOG pathway does play a role in regulating cell morphogenesis but apparently only in response to salt.

It is interesting that the other osmosensing signal transduction pathway, the PKC1 pathway, has also been implicated in regulation of growth from the bud. A mutant allele of *BCK1* (*slk1*) was isolated by its requirement for the bud formation protein, Spa2p, for growth (Costigan *et al.*, 1992). Other evidence for the involvement of this pathway in the regulation of budding comes from a mutant *mpk1* allele which causes delocalization of chitin deposition and actin cortical spots (Mazzoni *et al.*, 1993). Thus it would appear that both the HOG pathway and the PKC1 pathway can effect the organisation of the cytoskeleton and growth at the bud. The study of protein-protein interactions at the bud during different physiological conditions may reveal further information about how these two pathways exert control over cell morphogenesis.

An interaction between the HOG pathway and another stress-responsive cell process may occur through the function of Sln1p. A strain containing a mutant allele of *SLN1* was first identified by its requirement for the ubiquitin N-end rule for degradation (Ota and Varshavsky, 1992; for a review of the N-end rule see Varshavsky, 1992). The lethality of the Δ*sln1* Δ*ubr1* double mutation (deleted for both Sln1p activity and the

recognition component of the N-end rule) was suppressed by high copy expression of the *PTP2* gene which encodes protein tyrosine phosphatase. As the *Δsln1* mutation can cause constitutive activation of the HOG pathway it seems likely that high copy Ptp2p can suppress the lethality by dephosphorylating and thereby deactivating Hog1p (Maeda *et al.*, 1994). The role of the N-end rule pathway is unclear but it is possible that it allows for tight regulation of the amount of protein in the HOG pathway. A model that would be consistent with the phenotypes observed would be that the N-end rule could be required for rapid turnover of Ssk1p. Ssk1p is apparently inactivated by phosphorylation by Sln1p. The constitutive activation of Ssk1p caused by loss of Sln1p activity could be counteracted by enhanced turnover of Ssk1p, thereby removing inappropriate signalling through the HOG pathway or, as mentioned before, by enhanced phosphatase activity down-regulating active Hog1p. *PTP2* is induced by heat and is required for certain aspects of thermotolerance (Ota and Varshavsky, 1992) suggesting another point of interaction between the HOG pathway and other stress responses.

Sln1p is also involved in Hog1p-independent cellular activity (Yu *et al.*, 1995). Deletion of *SLN1* severely reduces the activity of the transcription factor Mcm1p, and certain alleles of *sln1* can enhance Mcm1p-mediated transcriptional activation. These responses were unaltered by deletion of *HOG1* showing that Sln1p can control functions independently of its role in osmoregulation.

It is apparent that Hog1p can bring about osmostress-induced changes at the level of both transcription and post-translational modification and as such is likely to phosphorylate an array of substrates.

1.4. The Vacuole and Osmohomeostasis

1.4.1. Characterisation of the vacuolar protein sorting (vps) mutants

The mechanisms involved in protein sorting to the vacuole have been an area of intense study for many years. The characterisation of strains which mislocalize vacuolar proteases has revealed mutations in over 50 complementation groups (Robinson *et al.*, 1988). The early studies described *vpt* mutants which mislocalize a vacuolar carboxypeptidase Y (CPY)-invertase fusion protein to the cell surface (Bankaitis *et al.*, 1986; Robinson *et al.*, 1988) and *vpl* mutants which have CPY located in the periplasm (Rothman *et al.*, 1989). The overlapping complementation groups of the *vpl* and the *vpt* mutants led to the revised nomenclature of *vps* genes for vacuolar protein sorting (Robinson *et al.*, 1988; Rothman *et al.*, 1989). One of the *vps* mutants, *vps11*, was

found to be allelic to the *end1* mutant which is defective in endocytosis thus providing the first genetic evidence for a link between the endocytotic and biosynthetic delivery routes to the yeast vacuole (Robinson *et al.*, 1988).

The *vps* strains can be classified according to their effects on vacuolar morphology. The original classifications (Banta *et al.*, 1988) have been refined to include six different classes (Raymond *et al.*, 1992).

Class A *vps* strains have vacuoles with similar morphology to 'wild-type'. In some strains the vacuolar structure is slightly perturbed but not severely. Segregation structures that transport maternal vacuolar material into the daughter bud (discussed later) are less prominent in some strains but all large buds contain a vacuolar structure. The severity of the sorting defect is variable for the class A *vps* strains.

Class B *vps* strains have fragmented vacuoles and severe defects in vacuolar protein sorting. These strains can form two sub-groups. In one the fragmented vacuolar compartments align along the mother-bud axis. In the other, vacuole fragments are randomly dispersed.

Class C *vps* strains lack coherent vacuoles and have severe sorting defects. Vacuolar proteins appear to be located in vesicular structures dispersed through the cytoplasm.

Class D *vps* strains display defects in vacuolar inheritance, acidification of the vacuole and vacuolar protein sorting.

Class E *vps* strains visualised using antibodies to alkaline phosphatase appear to have normal vacuoles but antibodies to the vacuolar H^+-ATPase reveal a densely-staining compartment adjacent to the vacuole. This small densely-staining compartment is termed the 'class E compartment'.

Class F *vps* stains appear to have small vacuolar compartments surrounding the main vacuole. Segregation structures are rarely observed but all large buds contain vacuoles.

The observation that some of the *vps* strains are also osmosensitive led to a mutagenesis study to create osmosensitive strains as a tool for isolating other components of the vacuolar protein sorting mechanism (Latterich, 1992). This approach led to the isolation of a further 14 complementation groups which were termed *ssv* for salt-sensitive vacuolar genes. The vacuoles of *ssv* strains and salt-sensitive *vps* strains are not restricted to one class of morphology, although all the class C mutations tested had an associated osmosensitivity phenotype (Banta *et al.*, 1988).

1.4.2. Vacuolar protein sorting

1.4.2.1. Golgi-to-vacuole protein sorting

Proteins destined for the vacuole are usually transported via the secretory pathway to the Golgi body. The study of *sec* mutants has given much information about the order of events in the secretory pathway (Novick *et al.*, 1981) and has also revealed some of the stages of vacuolar protein maturation and transport. The secretory pathway is the default pathway for soluble proteins, and vacuolar proteases, such as CPY, contain a signal sequence, QRPL, that direct them to the vacuole instead of the plasma membrane (Valls *et al.*, 1990). However, integral membrane proteins, e.g. alkaline phosphatase, rely on a different mechanism for transport to the vacuole as suggested by their relative sensitivity to different *vps* mutants with respect to the soluble enzymes (Klionsky and Emr, 1989). Dipeptidyl aminopeptidase A (DPAP A) normally resides in the Golgi but its overproduction results in activity located to the vacuole (Roberts *et al.*, 1992). If the Golgi retention signal is deleted then again DPAP A activity can be located to the vacuole (Nothwehr *et al.*, 1993) suggesting that for membrane-bound proteins it is transport to the vacuole not to the plasma membrane which is the default route.

Vacuolar protein sorting requires a complex transport machinery to recognise the signal sequence of soluble proteases and to regulate vesicle streaming from the Golgi. Subcellular fractionation studies demonstrate the presence of a prevacuolar compartment (Vida *et al.*, 1993) and transport may also require recognition of this compartment to ensure sequential stages in trafficking. After delivery of proteins to the vacuole or the prevacuolar compartment vesicular proteins and membrane are recycled back to the Golgi to maintain the flow of traffic.

One component of the transport machinery which cycles between the Golgi and the prevacuolar compartment is the CPY receptor, Vps10p (Cooper and Stevens, 1996; Marcusson *et al.*, 1994). Vps10p apparently recognises both CPY and proteinase A (PrA) (Cooper and Stevens, 1996) although previous evidence suggested separate sorting mechanisms for CPY and PrA (Marcusson *et al.*, 1994; Rothman *et al.*, 1986; Stevens *et al.*, 1986). Chemical cross-linking experiments show that the sorting signal of CPY is required for direct interaction of Vps10p and the Golgi-modified CPY precursor (Marcusson *et al.*, 1994). The recycling of Vps10p is dependent on a tyrosine-based signal within the cytosolic domain of the protein.

Details of the nature of the prevacuolar compartment are emerging through the study of class E *vps* strains. *VPS27* appears to be particularly important in the control of traffic through the prevacuolar compartment for both vacuolar proteins and for endocytotic complexes (Piper *et al.*, 1995). In the *vps27* deletion strain, both Vps10p and Ste3p (**a**-

factor receptor) are located in the class E compartment. It is likely that the class E compartment forms when there is a block in transport which results in dense accumulation of vacuolar material at a prevacuolar stage. Temperature-sensitive alleles of *vps27* have shown that restoration of Vps27p function will allow Ste3p to be transported into the vacuole and Vps10p to be recycled. Overexpression of Vps10p can suppress the Δ*vps27* CPY sorting defect showing that it is inhibition of recycling of the receptor that results in CPY secretion. Vps27p has two putative zinc-finger domains which are necessary for its function and are likely to be involved in protein-protein recognition. It is over this region that it has homology to two other proteins involved in vacuolar function; Fab1p and Vac1p (Weisman and Wickner, 1992; Yamamoto *et al.*, 1995) which will be discussed later.

Vesicle trafficking from the Golgi to the vacuole requires Vps15p and Vps34p. Vps15p and Vps34p interact to form a peripheral membrane complex and both are capable of autophosphorylation (Stack and Emr, 1994; Stack *et al.*, 1993). Active Vps15p recruits Vps34p to the membrane where the complex regulates transport. Vps34p is a dual specificity kinase capable of phosphorylating both protein and phosphatidylinositol (Stack and Emr, 1994). Vps15p activity is required for stimulation of Vps34p phosphatidylinositol-3-kinase activity which is required for correct sorting of vacuolar proteins (Stack *et al.*, 1995). This suggests that the formation of phosphatidylinositol 3-phosphate from phosphatidylinositol may function to regulate trafficking from the Golgi body.

Vacuolar protein sorting from the Golgi also requires the GTP-binding protein Vps1p. Antibody labelling of Vps1p shows it is distributed in punctate cytoplasmic structures and in a *vps1* strain membrane-enclosed structures accumulate (Rothman *et al.*, 1990). Vps1p is a homologue of dynamin (Vater *et al.*, 1992) with amino-terminal domain GTPase activity which is required for vacuolar protein sorting. The carboxy-terminal domain may associate with a component of the transport machinery. A mutant allele of *vps1* disrupts retention of the Kex2p protease in the Golgi (Wilsbach and Payne, 1993). The phenotype caused suggests that Golgi membrane proteins are retained in the Golgi by recycling from a prevacuolar compartment in a Vps1p-dependent manner.

1.4.2.2. Endocytosis

Endocytosis of proteins from the plasma membrane for degradation in the vacuole occurs in two stages with a detectable intermediate transport compartment (Singer and Riezman, 1990). At lower temperature (15°C) uptake of α-factor pheromone is slowed slightly whereas the rate of delivery to the vacuole and subsequent degradation by PrA is severely impaired (Singer and Riezman, 1990). Degradation of α-factor is also impaired in Δ*ypt7* cells (Wichmann *et al.*, 1992). Ypt7p is a *rab* family GTP-binding

protein and its disruption results in fragmented vacuoles. In Δ*ypt7* strains, CPY is not secreted but its maturation occurs at a severely reduced rate. This suggests that Ypt7p acts late in endocytosis, perhaps from the prevacuolar compartment that is common to both endocytosis and vacuolar protein targeting.

The endocytosis of uracil permease requires the ubiquitin-protein ligase, Npi1p (Galan *et al.*, 1996). In adverse conditions the uracil permease is ubiquitinated which appears to act as a signal for endocytosis. The breakdown of uracil permease requires proteinase A and in a *pep4* mutant ubiquitin-permease conjugates can be observed intact in the vacuole. Endocytosis and thus permease degradation are also defective in an *act1* mutant strain demonstrating the importance of the cytoskeleton in this process (Galan *et al.*, 1996).

1.4.2.3. Vacuole integrity

A collection of mutant strains defective in vacuolar morphology, *vam* strains, have been described (Wada *et al.*, 1992). These were divided into two classes: one with defects in the pathway of sorting and targeting vacuolar proteins; and the other with mature vacuolar proteins but in several vesicles instead of a coherent vacuole. The study of two of the class II mutants revealed that they were allelic to *vps41* and *vps42*. The phenotype of these strains suggest the genes may be involved in the recognition and fusion of vacuolar compartments.

There is a role for microtubules in maintaining vacuolar integrity. Treatment of cells with drugs which inhibit microtubule polymerization results in vacuole fragmentation (Guthrie and Wickner, 1988). The large number of class B and class C *vps* strains (Raymond *et al.*, 1992), in which vacuoles are fragmented or even completely disrupted, implies that a large number of gene products are involved in maintaining vacuolar integrity, many of which have yet to be characterised.

Figure 1.4. shows a scheme for vacuolar protein sorting and the stage at which certain gene products are involved. In summary, trafficking to the vacuole requires:

- sorting signals within soluble vacuolar enzymes and receptors for these signals
- phosphatidylinositol kinase activity, provided by Vps34p
- GTPase activity at more than one stage of trafficking (as demonstrated by the requirement for Vps1p and Ypt7p)
- proteins for vacuole compartment recognition.

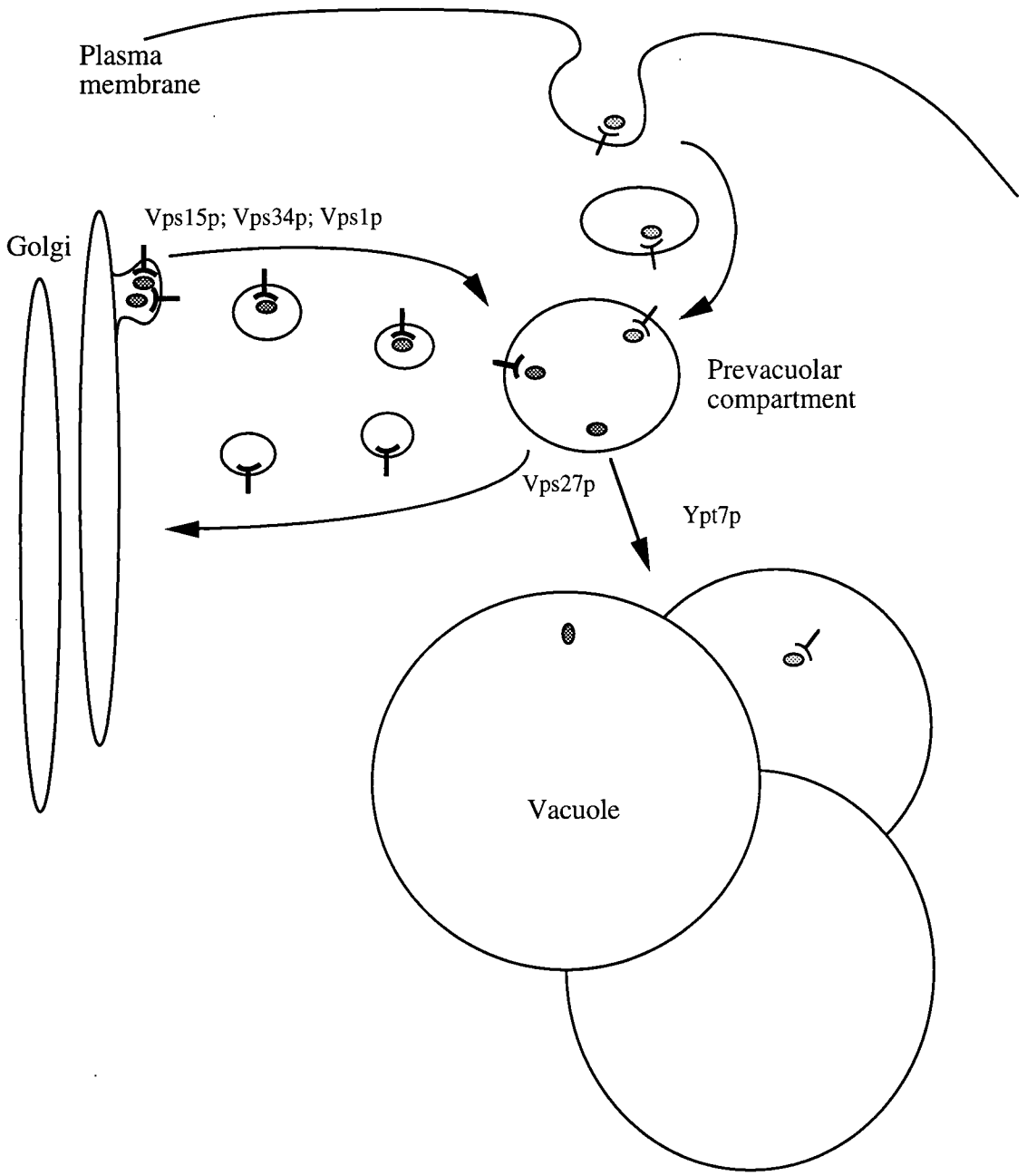

Figure 1.4. Protein sorting to the vacuole

Figure 1.4 is a diagrammatic representation of protein transport to the vacuole. Soluble vacuolar proteins such as CPY (⬭) are recognised by receptors (Vps10p; ⊥) and then transported to the prevacuolar compartment. Transport from the Golgi is regulated by Vps34p PI 3-kinase activity, which is stimulated by Vps15p, and Vps1p GTPase activity. Transport out of the prevacuolar compartment to the vacuole or for recycling of receptors requires Vps27p. Vacuole degradation of cell surface proteins also involves trafficking through the prevacuolar compartment. For exmaple, α-factor (⬭) binds to its receptor (⊥) and is then internalised. Final transport of the complex to the vacuole requires Ypt7p.

1.4.3. Vacuole inheritance

The study of *ade2* mutants which accumulate fluorophore in adenine-depleted medium showed that as *ADE2* and *ade2* strains mate and form a schmoo, vacuole inheritance is a dynamic process with exchange of vacuolar material from the parental cells to the bud and vice versa (Weisman and Wickner, 1988). In normal mitotic cell division, emerging buds inherit maternally-derived vacuolar material early in the cell cycle (Weisman and Wickner, 1988). Strains have been isolated which are defective in vacuolar inheritance where segregation structures are not formed and large buds are observed with no apparent vacuolar material (Weisman *et al.*, 1990). These so-called *vac* mutants have given some insight into the mechanisms for vacuolar inheritance.

The *vac1-1* allele is a temperature-sensitive, conditionally lethal mutation and at the non-permissive temperature cells accumulate with multiple buds (Weisman *et al.*, 1990). At the permissive temperature buds do eventually form vacuoles but with very little maternal vacuolar material suggesting that cells have mechanisms to form vacuoles *de novo* by a biosynthetic route. Defects in *VAC1* also have an associated vps phenotype and *VAC1* was subsequently shown to be identical to *VPS19* (Raymond *et al.*, 1992). The *VAC1* sequence shows that it encodes three putative zinc-finger domains and its product is likely to be cytosolic (Weisman and Wickner, 1992). As mentioned before, the zinc-finger domains of Vac1p are homologous to regions of Vps27p and Fab1p. Fab1p is a PI(4)P 5-kinase homologue (Yamamoto *et al.*, 1995). Loss of Fab1p function results in defects in vacuolar function and morphology, cell surface integrity and chromosomal segregation. In *fab1* mutants, the vacuole enlarges and segregation structures between mother cells and daughter buds are not observed. Acidification of the vacuole is also perturbed. Fab1p may therefore be involved in efficient efflux and turnover of the vacuole membrane. It is not yet known whether the effects in chromosome segregation are from steric inhibition by the enlarged vacuole or whether Fab1p may be involved in the segregation directly (or metabolically through PIP_2). This is another instance where the regulation of an aspect of vacuolar function appears to require a derivative of phosphatidylinositol.

A gene which distinguishes vacuolar segregation from vacuolar protein sorting is the *VAC2* gene (Shaw and Wickner, 1991). *vac2-1* cells have a temperature-sensitive defect in vacuolar segregation but not in protein targeting from the Golgi. *VAC2* is apparently required for partitioning maternal vacuolar contents into emerging buds. At the time of characterisation, *VAC2* was unusual for its lack of influence in vacuolar protein sorting; defects in *VAC1*, *VAC3* and *VAC4* all have an associated vps phenotype (Shaw and Wickner, 1991). More recently a mutant allele, *vac5-1* has been described which also appears to only affect vacuolar inheritance and not vacuolar protein sorting (Nicolson

et al., 1995). *vac5-1* was found to encode a truncated form of Pho80p. Pho80p is a cyclin which acts in a complex with Pho85p to regulate transcription factors involved in metabolic phosphatase expression. Neither Δ*pho80* or Δ*pho85* cause vacuole inheritance defects suggesting that the phenotype is not caused by loss of function of Pho80p/Pho85p but that the *vac5-1* allele may interfere with the regulation of the transcription factors, perhaps altering their specificity (Nicolson *et al.*, 1995).

The link between vacuolar protein sorting and vacuolar inheritance has also been demonstrated by *vps* mutants which are unable to form segregation structures. The *vps3* mutant has a defect in vacuolar acidification but this is apparently unrelated to its aberrant vacuolar morphology (disruption of acidification by other means cannot confer the same phenotype) (Raymond *et al.*, 1990). In Δ*vps3* cells, the vacuoles form spheres which cannot form segregation structures during budding. As for the *vac1-1* strain, nearly all the mother cells contain vacuoles suggesting assembly does occur during the cell cycle. In some ways (enlarged vacuole and disrupted acidification) the *vps3* mutant has a similar phenotype to the *fab1* strain (Yamamoto *et al.*, 1995). It is possible that these two gene products operate at a similar stage of vacuole function although this has yet to be tested. The *VPS3* gene does not appear to encode an ER signal sequence for entry into the secretory pathway nor a transmembrane domain and is therefore likely to be cytosolic.

In vitro studies are revealing further information about the processes involved in vacuolar inheritance. An assay that makes use of maturation and activation of vacuole membrane-bound pro-alkalinephosphatase by PrA after vacuole-vacuole fusion has shown that vacuole fusion (*in vitro*) requires a membrane potential (Haas *et al.*, 1994). The involvement of a G protein is also implicated as non-hydrolyzable guanosine derivatives inhibit fusion in the *in vitro* assay.

There are other aspects of vacuolar inheritance yet to be characterised. The *ssv17-101* mutation causes an unusual vacuole inheritance defect (Hartley, 1995; Latterich *et al.*, 1993). Unlike defects in *vac1* and *vac2*, this strain appears to have a breakdown in the regulation of vacuolar inheritance. Vacuolar material is segregated to the daughter bud in most cases but in a proportion of the cells, no vacuole is observed in the emerging bud and interestingly mother-daughter pairs can be observed with neither cell containing a coherent vacuolar structure. *SSV17* is also involved in vacuolar protein targeting and the *ssv17-101* mutation causes a severe sorting defect.

A scheme for vacuole inheritance is shown in figure 1.5. It is likely that some of the reactions required for vacuole inheritance share proteins which are common to both segregation and vacuolar protein sorting mechanisms, whereas others are specific to segregation only.

1.4.4. The role of the vacuole in osmohomeostasis

The vacuole could play a variety of roles in osmohomeostasis. It could help maintain the intracellular Na^+/K^+ ion ratio, the importance of which was discussed in section 1.2. The vacuole may also be involved in osmohomeostasis by degrading proteins that are not required in a particular physiological state.

Of the *vps* mutant strains described as being osmosensitive, three, namely *vps1*, *vps15* and *vps34* (isolated as *vpt26*, *vpt15* and *vpt29* respectively; Banta *et al.*, 1988), are involved in the early stages of vacuolar protein sorting from the Golgi. As described in section 1.4.2, Vps15p and Vps34p form a complex that regulates trafficking (Stack *et al.*, 1993). *vps15* and *vps34* mutations both confer class D morphology and thus also have a segregation defect (Raymond *et al.*, 1992). Vps1p is also involved in transport from the Golgi. It has GTPase activity (Vater *et al.*, 1992), and is required for retention of Golgi proteins, such as Kex2p (Wilsbach and Payne, 1993). The reason for the osmosensitivity displayed by *vps1*, *vps15* and *vps34* strains is not known. It is possible that the stage of sorting from the Golgi is particularly sensitive to fluctuations in ion concentration.

All four *vps* strains with class C vacuole morphology, *vps11*, *vps16*, *vps18* and *vps33* (Banta *et al.*, 1988) have an associated osmosensitive phenotype. This implies that a coherent vacuolar structure is required for some aspect of osmohomeostasis. Vps33p is a cytoplasmic ATPase (Banta *et al.*, 1990). A temperature-sensitive *vps33* strain which contains a vacuole was found to be defective in vacuolar inheritance. This suggests the protein has a function common to both vacuole segregation and integrity. A defect in vacuole inheritance does not always confer osmosensitivity. For example, Δ*vac1* is not osmosensitive, so it is more likely that it is the structural defect caused by *vps33* that disrupts osmohomeostasis.

The degradation of proteins in the vacuole may play a general role in homeostasis in a variety of conditions. Endocytosis and degradation of plasma membrane proteins can require ubiquitin-protein ligase, a functional actin cytoskeleton and mature vacuolar proteins (Galan *et al.*, 1996). If the vacuole is the route of degradation for proteins involved in metabolism and homeostasis, then disruptions in vacuolar integrity or transport to the vacuole could have pleiotropic effects on osmosensitivity. A link

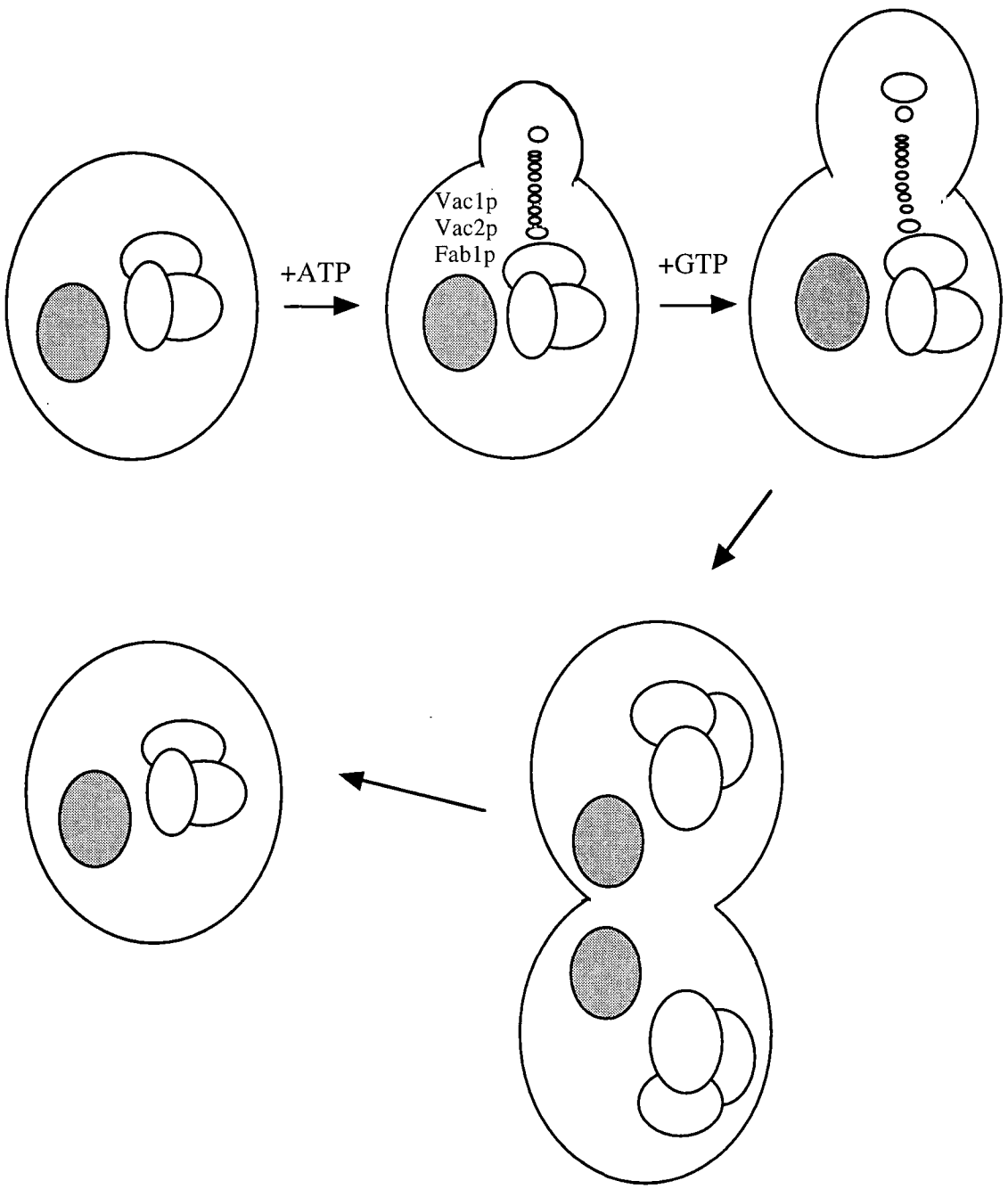

Figure 1.5 Vacuole inheritance in yeast.

The vacuole (◯) begins segregation early in the cell cycle before nuclear (◉) division. Vesicles stream into the daughter bud forming segregation structures. The whole process of vacuolar segregation requires many genes, including Vac1p, Vac2p, Fab1p, Vps3p and Ssv17p. The process also requires ATP, GTP and a membrane potential (see text for further details).

between vacuole function and metabolism has been demonstrated. Defects in *gut1* and *aro7*, encoding glycerol kinase and chorismate mutase, have an associated CPY secretion phenotype (Latterich *et al.*, 1993). Mutations in *aro7* also confer osmosensitivity.

1.5. Aims of Project

The aim of this project was to characterise *ssv* strains from the laboratory collection of mutants (Latterich, 1992). These mutants were isolated by their lack of growth on media containing 1.5M NaCl. The vacuolar morphology and protein sorting defects for the strains were tested previously.

Part of the project was dedicated to screening the strains for phenotypes which may signify a defect in osmosensing signal transduction. The screen was initiated by B. Pöpping who tested all the strains for glycerol accumulation. The strains which showed depressed levels of glycerol accumulation in response to salt stress were selected for this project. The aim was to show that the low levels of glycerol accumulation correlate with low GPDH activity and that these strains may therefore be defective in signalling to enhance *GPD1* transcription.

The other aspect of the project was to characterise the *SSV17* gene. Mutations in this gene confer a particularly unusual pattern of vacuolar inheritance. A candidate gene for *SSV17* was revealed by the EC yeast genome sequencing project. This gene was tested for ability to complement the osmosensitivity of *SSV17*. The aim was to gain insight into the mechanisms of vacuole inheritance by characterising the role of *SSV17*.

CHAPTER 2

MATERIALS AND METHODS

2.1. Materials

2.1.1. Reagents and Suppliers

All chemicals were of AnalaR quality and were from BDH Chemicals Ltd., Poole, Dorset, U.K. or Sigma Chemicals Plc., Poole, Dorset, U.K. unless otherwise specified.

Yeast extract was from Oxoid Ltd., Basingstoke, Hants., U.K..

Trypticase Peptone was from BBL, Cockeysville, U.S.A..

Bacto Peptone and Yeast Nitrogen Base without Amino Acids were from Difco Laboratories, Detroit, MI, U.S.A..

Select agar and agarose were from Gibco BRL, Gaithersburg, U.S.A..

Restriction endonucleases and buffers, T4 DNA ligase, Klenow enzyme, 5-bromo-4-chloro-3-indoyl-β-D-galactoside (X-gal) and wild-type λ DNA were from NBL, Cramlington, Northumberland, U.K., Boehringer Mannheim (U.K.) Ltd., Lews, U.K., or New England Biolabs, CP Labs Ltd., Bishop's Stortford, Hertfordshire, U.K..

Filter paper (3MM) and laboratory sealing film were from Whatman International Ltd., Maidstone, U.K..

Nitrocellulose was from Bio-Rad Laboratories Ltd., Hemel Hempstead, U.K..

Polaroid film was from Polaroid (U.K.) Ltd., St. Albans, Hertfordshire, U.K..

2.1.2. Buffers and Stock Solutions (Listed in Alphabetical Order)

Amino Acid Stock Solutions

Stock solutions of individual amino acids and nucleotide bases were prepared at 2mg/ml and then autoclaved. They were used at a final concentration of 20μg/ml as supplements of yeast minimal medium as required.

Antibiotic Stock Solutions

Ampicillin was prepared as a 50mg/ml stock solution in 70% ethanol, and used at a final concentration of 50µg/ml. Kanamycin was prepared as a 20mg/ml stock solution in dH_2O, filter sterilised and used at final concentration of 20µg/ml.

6x Agarose Gel Loading Buffer

Bromophenol Blue	25mg
Xylene Cyanol	25mg
Sucrose	4g

in 10ml dH_2O.

20x SSC

NaCl	175.3g
Sodium Citrate	88.2g

in 1l dH_2O. The solution was adjusted to pH7.0 with 10M NaOH.

50x TAE Buffer

Tris.HCl	242.0g
EDTA	18.5g
Glacial Acetic Acid	57.1ml

in 1l dH_2O.

TE Buffer pH 8.0 (10mM Tris.HCl, 1mM EDTA)

1M Tris.HCl pH 8.0	10ml
250mM EDTA pH 8.0	4ml

in 1l dH_2O.

2.1.3. Growth Media (Listed in Alphabetical Order)

All growth media described below can be used as liquid media or can be solidified by the addition of 2% agar.

Luria-Bertani Broth (L-Broth)

Trypticase Peptone	10g
Yeast Extract	5g
NaCl	5g

in 1l dH_2O.

Sporulation Agar

Yeast Extract	1g
Glucose	0.5g
Potassium Acetate	10g
Agar	20g

in 1l dH_2O. Required amino acids were added to a final concentration of 20µg/ml.

Yeast Minimal Medium

Yeast Nitrogen Base without Amino Acids	6.7g
Glucose	20g

in 1l d H_2O. Required amino acids were added to a final concentration of 20µg/ml.

YPD(A)

Yeast Extract	10g
Bacto Peptone	20g
Glucose	20g
(Adenine	20mg)

in 1l dH_2O.

2.2. Strains and Plasmids

2.2.1. Bacterial Strains

The bacterial strain used in this study was *Escherichia coli*, and strains are listed in table 2.1. All strains represent laboratory stocks.

E. coli strains were cultured in L-Broth at 37°C. Cultures of bacteria containing plasmids were grown in media containing the appropriate antibiotic selection. Strains were maintained for short periods of time on L-Agar and stocks of all bacteria were maintained in 15% glycerol at -80°C.

Strain	Genotype	Source
DH5α	*supE*44 Δ*lac*U169 (ϕ80 *lacZ*ΔM15) *hsdR*17 *recA*1 *endA*1 *gyrA*96 *thi*-1 *rel*A1	laboratory stock
GM119	*dcm*6 *dam*3 *met*B1 *thi*1 *lacY*1 *gal*K2 *galT*22 *mtl*2 *ton*A2 *tsx*78 *supE*44	laboratory stock

Table 2.1. Bacterial strains used in this study.

2.2.2. Plasmids

All plasmids used in this study were maintained in DH5α except for plasmids to be restricted with *Bcl*I which were maintained in GM119. Plasmids and their prominent features are listed in table 2.2. The plasmid pL2 was kindly supplied by T.H. Stevens and C. R. Raymond, Oregon (personal communication).

Plasmid	Genotype	Reference
pUCI9	amp^R	(Yanisch-Perron *et al.*, 1985)
pFA6a	amp^R	(Wach *et al.*, 1994)
pFA6a-lacZMT-KanMX3	amp^R, *lacZ*, kan^R	(Wach e*t al.*, 1994)
pL2	amp^R, *LEU2*	C. Raymond, Oregon
AW1N	amp^R, *URA3*	(Belazzi *et al.*, 1991)
YCp50	tet^R, amp^R, *URA3*	(Rose *et al.*, 1987)

Table 2.2. Plasmids used in this study.

2.2.3. Yeast Strains

Saccharomyces cerevisiae strains used in this study are listed in table 2.3. MLY *ssv* strains are laboratory strains derived from the parental strains SEY6210 and SEY6211 (Latterich, 1992). MLY strains which are MATα are derived from SEY6210 and have the genotype *leu2-3,112 ura3-Δ52 his3-Δ200 trp1-Δ901 lys2-801 suc2-Δ9 GAL.* MLY strains which are MATa are derived from SEY6211 and have the genotype *leu2-3,112 ura3-Δ52 his3-Δ200 trp1-Δ901 ade2-101 suc2-Δ9 GAL.*

JBY10 and JBY40 were derived from the parental strain YPH499 and were kindly donated by M. Gustin. *vps27* was originally isolated as *vpl23* (Raymond *et al.*, 1992) and was kindly donated by T. H. Stevens.
Stocks of all yeast strains were kept in 40% glycerol at -80°C.

Strain	Genotype	Reference
SEY6210	MATα *leu2-3,112 ura3-Δ52 his3-Δ200 trp1-Δ901 lys2-801 suc2-Δ9 GAL*	(Robinson *et al.*, 1988)
SEY6211	MATa *leu2-3,112 ura3-Δ52 his3-Δ200 trp1-Δ901 ade2-101 suc2-Δ9 GAL*	(Robinson *et al.*, 1988)
MLY0108	MATα *ssv1-3*	(Latterich, 1992)
MLY0145	MATα *ssv1-5*	
MLY0402	MATa *ssv8-3*	
MLY0419	MATa *ssv18-100*	
MLY0508	MATa *ssv17-101*	
MLY0712	MATa *ssv-124*	
MLY0905	MATα *ssv-112*	
MLY1005	MATα *ssv7-2*	
MLY1143	MATa *ssv1-8*	
MLY1164	MATa *ssv-118*	
MLY1176	MATa *ssv-119*	
MLY1218	MATa *ssv-121*	
MLY1510	MATα *ssv6-1*	
YPH499	MATa *ura3-52 lys2-801 ade2-101 trp1-Δ1 his3-Δ200 leu2-Δ1*	(Sikorski and Hieter, 1989)
JBY10	MATa *ura3-52 lys2-801 ade2-101 his3-Δ200 leu2-Δ1 hog1-Δ1*	(Brewster *et al.*, 1993)
JBY40	MATa *lys2-801 ade2-101 trp1-Δ1 his3-Δ200 leu2-Δ1 pbs2-Δ1*	(Brewster *et al.*, 1993)
vps27	MATa *his4 ura3-52 leu2 ade6 pep4-3 vps27*	T. Stevens

Table 2.3. Yeast strains used in this study.

2.3. General Methods

2.3.1. Sterile Working Practices

Sterile working practices were maintained throughout. All media and materials were autoclaved at 15 p.s.i. for 15 minutes, unless heat sensitive, in which case they were filter sterilised by passing through a 0.22μm nitrocellulose membrane filter. Heat sensitive plastic ware was sterilised by leaving overnight in 70% ethanol then washing in sterile dH_2O.

All bottle necks were flamed before and after use, and caps were replaced on all containers as soon as possible. Culture plates were sterilised after pouring by flaming the surface of the molten agar with a roaring Bunsen flame.

2.4. Transformation Methods

2.4.1. Transformation of *E. coli* - Heat Shock

Transformation of *E. coli* by heat shock was based on the method of Mandel and Higa (1970).

100ml of L-broth were inoculated with 1ml of an overnight culture of *E. coli* and incubated, with shaking, at 37°C until the absorbance at 550nm was 0.4-0.5 (2-4 hours). The culture was chilled on ice for 10 minutes before the cells were pelleted in chilled centrifuge tubes at 4000g for 5 minutes at 4°C. After removal of the supernatant, the pellet was gently resuspended in 50ml of ice-cold 0.1M $CaCl_2$ and the suspension stored on ice for 15 minutes. The cells were then re-centrifuged as before and finally resuspended in 6ml of the same solution. 0.2ml aliquots were dispensed into microcentrifuge tubes which were stored on ice for a further 1-2 hours. Cells were either used straight away for transformation or stored for future use. For storage of the competent cells, 70µl of 80% glycerol were added to each tube and the cells were kept at -80°C. Frozen cells were thawed on ice before transformation.

For transformation of the competent cells, pure DNA in TE buffer or a ligation mixture (typically 200ng of DNA in a volume of 5µl) was added to a 0.2ml aliquot of cells and mixed gently by inversion before incubation on ice for 30-60 minutes. The cells were heat-shocked for 2 minutes at 42°C before the addition of 1ml L-broth. The tube was then incubated at 37°C in a heating block for 1 hour before appropriate aliquots, usually 1/10th and 9/10ths of the tube, were spread on selective agar plates.

2.4.2. Transformation of *S. cerevisiae* - Electroporation

Transformation of *S. cerevisiae* by electroporation was based on a method from B. Stevenson (personal communication).

10ml YPDA were inoculated with a colony of the yeast strain to be transformed and incubated overnight with agitation at 30°C. 100µl were used to inoculate 100ml of YPDA and incubated as above until a cell density of approximately $1x10^7$ cells/ml was reached (16-18 hours). The culture was then centrifuged at 2400g for 5 minutes and the

pellet resuspended in 20ml ice-cold dH_2O. The cells were washed twice in ice-cold 1M sorbitol by resuspending the pellet and centrifuging the cells as above, before resuspending the final pellet in 0.3-0.5ml of 1M sorbitol and storing on ice until transformation. Up to 5µl of DNA solution were pre-mixed with 1µg of carrier DNA (single-stranded Salmon sperm DNA). 100µl of cells were added to the DNA, mixed and transferred into a cold genepulser cuvette (Bio-Rad 0.2cm electrode gap). The cells were pulsed at 1.5kV (7.5kV/cm), 25µF, 200Ω for about 4.8ms (Bio-Rad gene pulser). 300µl 1M sorbitol were added to the transformation mixture and 100µl aliquots were plated out onto selective media. The plates were incubated at 30°C for at least 4 days.

2.4.3. Transformation of *S. cerevisiae* - Heat Shock

Transformation of *S. cerevisiae* was based on the methods of Gietz *et al.* (1992) and Hill *et al.* (1991).

A single colony of the yeast to be transformed was used to inoculate a 10ml culture of YPDA and incubated overnight at 30°C with shaking. 50ml of YPDA were inoculated with 5ml of this overnight culture and then incubated as above for 3 hours. The cells were harvested by centrifugation at 1000g for 5 minutes at room temperature and then resuspended in 25ml dH_2O. The suspension was centrifuged as above and the cell pellet was resuspended in 1ml LiAc solution (TE, 0.1M lithium acetate pH7.5). For each transformation 100µl of cell suspension were added to a microcentrifuge tube along with 0.1µg plasmid DNA and 100µg of single-stranded carrier DNA. 0.6ml of freshly-prepared PEG/LiAc solution (40% PEG 4000, TE, 0.1M lithium acetate pH7.5) was added to each tube and mixed by vortexing before incubation for 30 minutes at 30°C with shaking. 70µl of 100% DMSO were added to the contents of the tube, mixed gently and then heat-shocked for 15 minutes at 42°C. The cells were pelleted by chilling on ice followed by centrifugation for 15 seconds at 12000g in a microcentrifuge. The supernatant was discarded and the pellet resuspended in 0.5ml TE before plating out onto selection plates (0.1ml per plate). The plates were incubated at 30°C for at least 3 days.

2.5. DNA Manipulations

2.5.1. Precipitation of DNA with Ethanol

0.1 volume of 3M sodium acetate (pH5.2) and 2.5 volumes of 100% ethanol were added to the DNA containing solution, mixed and stored at -80°C for at least 30 minutes.

DNA was pelleted by centrifugation at 12 000 g for 10 minutes. Pellets were washed in ice-cold 70% ethanol, the supernatant removed and the pellet allowed to dry before resuspension in TE buffer.

2.5.2. Spectrophotometric Quantification of DNA

The DNA sample was diluted 1:50 or 1:100 with TE to give final volume of 0.1ml. This was put into a quartz cuvette and the absorbance of the solution at 260 and 280nm measured with a UV spectrophotometer (LKB) using TE as a blank. A pure DNA sample has an $A_{260/280}$ ratio of 1.8. An A_{260} value of 1.0 is equivalent to a concentration of 50$\mu g ml^{-1}$ of double stranded DNA or 20$\mu g ml^{-1}$ of single stranded oligonucleotides.

2.5.3. Plasmid DNA Preparation from *E. coli* - Alkaline Lysis

Small amounts of plasmid DNA were prepared according to Sambrook *et al.* (1989). A single colony of plasmid-containing bacteria was grown overnight in 5ml of L-broth with appropriate antibiotic selection and 1.5ml transferred to a sterile microcentrifuge tube. The culture was centrifuged for 1 minute (12000g) and the supernatant discarded. The pellet of cells was resuspended in 100µl TE and allowed to stand at room temperature for 5 minutes. 200µl of solution 2 (0.2M NaOH, 1% SDS) were then added and the contents of the tube mixed by gentle inversion before incubation on ice for 5 minutes. 150µl of ice-cold solution 3 (11.5ml glacial acetic acid, 28.5ml dH_2O and 60ml 5M potassium acetate pH4.8 with no correction) were then added and the tube vortexed briefly. After a further 5 minutes on ice, the tube was centrifuged for 10 minutes in a microcentrifuge to remove bacterial debris. The supernatant was transferred to a clean tube and the DNA was ethanol precipitated (section 2.5.1). The pellet was resuspended in TE with RNase A added to a concentration of 20$\mu g ml^{-1}$.

2.5.4. Plasmid DNA Preparation from *E. coli* - High Purity

Plasmids to be sequenced or required in high concentration were prepared by a modified alkaline lysis method using the Promega Wizard Minipreps (DNA Purification System) kit according to the manufacturer's instructions.

2.5.5. Rapid Screen for Plasmid DNA

This procedure (T. Fawcett, personal communication) was used for screening of plasmids of different sizes when no other selection was available. Colonies to be tested and a control of a known plasmid size were picked with broad-ended toothpicks and

transferred to a fresh plate in 2cm streaks for overnight incubation at 37°C. For screening, 80% of a streak was resuspended by vortexing in 40µl of STE (100mM NaCl, 20mM Tris.HCl, 10mM EDTA). 40µl of phenol: chloroform were added to the tube which was then vortexed for 1 minute and centrifuged for 2 minutes in a microcentrifuge. 30µl of the upper, aqueous phase were removed and added to 1µl of 10mg/ml RNase A in a fresh tube. The mixture was incubated for 2 minutes at room temperature before 6x loading buffer was added and the sample analysed by gel electrophoresis alongside controls and the other samples selected for rapid screening. Each gel lane should contain a smear of chromosomal DNA at the top of the gel and also a single band containing covalently closed circular DNA which migrates according to size.

2.5.6. Restriction Digests

Restriction digests were carried out using commercial sources of enzymes and their corresponding buffers, as supplied by the manufacturer. Restriction enzymes were used at at least 1 unit per µg of DNA to be digested. Digests were carried out for a minimum of 2 hours at 37°C, except for digests with *Bcl*I which were carried out at 50°C. Manufacturer's guidelines were followed for the most appropriate buffer to use in digests involving more than one enzyme.

If digestions were to be analysed by gel electrophoresis, 0.2 volumes of 6x gel loading buffer were added. If the digestion was to be used in further subcloning steps, the digestion was stopped by removing the restriction enzyme(s) using Promega Wizard Clean Up System spin-columns according to the manufacturer's instructions (or the DNA was purified by fragment isolation as described in section 2.5.10).

2.5.7. Ligation Reactions

T4 DNA ligase was used to ligate DNA fragments with compatible cohesive or blunt-ended termini. The fragments of insert and vector were mixed so that there was an excess of insert, typically a ratio of 3:1 (insert:vector) for cohesive and 10:1 (insert:vector) for blunt-end ligations. 5x ligase buffer containing ATP (supplied with the enzyme) and 1 unit of DNA ligase were added to give a final concentration of 1x buffer in the reaction. The ligation mix was incubated overnight at 15°C. 1 to 10µl of the ligation reaction were used in transformations of competent *E. coli*.

2.5.8. DNA Molecular Weight Markers

DNA molecular weight markers were prepared by digestion of phage λ DNA with *Pst*I to completion. A typical preparative digest was performed in the following reaction:

λ DNA (300µg/ml)	100µl
dH_2O	780µl
10x Restriction Enzyme Buffer	100µl
Restriction Enzyme (10U/µl)	20µl

Digestion was carried out for 7 hours at 37°C. 200µl 6x loading buffer were added, and the markers stored at -20°C. 15µl were loaded onto agarose gels as a size standard.

A λ*Pst*I digest produces DNA fragments of the following sizes (in kb):
14.05, 11.49, 5.07, 4.75, 4.51, 2.84, [2.56, 2.46, 2.44], 2.14, 1.99, 1.70, 1.16, 1.09, 0.81, 0.52, 0.47, 0.45, 0.34.
The fragments in brackets run together on an agarose gel.

2.5.9. Agarose Gel Electrophoresis

Agarose gel electrophoresis was performed in an Appligene or Bio-Rad mini-gel system for mini gels or in a Scotlab gel system for larger gels. Agarose was added to a measured quantity of 1x TAE buffer, usually to a concentration of 0.7% (w/v) which efficiently separated linear DNA between 10-0.8 kb. The concentration of agarose could be varied according to the size of DNA to be separated (Sambrook *et al.*, 1989). The agarose was dissolved by microwaving the mixture. After cooling, ethidium bromide was added to a final concentration of 0.5µg/ml and the agarose poured into the mould with a well comb in place. Once the agarose had set, the gel was placed into the tank and covered with 1x TAE buffer containing 0.5µg/ml ethidium bromide. DNA samples in loading buffer were loaded and electrophoresis performed, usually at 80mV, until the marker dyes had migrated to appropriate distances. The gel was then placed onto a UV illumination apparatus and photographed using a red-filter and a Polaroid camera.

2.5.10. DNA Fragment Isolation

DNA fragments were isolated from agarose gels using the QIAGEN QIAquick Gel Extraction Kit according to the manufacturer's instructions. The procedure makes use of chaotropic agents to solubilise the gel and the DNA is recovered using spin columns.

2.5.11. Genomic DNA Isolation from *S. cerevisiae*

Genomic DNA isolation was based on a method from E. Broomfield (personal communication).

The yeast colony from which genomic DNA was to be isolated was incubated overnight at 30°C in 10ml of YPDA. The cells were pelleted by centrifugation at 3000g for 5 minutes, resuspended in 1ml dH_2O and transferred into a fresh microcentrifuge tube. The tube was then centrifuged for 1 minute, the supernatant discarded and the pellet resuspended in 0.5ml of breaking buffer (2% TritonX-100, 1% SDS, 100mM NaCl, 10mM Tris.HCl pH8.0, 1mM EDTA). 0.2g of acid-washed glass beads and 500µl of phenol:chloroform:isoamyl alcohol (25:25:1) were added and the tube was vortexed at high speed for two times 1 minute to break open the cells and precipitate the protein and cell debris. The tube was centrifuged for 5 minutes and the upper, aqueous layer (which contains DNA and RNA) was removed and extracted once with chloroform. The aqueous layer was transferred to a fresh tube and the nucleic acid was precipitated with 2 volumes of 100% ethanol and 0.1 volume of 3M sodium acetate for 2 hours at room temperature. The tube was centrifuged at high speed (12 000g) for 30 minutes and the pellet was washed in ice-cold 70% ethanol. The DNA/RNA pellet was then air-dried and resuspended in 50-100µl TE containing 1 unit of RNase to digest the RNA.

2.5.12. Polymerase Chain Reaction (PCR)

PCR reactions were performed in a thermal cycler (PHC-3, Techne). Typically reactions contained 80pmoles of each primer, 20nmol of each dNTP, PCR buffer (provided with the enzyme) and 1 unit of *Taq* DNA Polymerase (Gibco-BRL) in a final volume of 100µl in a 0.5ml microcentrifuge tube. The quantity of template and $MgCl_2$ in each reaction and the cycling conditions varied according to what was to be amplified and are therefore described where individual PCR reactions appear in the results chapters. *Taq* polymerase was the last component to be added to the reaction before mixing by brief centrifugation. The reaction mixture was then overlaid with sterile mineral oil (100µl) to prevent evaporation during the heat cycles.

After completion of the PCR, samples were kept at 4°C until analysis by gel electrophoresis. PCR products could then be purified by band fragment isolation as described in section 2.5.10.

2.6. DNA Hybridisation Procedures

2.6.1. Labelling DNA Fragments

DNA fragments were labelled for use as probes in hybridisations using the Boehringer Mannheim DIG DNA Labelling and Detection Kit. A 15µl aliquot of 200ng of DNA was boiled for 10 minutes to denature the DNA and then cooled rapidly on ice-water to prevent re-annealing of the strands. dNTPs, hexanucleotide and Klenow enzyme were added according to the manufacturer's instructions and the sample was incubated overnight at 37°C. 1µl of 0.5M EDTA was added to stop the reaction and the DNA was ethanol precipitated. The DNA was washed in ice-cold 70% ethanol, dried and then resuspended in 100µl TE.

The probe was denatured by boiling and rapid cooling on ice before use in hybridisation reactions.

2.6.2. Southern Blotting

Southern blotting and hybridisation reactions were based on the method of Southern (1975).

DNA for hybridisation was separated on an agarose gel, visualised under UV illumination and photographed. The DNA was depurinated by soaking the gel in 0.25M HCl for 7 minutes with shaking. The gel was then rinsed twice with dH_2O before being soaked in denaturing solution (0.5M NaOH, 1.5M NaCl) for 20 minutes again with shaking. The gel was rinsed and neutralised in 0.5M Tris.HCl, 3.0M NaCl, pH7.0 for two times 15 minutes. A DNA blot transfer system was assembled as described in (Sambrook et al., 1989). The gel was placed, wells uppermost, on a long piece of 3MM paper that was soaked in 20xSSC and positioned over a glass plate with its ends dipped in a reservoir of 20xSSC. A nylon or nitrocellulose membrane cut to the same size as the gel was pre-wetted with dH_2O, put on top of the gel and any air bubbles were removed. The transfer membrane was covered with 3 pieces of 3MM paper soaked in 20xSSC followed by 2 layers of disposable nappies and these were covered with a glass plate with a 1kg weight placed on top. Care was taken that everything placed on top of the filter was cut to the same size as the gel and nothing touched the bottom layer of 3MM paper. After 2-16 hours (usually overnight) the system was disassembled and the membrane rinsed in 2xSSC for 5 minutes. The membrane was air dried for 1 hour before fixing of the DNA by baking for 45 minutes in a vacuum oven at 80°C. The membrane could then be used in hybridisation reactions.

2.6.3. Hybridisation of Labelled Probes to Southern Blots

Hybridisation reactions were carried out using Techne Hybridisation tubes in a Techne Hybridiser HB-1 oven. Southern blot membranes were pre-hybridised at 68°C for 30 minutes in 50ml pre-hybridisation solution consisting of 6xSSC, 5x Denhardt's solution (100x: 2% (w/v) bovine serum albumin, 2% (w/v) Ficoll, 2% (w/v) polyvinylpyrollidone), 0.5% (w/v) SDS and 100µg/ml of 10mg/ml single-stranded salmon sperm DNA (denatured at 95°C for 10 minutes and placed on ice immediately). Denatured, labelled probe was added and the membranes were incubated overnight with rotation at 68°C for hybridisation. To remove non-specifically bound probe the membrane was washed at room temperature in 2x SSC, 0.5% (w/v) SDS for 5 minutes and then in 2x SSC, 0.1% (w/v) SDS for 15 minutes. The final wash was in 0.1x SSC, 0.5% (w/v) SDS at 68°C for 60 minutes. The filters could then be used in the detection procedure described below.

2.6.4. Detection of Hybridising Probes

Anti-digoxigenin antibody conjugated to alkaline phosphatase (Boehringer) was used to detect the labelled probe. All incubations for this procedure were at room temperature. The hybridised membrane was first rinsed in Tris-salt (0.15M NaCl, 1.5mM KCl, 25mM Tris.HCl pH7.4) for 5 minutes and then blocked in 50ml of fresh blocking solution (Tris-salt, 1.5% dried milk powder, 0.2% Tween-20) for 30 minutes. The membrane was transferred into fresh blocking solution with 5ml of anti-digoxigenin antibody and incubated for 4 hours to allow the antibody to bind to the attached probe. The membrane was washed twice in Tris-salt + 0.2% Tween-20 for 5 minutes each time and then in Tris-salt (no Tween-20) for another 5 minutes to remove all the unbound antibody.

Antibody binding was visualised using solutions provided in the DIG DNA Labelling and Detection Kit. The filter was rinsed in alkaline phosphatase buffer (100mM NaCl, 50mM $MgCl_2$, 0.1M Tris pH9.5) and then placed in a clean petri dish. Alkaline phosphatase buffer was added until the liquid just covered the membrane and 15µl XP and 15µl NBT were added. Alkaline phosphatase cleaves the XP resulting in a colour change. Membranes were stored in the dark during signal development (10 minutes - 15 hours depending on the strength of the signal) and care was taken not to agitate the solutions. The colour development was stopped by the addition of 0.5M EDTA and the membranes were rinsed, dried and stored in the dark.

2.7. Yeast Methods

2.7.1. Sporulation of Diploids

Diploids of the cells to be sporulated were patched onto YPDA agar, incubated overnight at 30°C and then replica plated onto sporulation agar. Spore plates were incubated at room temperature for 6 to 8 days, until tetrads had formed as detected by light microscopy. A loopful of the sporulated diploids (about the size of a match head) was resuspended in 100µl 1:10 dilution of β-glucuronidase. The suspension was incubated at room temperature for 5 minutes and 5-10µl were streaked along one side of a YPDA plate. The plate was inverted over the microscope on a specially designed plate holder.

Spores were visualised under a Nikon, Labophot-2 microscope (Nikon, Japan) using a 20x objective lens and 10x eyepieces. The spores were dissected by picking up a tetrad on a needle mounted in a micromanipulator (Narishige Co., Ltd, Tokyo, Japan. Model MO-202). The four spores were separated and plated at 5mm intervals across the plate. The plate was incubated at 30°C for 2-3 days until small colonies appeared. These haploids were picked and tested for various markers.

2.7.2. Microscopy

Vacuoles were visualised under UV microscopy by staining with FM4-64 which binds to the vacuolar membrane (Vida and Emr, 1995).

Yeast cells were grown overnight in YPDA, diluted in YPDA to obtain an absorbance reading of 0.3 OD/ml and then incubated for a further 3 hours at 30°C. A 1ml aliquot of this culture was transferred to a microcentrifuge tube and the cells were pelleted by low speed centrifugation (6000 rpm) for 2 minutes. 1µl of FM4-64 stock (1.6µM in DMSO) was diluted in 100µl pre-warmed YPDA and 50µl were used to gently resuspend the cell pellet. The tube was incubated for 15 minutes at 30°C with agitation to allow the stain to be taken up by the cells. 1.2ml of pre-warmed YPDA were added to dilute the dye at the plasma membrane to aid the visualisation of the internal membranes. The cells were then incubated at 30°C for a further 30 minutes. Meanwhile a microscope slide was coated with 10µl of 2mg/ml concanavilin A and allowed to dry. The cells were pelleted by low speed centrifugation and gently resuspended in 150µl YPDA. 5µl of the stained cells were placed on the coated slide, covered with a coverslip and observed under UV with a rhodamine filter. Oil-immersion was used to observe the cells with a 100x objective lens.

2.7.3. Immunoblotting of Carboxypeptidase Y (CPY)

A vacuolar protein sorting (vps) defect could be measured qualitatively with an immunoblotting method (Roberts *et al.*, 1991). Yeast colonies were grown at 30°C overnight as patches on a Yeast Minimal Medium (YMM) plate with amino acid supplements. Using a sterile velvet the colonies were replica plated onto a fresh YMM plate with amino acid supplements, covered with a nitrocellulose filter which had been pre-soaked in Tris-NaCl buffer (0.1M Tris.HCl pH 7.2, 0.15M NaCl) and grown overnight as above. The filter was carefully removed from the plate and washed 1x 5 minutes in dH_2O and 3x 10 minutes in TTBS (0.15M NaCl, 1.5mM KCl, 25mM Tris.HCl pH8.0, 0.1% Tween-20) containing 1% dried milk powder. 150µl of primary antibody (rabbit polyclonal anti-CPY antibody (Latterich, 1992)) were added to 10ml TTBS with 1% dried milk powder which was then used to cover the filter. The filter was incubated at room temperature for 6 hours with gentle rocking to allow antibody binding to (extracellular) CPY. Unbound antibody was then removed by washing the filter three times with fresh TTBS containing 1% dried milk powder; 10 minutes for each wash. 6µl of the secondary antibody (anti-rabbit IgG alkaline phosphatase conjugate) was added to 10ml of TTBS with 1% dried milk powder which was then used to cover the filter. The filter was incubated for 1.5 hours before being washed as before. A final wash in Tris-NaCl buffer was performed. The presence of bound antibody was detected using alkaline phosphate substrates which undergo a colour change when cleaved enzymatically. The filter was covered in alkaline phosphatase buffer (100mM NaCl, 50mM $MgCl_2$, 0.1M Tris pH9.5) to which 67µl of 50mg/ml NBT (nitro blue tetrazolium) and 33µl of 50µg/ml BCIP (bromo-chloro-indolyl phosphate) were added and mixed thoroughly. The filter was kept stationary and in the dark while the signal developed. The reaction was stopped by washing in dH_2O and EDTA.

2.8. Protein Assays

2.8.1. Determination of Protein Concentration - Lowry Method

The Lowry Method of determining protein concentration (Lowry *et al.*, 1951) used the following buffers:

Buffers: A 2% Na_2CO_3 in 0.1M NaOH

B1 1% $CuSO_4.5H_2O$

B2 2% Na-K-Tartrate

B Buffer B1 (500µl) + Buffer B2 (500µl)

C 49ml Buffer A + 1ml Buffer B

Folin & Ciocalteu's Phenol Reagent diluted 1:1 with dH_2O

An 100µl aliquot of protein diluted with a known volume of dH_2O was added to 1ml of buffer C. The sample was incubated at room temperature for 10 minutes and then 100µl of diluted Folin & Ciocalteu's Phenol Reagent were added. The sample was shaken vigorously (but with care as Folin & Ciocalteu's Phenol Reagent is highly toxic) and then incubated at room temperature for 30 minutes. The absorbance was read at 578nm and could be used to calculate protein concentration by comparison with a standard curve using bovine serum albumin (BSA) as a protein source which was prepared at the same time. Protein samples were tested in duplicate.

2.8.2. Determination of Protein Concentration - Bio-Rad®

The Bio-Rad Protein Assay was used for protein determinations carried out later in the study. The method was according to the manufacturer's instructions and uses a Coomassie Blue dye reagent according to Bradford (1976).

2.8.3. Quantification of β-Galactosidase Activity

β-Galactosidase was assayed in protein extracts according to Sambrook *et al.* (1989). The following buffers were required:

100x Mg solution	0.1M $MgCl_2$
	4.5M β-mercaptoethanol
0.1M NaP_i pH 7.5	41ml 0.2M $Na_2HPO_4.2H_2O$
	9ml 0.2M $NaH_2PO_4.2H_2O$
	50ml dH_2O
1x ONPG	4mg/ml ONPG in 0.1M NaP_i pH7.5.

For each cell extract to be measured, duplicate reactions of 30µl cell extract, 3µl 100x Mg solution, 66µl 1xONPG and 201µl 0.1M NaP_i pH7.5 were mixed and incubated for 30 minutes at 37°C. The reactions were stopped by the addition of 500µl of 1M Na_2CO_3 and the absorbance was read at 420nm.

2.9. DNA Sequencing

2.9.1. DNA Sequencing

Double stranded DNA was prepared using a modified alkaline lysis preparation (see section 2.5.4).

DNA sequencing was always carried out using the departmental sequencing service with an Applied Biosystems 373A DNA Sequencer using double stranded DNA templates. Usually fluorescently labelled universal M13 primers from the Applied Biosystems PRISM™ Ready Reaction Dye Primer Cycle Sequencing Kit were used, according to the manufacturer's instructions. Occasionally custom-synthesised primers (synthesised on an Applied Biosystems 381A DNA Synthesiser) were used in conjunction with the Applied Biosystems Taq DyeDeoxy™ Terminator Cycle Sequencing Kit.

2.9.2. DNA Sequence Analysis

The DNA sequences generated were initially analysed using the Macintosh computer programmes DNA Strider™1.2 and Sequencher. Primary DNA sequence analysis involved aligning DNA fragments, analysing restriction sites, creating graphical maps of the sequenced fragments, and translating all six hypothetical reading frames.

CHAPTER 3

GLYCEROL-3-PHOSPHATE DEHYDROGENASE ACTIVITY

3.1. Introduction

The yeast *Saccharomyces cerevisiae* adapts to increasing external osmolarity, or salt stress, by producing higher levels of glycerol within the cell to act as a buffer (Blomberg and Adler, 1992). The change in osmotic pressure is probably detected by the Sln1p receptor (Maeda *et al.*, 1994). The signal is then transduced via an osmosensing signal transduction pathway, termed the HOG pathway for High Osmolarity Glycerol response (Brewster *et al.*, 1993). This pathway consists of a MAP kinase cascade, the details of which were discussed more fully in Chapter 1. One of the targets of the signalling cascade is the key metabolic enzyme glycerol-3-phosphate dehydrogenase (GPDH). GPDH uses the substrates dihydroxyacetone phosphate (DHAP) and reduced nicotinamide adenine dinucleotide (NADH) to produce glycerol-3-phosphate (G3P) and NAD^+. This reaction is rate-limiting and controls glycerol production by limiting the supply of the substrate G3P. The transcription of GPDH is enhanced during salt stress (Albertyn *et al.*, 1994a) and mutations in the HOG pathway can be identified by either depressed levels of glycerol production in stressed cells or by lack of induction of GPDH.

A collection of salt sensitive strains of *Saccharomyces cerevisiae* was created in the laboratory (Latterich, 1992). To determine if any of these mutants may be defective in the osmosensing signal transduction pathway, intracellular glycerol concentrations were measured in stressed and unstressed cells using the parental strains as a reference. This work was carried out by B. Pöpping and the results are included later in this chapter for discussion. From this screening procedure salt-stressed mutant strains that accumulated significantly lower glycerol concentrations than the parent strains could be selected as potentially being defective in the osmosensing signal transduction pathway. Some strains were found to have enhanced levels of glycerol accumulation and one of these strains was also selected for further investigation. Possible reasons for elevated levels of glycerol could be lack of feedback control or constitutive activation of the pathway.

This chapter describes the development and use of a GPDH assay to complement the glycerol concentration assays performed previously. GPDH activity was measured to confirm the possibility of mutants being defective in the HOG pathway allowing the selection of one or two mutant strains for further investigation. Complementation of

mutants selected in this way could reveal previously unidentified components of the HOG pathway and give insight into the intracellular mechanisms for responding to osmotic stress.

3.2. Measuring Glycerol-3-Phosphate Dehydrogenase Activity

The assay for glycerol-3-phosphate dehydrogenase was based on a combination of previous methods (Albertyn *et al.*, 1992; Blomberg and Adler, 1989; Gancedo *et al.*, 1968). GPDH activity was measured spectrophotometrically as an absorbance change at 340nm caused by the oxidation of NADH in a reaction mixture of 20mM imidazole.HCl pH7.0, 1.5mM dihydroxyacetone phosphate (DHAP) and 0.2mM nicotinamide adenine dinucleotide (NADH) . The activity of GPDH in this reaction mixture was confirmed by testing with commercially available purified rabbit glycerophosphate dehydrogenase. The reaction mixture without NADH was used as a blank and the reaction was started by the addition of the enzyme. A typical trace obtained in an assay containing 1µl pure enzyme is shown in figure 3.1. GPDH activity is described as a change in absorbance per minute ($Amin^{-1}$) as calculated over the linear portion of the trace, in this case 5.04 $Amin^{-1}$.

3.3. Enzyme Extraction

For the strain to be analysed, a loopful of cells was used to inoculate 10ml YPDA and grown with agitation overnight at 30°C. Two flasks of 100ml YPDA were inoculated with 100µl aliquots of this overnight culture and incubated for a further 15-18 hours to late log phase. The contents of one of the flasks were harvested and subjected to salt stress by resuspension in YPDA containing 0.9M NaCl and incubation for 4 hours at 30°C. A salt concentration of 0.9M NaCl was used because this was the concentration used in the glycerol assays which preceded this work and was also the concentration used by Albertyn *et al.* (1992). The salt stress was applied for four hours because application of salt stress for 90 minutes was not found to give distinguishable rates of GPDH activity (results not shown). Both cultures were then harvested by centrifugation at 3000g for 5 minutes, washed twice and resuspended in 1ml of dH_2O. Washes were in dH_2O except for the first wash of the stressed cells which was in 0.4M NaCl to prevent osmotic down shock. The cell suspensions were transferred into 1.5ml microfuge tubes and approximately 0.2g acid-washed glass beads added to each. The suspensions were then vortexed at high speed for 10 minutes to lyse the cells and the tubes were spun briefly in a microcentrifuge at 12000g to pellet the beads and any remaining intact cells. The supernatants were transferred to fresh tubes and then centrifuged for 20 minutes to

Figure 3.1. Original trace showing change of absorbance on addition of glycero-phosphate dehydrogenase

Figure 3.1. is a copy of an original trace showing the rate of change in absorbance at 340nm when 1µl of rabbit glycerophosphate dehydrogenase was added to the reaction mixture (20mM imidazole.HCl pH7.0, 1.5mM DHAP and 0.2mM NADH). The rate of change of absorbance was measured by extrapolation from the initial linear portion of the trace when availability of substrates is not rate limiting giving an enzyme activity of 5.04 $Amin^{-1}$.

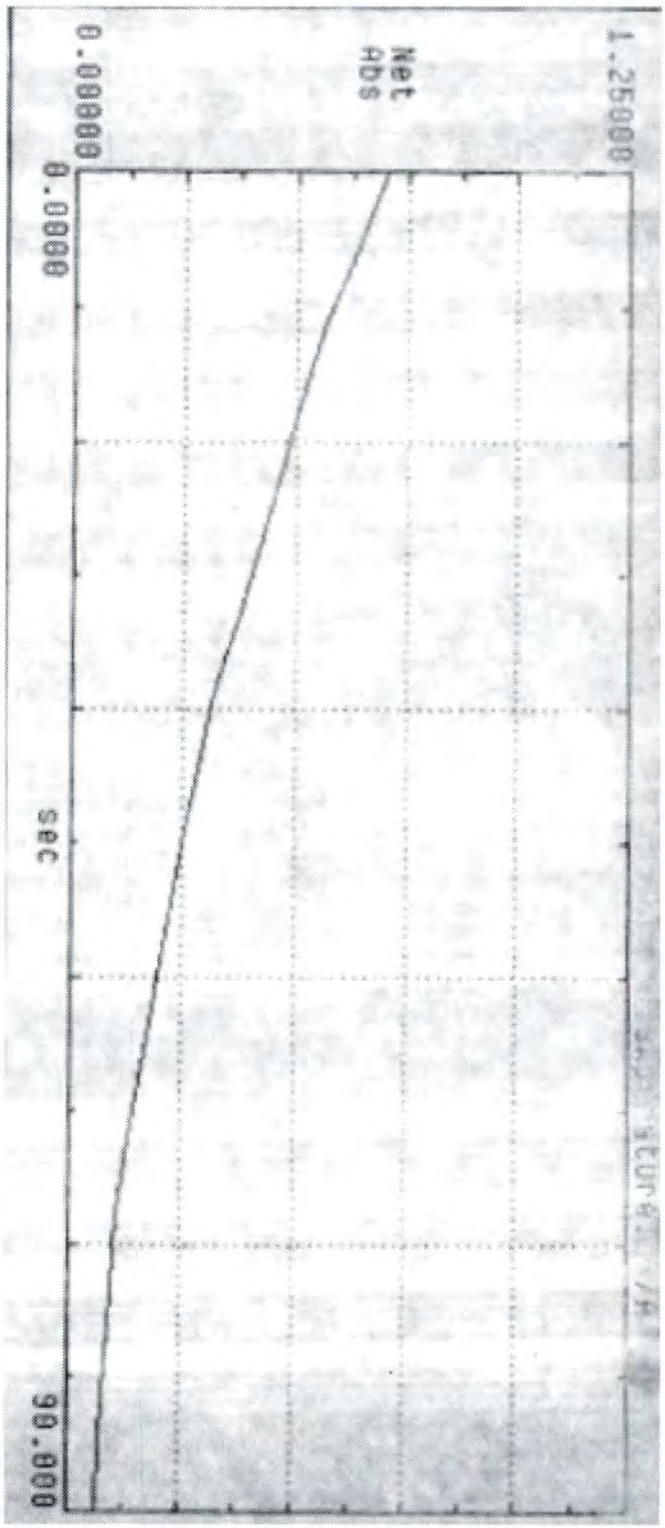
1.25000
Net
Abs
0.00000
0.0000
sec
90.000

remove the cell debris from the protein extract. The supernatant was stored on ice before the measurement of GPDH activity, as described in section 3.2, and determination of protein concentration.

Extracts from the parental strain SEY6211 were prepared in this way and 10µl of each extract were assayed in duplicate. 10µl were found to give a detectable rate of change in absorbance at 340nm with a higher rate in the extract from stressed cells (see example traces in figure 3.2). The protein concentrations in these extracts were 29.1mg/ml in the unstressed cells and 23.2mg/ml in the stressed cells which gave enzyme activities of $0.31 Amin^{-1}mg^{-1}$ and $0.78 Amin^{-1}mg^{-1}$ respectively and thus showed a measurable induction of GPDH activity. It was therefore decided that 10µl would be used as a standard volume of extract in the GPDH assays.

3.4. Testing Suitability of Assay with *Δhog1* and *Δpbs2* Strains

GPDH activity was measured in cells with known mutations in the HOG pathway to demonstrate that assaying GPDH activity is a suitable screen for such defects. GPDH activity was measured in the strains JBY10 (*hog1-Δ1*), JBY40 (*pbs2-Δ1*) (Brewster *et al.*, 1993) and their parent strain (YPH499) grown in the presence or the absence of salt stress. The results from these assays are shown in table 3.1 and depicted graphically in figure 3.3. The values correspond to the average of the duplicate samples tested.

The GPDH activities in the mutant cells were less than those of the parent strain, particularly when salt-stressed, confirming that this method is an appropriate screen for mutations in the HOG pathway from the laboratory collection of salt-sensitive mutants.

3.5. Preliminary Results from Screen of Salt-Sensitive Mutants

The salt-sensitive strains MLY0145, MLY0419, MLY0712, MLY0803, MLY0905, MLY1164, MLY1218, MLY1510 and the parental strain SEY6211 were screened for GPDH activity in stressed and unstressed cultures. Each culture was tested in duplicate and the results are shown as averages in table 3.2 and figure 3.4.

Figure 3.2. GPDH activity in extracts from stressed and unstressed SEY6211.
Figure 3.2. shows original traces obtained when 10µl of protein extract from SEY6211 a) unstressed and b) stressed with 0.9M NaCl were assayed for GPDH activity.

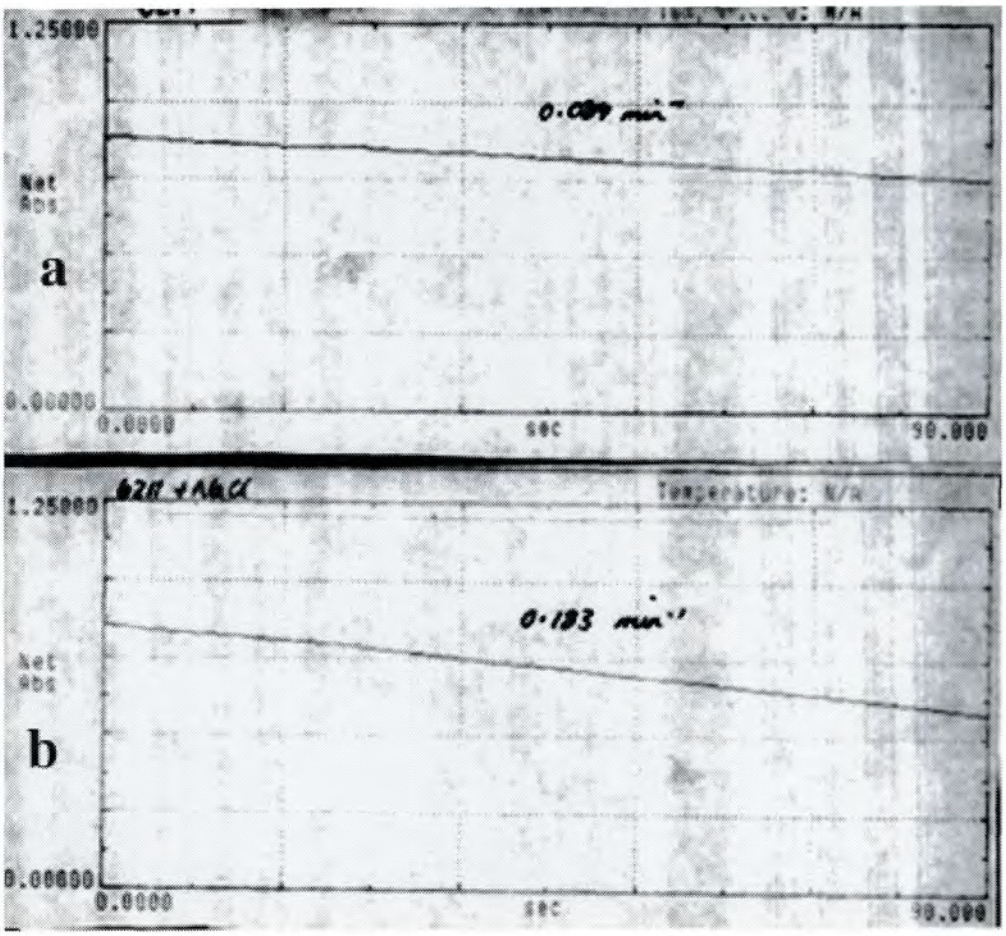
1.25000
0.089 min⁻¹
Net
Abs
a
0.00000
0.0000
sec
90.000
1.25000
Temperature: N/A
0.193 min⁻¹
Net
Abs
b
0.00000
0.0000
sec
90.000

Strains	Protein (mg/ml)		GPDH Activity in 10µl Extract ($Amin^{-1}$)		GPDH Activity ($Amin^{-1}mg^{-1}$)	
	unstressed	stressed	unstressed	stressed	unstressed	stressed
YPH499	24.6	24.7	0.052	0.12	0.211	0.486
JBY10	25.2	19.9	0.036	0.061	0.143	0.307
JBY40	28.4	13.0	0.036	0.028	0.127	0.215

Table 3.1. GPDH activities in extracts from YPH499, JBY10 and JBY40, stressed and unstressed.

Table 3.1. shows the protein concentration, the GPDH activity for 10µl of extract and the GPDH activity per mg of protein from unstressed cultures and from cultures stressed with 0.9M NaCl. Duplicate samples were measured from YPH499, JBY10 (Δ*hog1*) and JBY40 (Δ*pbs2*) and the figures shown represent the averages of the duplicates.

Figure 3.3. Graph of GPDH activities in extracts from YPH499, JBY10 and JBY40, stressed and unstressed.

Figure 3.3. shows a graphical representation of the GPDH activities measured in protein extracts from unstressed and stressed cultures of YPH499, JBY10 (Δ*hog1*) and JBY40 (Δ*pbs2*). The numerical values were shown in table 3.1.

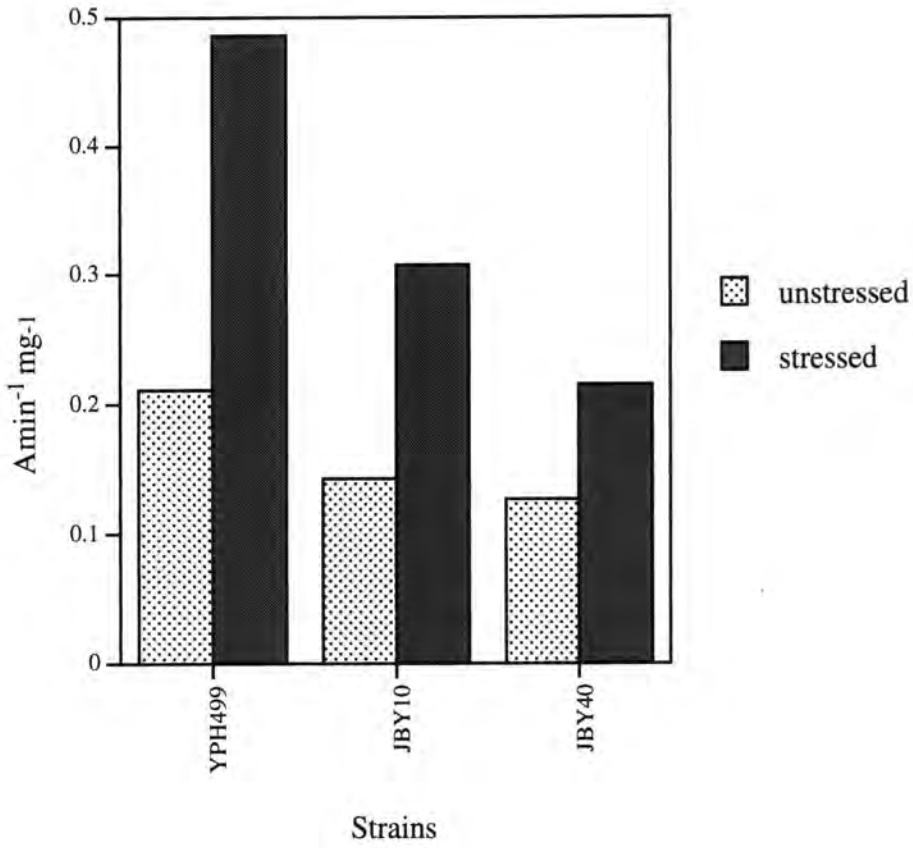

Figure 3.3. GPDH Activities in Protein Extracts from Unstressed and Stressed YPH499, JBY10 and JBY40

Strains	Protein (mg/ml)		GPDH Activity in 10µl Extract ($Amin^{-1}$)		GPDH Activity ($\mu Mmin^{-1}mg^{-1}$)	
	unstressed	stressed	unstressed	stressed	unstressed	stressed
SEY6211	29.6	26.5	0.09±0.5%	0.18±0.5%	0.05	0.11
MLY0145	21	8.4	0.09±3.4%	0.15±13%	0.07	0.28
MLY0402	34.8	22.8	0.08±2.5%	0.12±2.5%	0.04	0.09
MLY0419	24.6	18.8	0.06±5%	0.28±1.2%	0.04	0.24
MLY0712	30.9	11.2	0.08±2.5%	0.09±0.0%	0.04	0.14
MLY0803	15	9	0.04±1%	0.12±2.5%	0.04	0.22
MLY0905	32	15.8	0.11±3%	0.20±1.5%	0.05	0.21
MLY1164	20.8	11	0.05±10%	0.20±15%	0.04	0.29
MLY1218	30.6	16.4	0.07±13%	0.18±2.5%	0.04	0.18
MLY1510	26	25.8	0.09±0.0%	0.24±3.5%	0.05	0.15

Table 3.2. Preliminary screen of salt-sensitive mutants.

Table 3.2. shows the protein concentrations, GPDH activities per 10µl protein extract and GPDH activities per mg of protein in the preliminary screen of the mutants MLY0145, MLY0419, MLY0712, MLY0803, MLY0905, MLY1164, MLY1218, MLY1510 and the parental strain SEY6211. The figures shown represent the averages of duplicate samples tested for both unstressed and stressed cultures.

Figure 3.4. Graph of GPDH activities obtained in the preliminary screen of salt sensitive mutants.

Figure 3.4. shows the GPDH activities in unstressed and stressed cultures from the preliminary screen of MLY0145, MLY0419, MLY0712, MLY0803, MLY0905, MLY1164, MLY1218, MLY1510 (results from table 3.2.) graphically with SEY6211 for comparison.

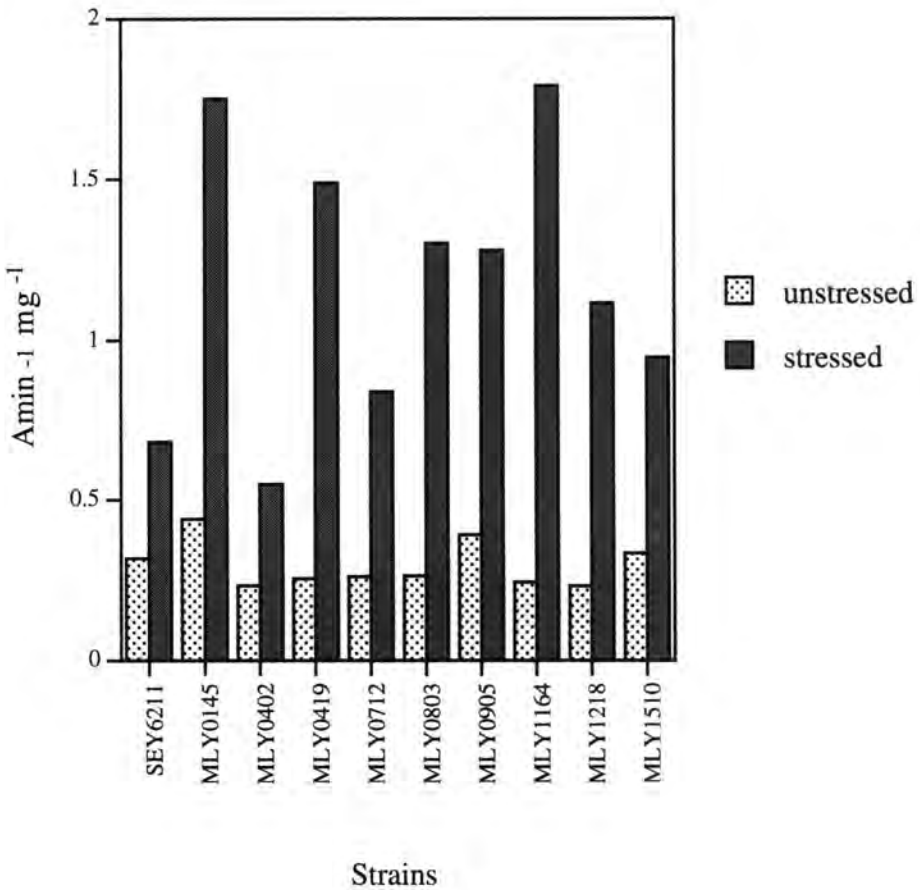

Figure 3.4. GPDH Activites in the Preliminary Screen of Salt-Sensitive Mutants

Table 3.2 also shows the amount of protein added in each 10µl. The protein concentrations of the extracts vary considerably from strain to strain, especially in the salt-stressed samples where the growth rate of the cells can be impaired. For example, the protein concentrations of the extracts from the salt-stressed cultures of MLY0145 and MLY0803 are 8.4mg/ml and 9.0mg/ml respectively which compares to an average of 26.0mg/ml for the reference strain SEY6210. MLY0145 and MLY0803 have relatively low rates of change in absorbance when described per 10µl but when corrected for protein concentration the rates are much higher. Because some of the absorbance changes are very small, errors could come into the calculations because a genuinely low rate could seem larger if the protein concentration was also low. The method was therefore modified slightly to prevent this type of error from entering into the calculations. Instead of adding a fixed volume of protein extract to the GPDH assay, protein concentration was measured beforehand so that a fixed quantity of protein, 200µg, could be added into each assay. The final centrifugation of the protein extracts was also modified to a centrifugation at 4°C for 30 minutes (previously at room temperature for 20 min) in order to maximise the removal of cell debris which may effect absorbance readings in the protein concentration assay.

3.6. Complete Screen of High and Low Glycerol Mutants

The following strains were tested for abnormal induction of GPDH: MLY0108, MLY0145, MLY0402, MLY0419, MLY0712, MLY0803, MLY0905, MLY1005, MLY1143, MLY1164, MLY1176, MLY1218 and MLY1510. SEY6210 and SEY6211 were also tested for reference. Each strain was tested on two separate days with each culture tested in duplicate. The data from this screen are shown in table 3.3. and figure 3.5 and are discussed in section 3.8.

3.7. Investigation of the Effect of pH on GPDH Activity

In *Debaryomyces hansenii*, the optimum pH for GPDH activity is between pH7.9-8.2 (Nilsson and Adler, 1990). In *Saccharomyces cerevisiae* the optimum pH was found to be pH7.6 with activity decreasing rapidly below pH 7.0 and above pH8.0 (Albertyn *et al.*, 1992). In this study, GPDH activity was measured at pH7.0, which was consistent with the methods of Gancedo *et al.* (1968) and Blomberg and Adler (1989). A small set of assays were therefore conducted to determine whether pH would have a significant effect on the results from this screen. The strains SEY6211 and MLY0419 were tested as before but using imidazole buffer at different pHs. GPDH activity was measured in triplicate at pH7.0, pH7.5 and pH8.0.

GPDH Activity ($\mu Mmin^{-1}mg^{-1}$)						
Strains	Unstressed			Stressed		
	Culture 1	Culture 2	Average	Culture 1	Culture 2	Average
SEY6210	0.04±12%	0.04±0.0%	0.04	0.11±4%	0.11±4%	0.11
SEY6211	0.07±11%	0.09±15%	0.08	0.14±0.0%	0.10±5%	0.12
MLY0108	0.04±0.0%	0.03±2.5%	0.04	0.08±3.5%	0.18±0.2%	0.13
MLY0145	0.07±9%	0.06±8%	0.06	0.22±0.0%	0.22±0.5%	0.22
MLY0402	0.03±8%	0.02±9%	0.03	0.08±9%	0.05±4%	0.06
MLY0419	0.08±3%	0.07±3.5%	0.08	0.24±1.0%	0.25±2.5%	0.24
MLY0712	0.05±0.0%	0.05±9%	0.05	0.14±7%	0.11±1%	0.12
MLY0803	0.07±13%	0.04±8%	0.06	0.23±0.5%	0.21±3.5%	0.22
MLY0905	0.07±4%	0.05±12%	0.06	0.13±3%	0.13±3%	0.13
MLY1005	0.03±5%	0.02±2%	0.03	0.13±6%	0.13±1.5%	0.13
MLY1143	0.02±4%	0.03±14%	0.02	0.07±0.0%	0.06±1.5%	0.06
MLY1164	0.03±5%	0.02±4%	0.02	0.12±5%	0.13±6%	0.12
MLY1176	0.03±7%	0.02±1.5%	0.03	0.11±6%	0.08±1.5%	0.10
MLY1218	0.04±1.0%	0.05±7%	0.04	0.15±3.5%	0.14±1.5%	0.15
MLY1510	0.07±5%	0.05±13%	0.06	0.21±1.5%	0.16±5%	0.19

Table 3.3. GPDH activities in the complete screen of salt-sensitive mutants.
Table 3.3. shows the results from the complete screen of unstressed and stressed MLY0108, MLY0145, MLY0402, MLY0419, MLY0712, MLY0803, MLY0905, MLY1005, MLY1143, MLY1164, MLY1176, MLY1218, MLY1510, SEY6210 and SEY6211. Each strain was tested in two separate cultures and the first two columns of each section show the average GPDH activities from duplicates measured from the extract of each culture. The third column of the section shows the overall average of GPDH activity measured for each strain with or without salt stress.

Figure 3.5. Graph of GPDH activities in the complete screen of salt-sensitive mutants.

Figure 3.5. shows the results from the complete screen of unstressed and stressed MLY0108, MLY0145, MLY0402, MLY0419, MLY0712, MLY0803, MLY0905, MLY1005, MLY1143, MLY1164, MLY1176, MLY1218, MLY1510, SEY6210 and SEY6211. The graph represents the overall average GPDH activity from duplicate samples of duplicate cultures, the numerical values of which were shown in table 3.3.

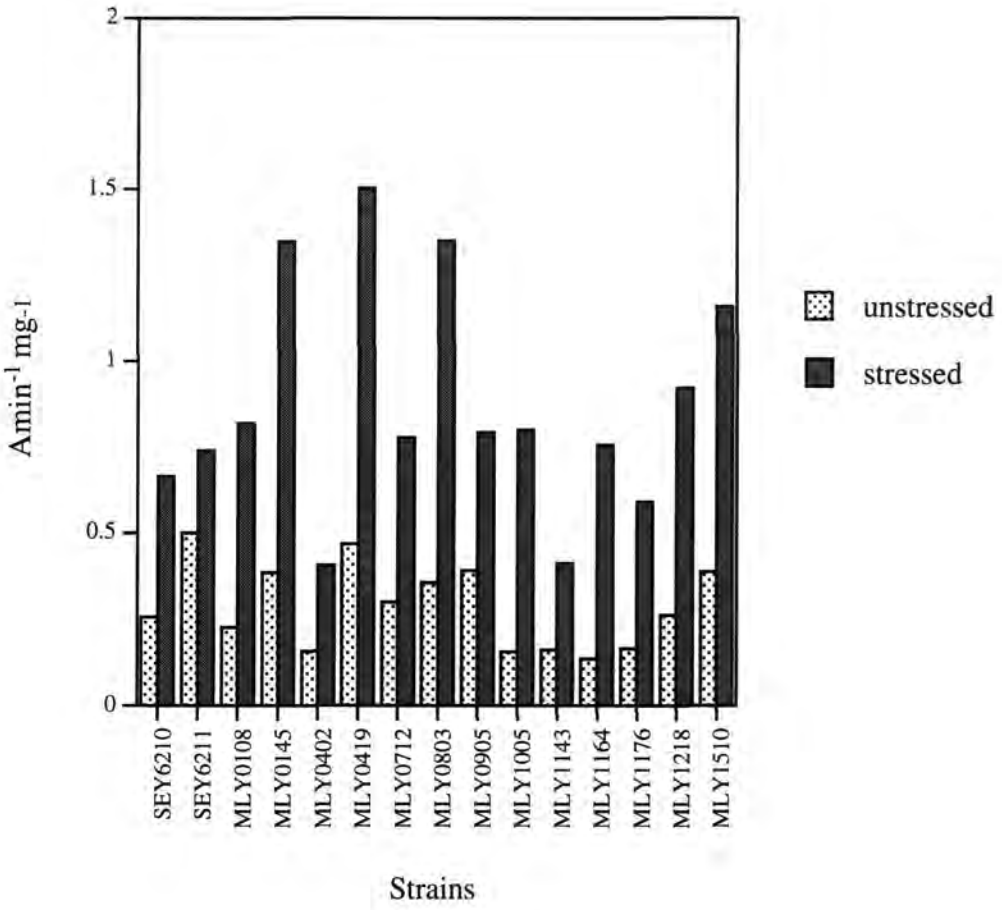

Figure 3.5. GPDH Activities in the Complete Screen of Salt-Sensitive Strains

The activity of GPDH was found to be higher at pH 8.0 but the pattern of results did not seem to alter significantly. Figure 3.6 shows graphically the level of GPDH activity at each pH. It was therefore concluded that although the enzyme activity would have been higher had it been measured in a buffer of pH8.0, the pattern of results would probably have been the same.

3.8. Discussion

The glycerol-3-phosphate dehydrogenase assays described in this chapter were initially conducted to confirm the findings of the glycerol concentration assays performed previously in the laboratory (B. Pöpping, unpublished data). Of the forty salt-sensitive mutants tested for glycerol concentration, eleven were found to accumulate lower glycerol levels than their parental strains in response to salt, three of which (MLY0108, MLY0419 and MLY1176) showed extremely depressed levels. The *HOG1* and *PBS2* genes, key components of the osmosensing signal transduction pathway, were isolated according to their ability to complement mutants that were unable to accumulate glycerol in response to salt stress (Brewster *et al.*, 1993). It was therefore proposed that the cells which were unable to efficiently accumulate glycerol could be defective in the HOG pathway. The GPDH assays were performed on these 'low glycerol' mutant cells to show the relationship between glycerol accumulation and induced enzyme activity. A small number of salt-sensitive mutants showed elevated levels of glycerol. One of these (MLY0402) was selected for the measurement of GPDH activity along with a mutant that showed 'wild-type' glycerol accumulation (MLY0712), giving a total of thirteen mutant strains and two parent strains. Figure 3.7 shows a comparison of the glycerol concentration assays and the GPDH assays for salt-stressed strains.

The results were not as originally expected because it became obvious that low glycerol concentration was not directly linked to low enzyme activity. Only one of the salt-sensitive mutants emerged as a possible candidate for defects in the HOG pathway, namely MLY1143. This strain has both low glycerol concentration and low GPDH activity in the presence of salt stress. Other strains with low glycerol concentrations appeared to fall into two categories. They either had GPDH activities which were the equivalent of the parent strain (e.g. MLY1164) or they in fact had elevated GPDH activity (e.g. MLY0419).

Cells which do not accumulate glycerol effectively in response to salt stress could be either suffering from metabolic defects; from structural defects; or from some other breakdown in the control of glycerol accumulation.

Figure 3.6. Comparison of GPDH activities assayed at different pH.

Figure 3.6. shows the effect of pH in the reaction mixture of the GPDH assay. The graph shows the averages of triplicate samples taken from duplicate cultures of SEY6211 and MLY0419 measured at pH7.0, 7.5 and 8.0.

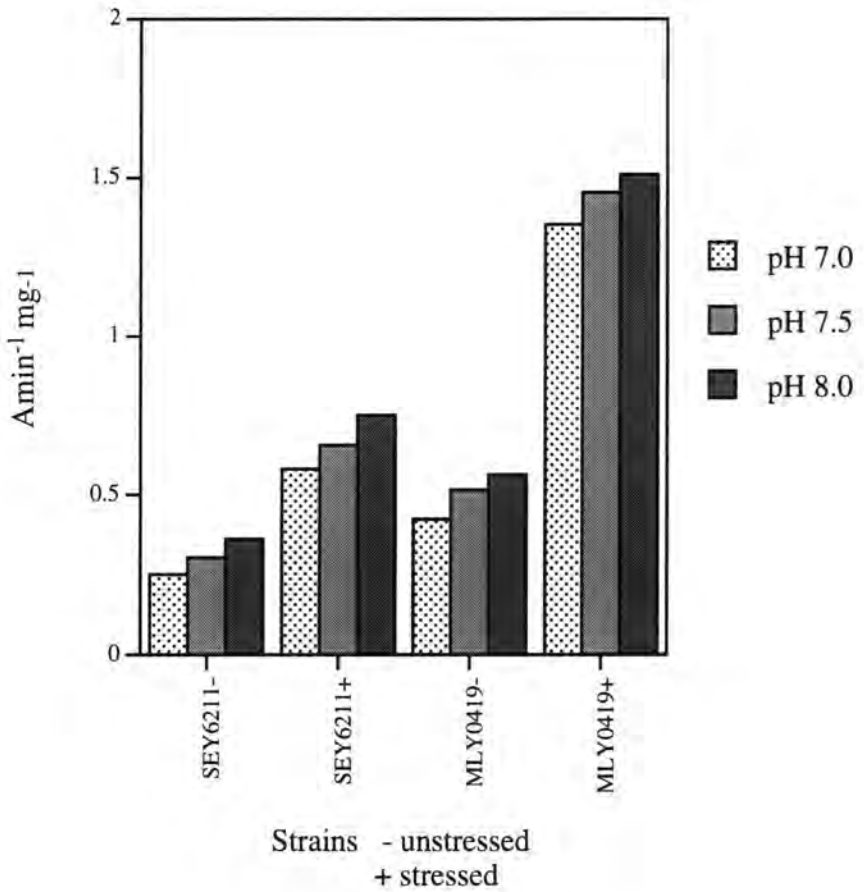

Figure 3.6. Comparison of GPDH Activities Assayed at Different pH

Figure 3.7. Comparison of glycerol concentration and GPDH activity assays. Figure 3.7. shows a comparison of intracellular glycerol concentration with GPDH activity in salt-stressed cultures of the laboratory salt-sensitive strains and their parent strains.

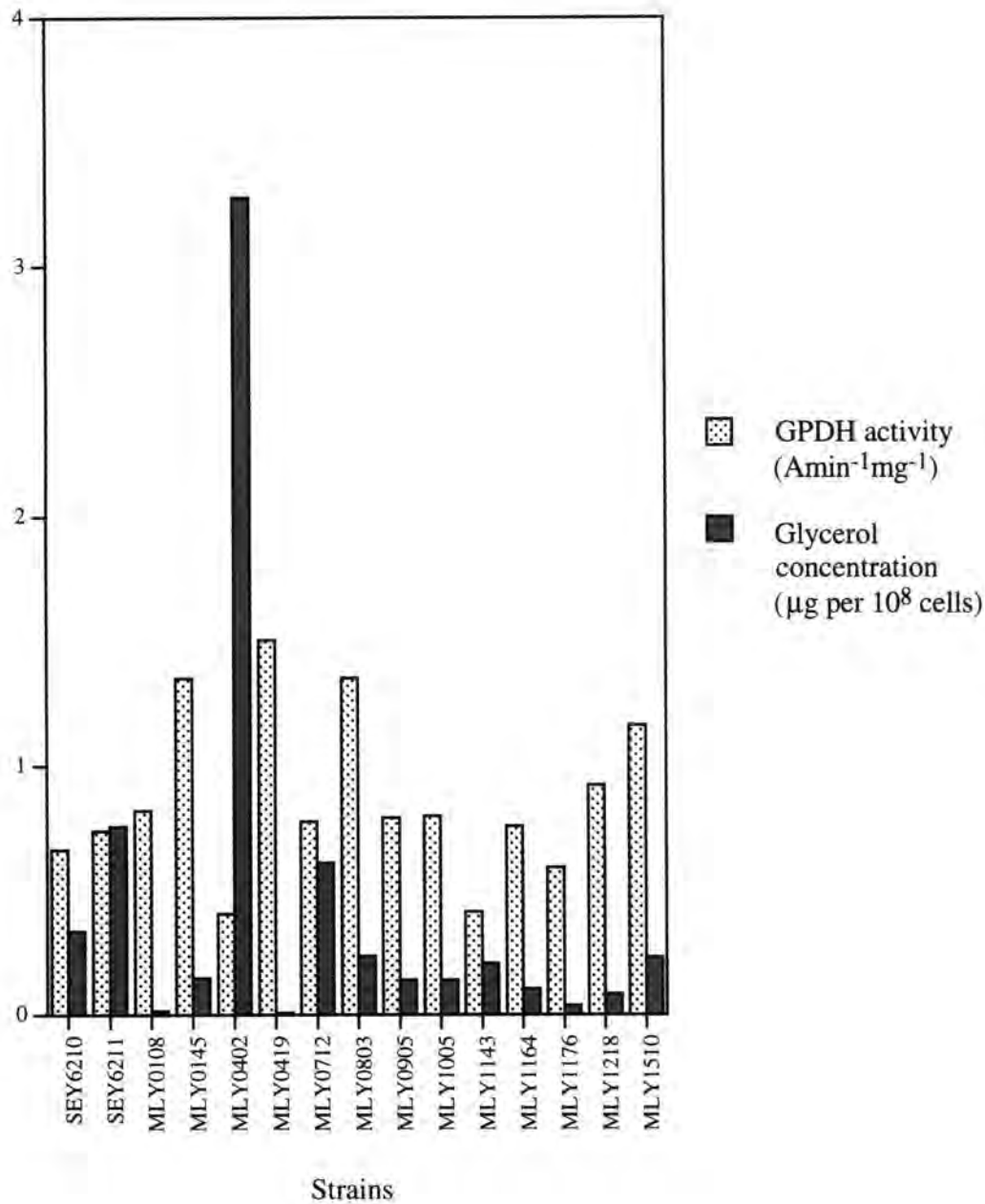

Figure 3.7. Comparison of glycerol concentration and GPDH activity assays

Production of glycerol-3-phosphate by GPDH requires DHAP and NADH. A metabolic defect which restricted the availability of these reactants would cause a relatively low internal glycerol concentration. DHAP is produced via glycolysis and in salt-stressed cells the activity of the glycolytic enzyme phosphofructokinase (PFK) is approximately doubled (Edgley and Brown, 1983). The availability of NADH is partly allowed by increasing the rate of acetate production from acetaldehyde which re-oxidises NAD^+ (Blomberg and Adler, 1989). A metabolic defect which restricts the availability of DHAP and NADH could be present in almost any of the mutants tested, except probably MLY0402 and MLY0712, but it is only a likely scenario in some of the cases. In cells such as MLY0419 where there is an extremely low glycerol concentration despite high enzyme activity, the metabolic defect to cause such an effect would have to be severe and would probably result in impaired growth under other conditions. It seems more likely that mutants suffering from restricted substrate availability would have a relatively low glycerol concentration but not extremely low as in the case of MLY0419 and would have a GPDH activity that is the equivalent to the parent strain. Mutants that fall into this category are: MLY0905, MLY1005, MLY1164, MLY1218 and MLY1510.

Some of the salt-sensitive strains are defective in vacuolar function and morphology (Latterich, 1992). In these cells there can be an abnormal distribution of proteins and other cell components. It has been reported that K^+ has an inhibitory effect on GPDH activity (Gancedo *et al.*, 1968; Meikle *et al.*, 1991) but that this is not normally of physiological significance because the majority of intracellular K^+ is located in the vacuole. An untested hypothesis would be that a defect in vacuolar morphology could lead to relatively high cytoplasmic concentrations of K^+ and in turn lead to GPDH inhibition. Of the salt sensitive mutants that have low glycerol concentrations but 'normal' or relatively high GPDH activities, MLY0108, MLY0419, MLY0905 and MLY1218 have unusual vacuolar morphology - fragmented, class B vacuoles. The ion distribution in these cells is not known and it is feasible that the GPDH activity could suffer from potassium inhibition. It is unlikely that any of these strains are directly defective in the HOG pathway.

Another defect that could occur to prevent glycerol accumulation in response to salt stress even in the presence of GPDH would be if glycerol was being lost to the extracellular medium at an unusually high rate. It has been reported that between 15-50% of glycerol is retained in the cell during salt stress (Andre *et al.*, 1991; Blomberg and Adler, 1989) and there is some evidence that glycerol uptake may occur (Albertyn *et al.*, 1994). Free diffusion of glycerol across the membrane can occur but a glycerol

channel has recently been discovered (Luyten *et al.*, 1995). This channel is encoded by the gene *FPS1* and contributes to the rapid loss of glycerol from the cell after salt stress has been relieved.

In Δ*fps1* mutants, salt-stressed cells accumulate the same amount of glycerol as 'wild-type' in response to salt stress but the loss of glycerol after the stress is removed is much slower. This suggests that the channel is inactive in stress conditions. J.M. Thevelein (Catholic University, Leuven; personal communication) has observed that Fps1p is rapidly ("instantaneously") switched off upon osmotic stress implying regulation of Fps1p activity by stress rather than inactivation or degradation of the protein or down-regulation of gene expression. Therefore it is possible that if regulation of Fps1p was defective, the channel could lose the ability to close in conditions of stress and glycerol could be lost to the medium. Strains with a defective glycerol channel would probably accumulate lower than 'wild-type' concentrations of glycerol in response to salt-stress but not severely depressed levels and would probably have equivalent to 'wild-type' levels of GPDH activity. Mutant strains that fall into this type of pattern (and have class A vacuolar morphology) are MLY1005, MLY1164 and MLY1176.

If there is a glycerol uptake mechanism, this could also be important in the maintenance of intracellular glycerol levels. A strain which has a defective uptake mechanism would be expected to be less efficient in the accumulation of glycerol in conditions of salt-stress. However, such a suggestion at this stage is purely speculative.

There is one other factor affecting the data that cannot be excluded and that is in the experimental design itself. In the measurement of intracellular glycerol, concentrations are expressed as μg glycerol per 10^8 cells. However, as cells are subjected to salt-stress there is an immediate cell shrinkage followed by a recovery period where the original cell volume is restored (Albertyn *et al.*, 1994a). It is possible that some of the salt-sensitive strains are unable to recover their original cell volume or may have unusually large cells and these discrepancies could lead to a natural variation in glycerol concentrations. The intracellular glycerol concentration per ml of cytosol could be the same for two strains but if the cell volumes are different, glycerol concentration per cell number will also be different. Therefore some of the cells with low or high intracellular glycerol concentrations may be behaving in the same way as the parent strain in terms of glycerol production but have an abnormal cell size or morphology. The GPDH activity screen has helped to determine which strains may fall into this category by showing GPDH activities within the same order. Strains with apparently 'normal' GPDH activity are MLY0905, MLY1005, MLY1164, MLY1176 and MLY1218.

The other interesting phenomenon encountered in this study is the enhanced GPDH activity observed in some cells that have very low glycerol concentrations. This is particularly noticeable in MLY0145, MLY0419 and MLY0803. MLY0419, which is the most extreme example, is a particularly interesting case. As mentioned above, this strain has fragmented vacuoles and a possible reason for its low GPDH activity could be potassium inhibition of the enzyme if K^+ cannot be sequestered in the vacuole as normal. However this does not provide any hypothesis for a high enzyme activity measured *in vitro*. Perhaps GPDH is normally turned over in cells subjected to salt stress but in these cases degradation is inhibited.

Another interesting strain is MLY0402. It was surprising to find that the high glycerol concentration for this strain was not matched by a correspondingly high GPDH activity and indeed the GPDH activity was relatively low. Although the cells for this strain may be abnormally large and thus contributing to glycerol concentration by the volume effect mentioned above the concentration is remarkably high. This would imply that this strain is particularly efficient at retaining intracellular glycerol. Perhaps this strain has an unusually active glycerol uptake mechanism or perhaps the cell membrane is less permeable to the leakage of glycerol out of the cell than would normally be the case. It is also possible that GPDH is down-regulated by the cell in response to the high glycerol content resulting in the lower enzyme activity measured.

The use of GPDH activity measurement as a screen for defects in the HOG pathway has raised more questions than it has answered, but it has probably not been unsuccessful. The strain MLY1143 can be picked for further investigation on the basis that it has low glycerol concentration and low GPDH activity during salt-stress. For the other low glycerol strains tested, the salt-sensitive phenotype could be a pleiotropic effect of a mutation in another cell process which interferes with glycerol accumulation.

CHAPTER 4

PROMOTER RESPONSE TO SALT STRESS

4.1. Introduction

A reporter gene construct was designed to further investigate the induction of glycerol-3-phosphate dehydrogenase (GPDH) in response to salt stress in the laboratory collection of salt-sensitive mutants described in chapter 3 (and Latterich, 1992). *GPD1* encodes the gene for GPDH (Albertyn *et al.*, 1994) and the construct was designed to link the promoter region of this gene to *lacZ* which encodes β-galactosidase. Increased promoter activity will result in increased transcription of β-galactosidase which can be measured spectrophotometrically using substrates which react to form coloured products. A selectable marker and the 3′ end of *GPD1* were also included to allow homology for integration of the construct into the yeast genome and selection thereof. Integration of the construct creates a Δ*gpd1* mutation and is also of interest for the phenotypic effects of combining the *ssv* mutations with *gpd1* disruption.

The functional analysis plasmids pFA6a and pFA6a-lacZMT-kanMX3 (Wach *et al.*, 1994), see figure 4.1, were selected for creation of the disruption construct because they were designed for yeast gene disruptions and promoter activity analyses of this type. They allow the cloning of a promoter in frame with the *lacZ* gene and selection of disruptants with *kanMX3*, which confers kanamycin resistance to bacteria and G418 (geneticin) resistance to many eukaryotes including *S. cerevisiae*. Figure 4.2 is a diagrammatic representation of the cloning strategy for creating the *gpd1*Δ::*lacZMT-kanMX3* construct.

This chapter describes the cloning of the promoter and 3′ regions of *GPD1*, the creation of the *gpd1*Δ::*lacZMT-kanMX3* disruption cassette and attempts to overcome problems encountered with selection of the disruption cassette.

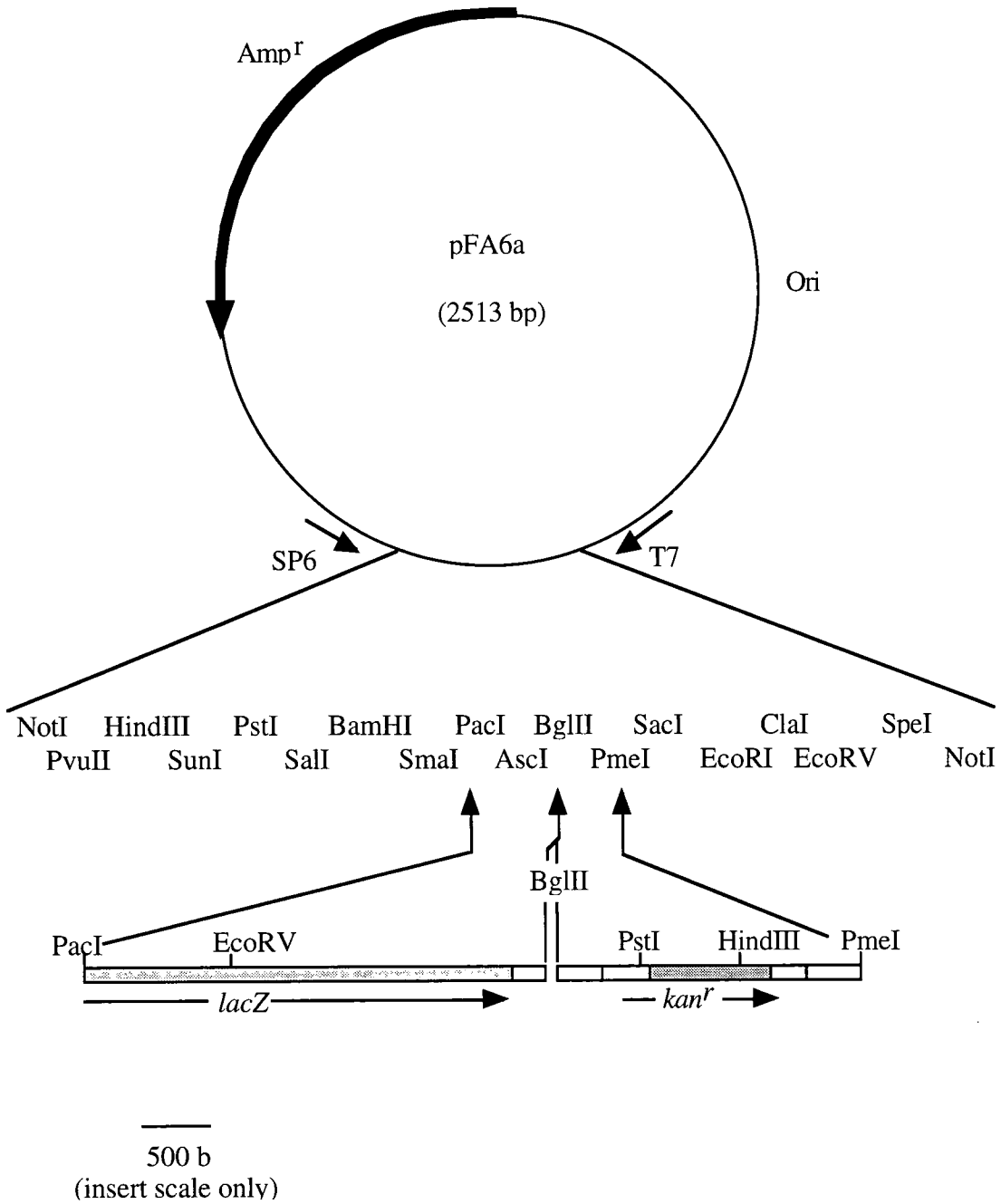

Figure 4.1. Restriction Map of the Plasmid pFA6a with lacZMT-kanMX3 Insert.

Figure 4.2. Cloning strategy for creating *gpd1Δ*::lacZMT-kanMX3.

Figure 4.2 shows the stages for cloning lacZMT-kanMX3 into *GPD1*.

1 *gpd1* 5′ (a) and *gpd1* 3′ (b) are amplified from *S. cerevisiae* genomic DNA by PCR.
2 *gpd1* 5′ PCR product is sub-cloned into pUC19 and then isolated by restriction digestion with *Pst*I (P) and *BamH*I (B). The isolated *gpd1* 5′ is ligated into pFA6a which has also been restricted with *Pst*I and *BamH*I.
3 *gpd1* 3′ PCR product is sub-cloned into pUC19 and then isolated by restriction digest with *EcoR*I (RI) and *EcoR*V (RV). The plasmid pFA6a-*gpd1* 5′ is then restricted with *EcoR*I and *EcoR*V into which the isolated *gpd1* 3′ is ligated.
4 *lacZMT-kanMX3* is isolated from pFA6a-lacZMT-kanMX3 by restriction with *Sma*I and *EcoR*I and then inserted into the above plasmid, pFA6a-*gpd1*5′-*gpd1*3′, which is also restricted with *Sma*I and *EcoR*I.
5 The resultant plasmid now contains the *gpd1*Δ::*lacZMT-kanMX3* disruption cassette which is excised by restriction with *NotI*.
6 The disruption cassette is transformed into competent yeast where it can integrate into the chromosome by homologous recombination.

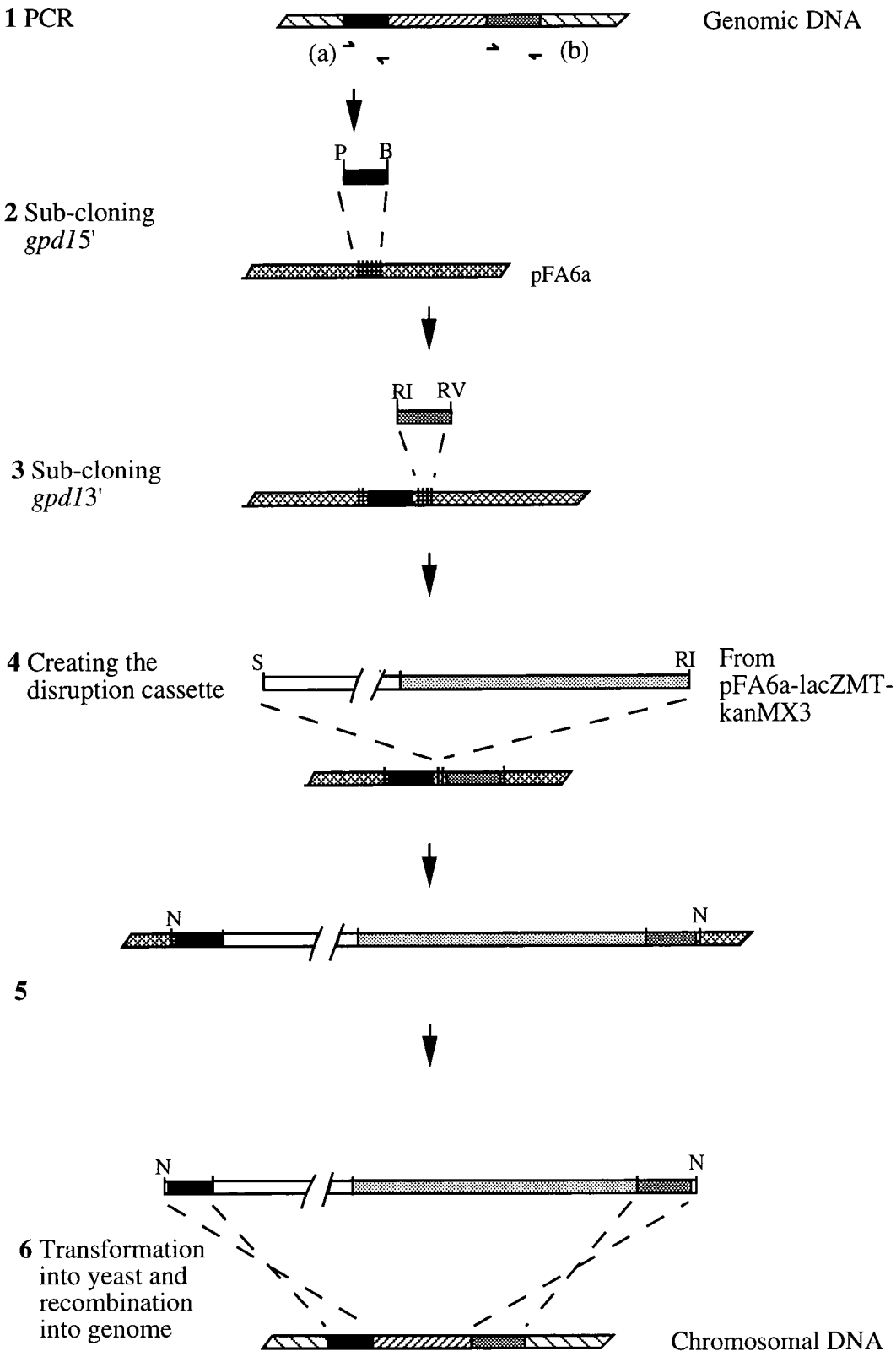
1 PCR
Genomic DNA
(a)
(b)
P
B
2 Sub-cloning
gpd15'
pFA6a
RI
RV
3 Sub-cloning
gpd13'
4 Creating the
disruption cassette
S
RI
From
pFA6a-lacZMT-
kanMX3
N
N
5
N
N
6 Transformation
into yeast and
recombination
into genome
Chromosomal DNA
GPD1 5'
GPD1 3'
pFA6a
lacZMT
kanMX3
genomic GPD1
genomic DNA (flanking GPD1)
500 bases

4.2. Cloning the 5′ Promoter Region of *GPD1*

4.2.1. Primer design

Primers were designed to amplify the 5′ promoter region of *GPD1* from *S. cerevisiae* genomic DNA using the polymerase chain reaction (PCR). Figure 4.3 shows the relative positions of the primers to the open reading frame map which shows start and stop sites for *GPD1* and flanking sequences. Restriction sites were incorporated into the sequence of the PCR primers to ease subsequent cloning steps for correct insertion into pFA6a. The sequence for the 5′ primer was as follows:

5′> CTA CTG CTG CAG CCC TCC TGC GC
*Pst*I site

The sequence for the 3′ primer included the complement of the start codon of *GPD1* and was as follows:

5′> CCC CGG ATC CTA TCA GCA GCA GCA GAC ATC
*BamH*I site Start codon

4.2.2. PCR conditions

Four PCR reactions were performed containing the above primers. The size of DNA fragment expected with these primers was 360 base pairs. Tubes 1 and 3 contained 8µl and tubes 2 and 4 contained 16µl of 25mM $MgCl_2$. Reactions 1 and 2 used genomic DNA as a template (approximately 1µg per reaction) whereas reactions 3 and 4 used a single yeast colony each as template. Thirty-five PCR cycles of 95°C for 1.5min, 50°C for 1.5min and 72°C for 1min were performed.

Figure 4.4 shows 10µl of each reaction mixture electrophoresed next to λ*Pst*1 size markers on a 2% agarose gel. A major band of approximately 360 base pairs, or slightly smaller, can be observed in each lane with minor larger bands in PCR reaction 2. The major bands were excised from lanes 1 and 2 of the gel and the DNA recovered as described in chapter 2.

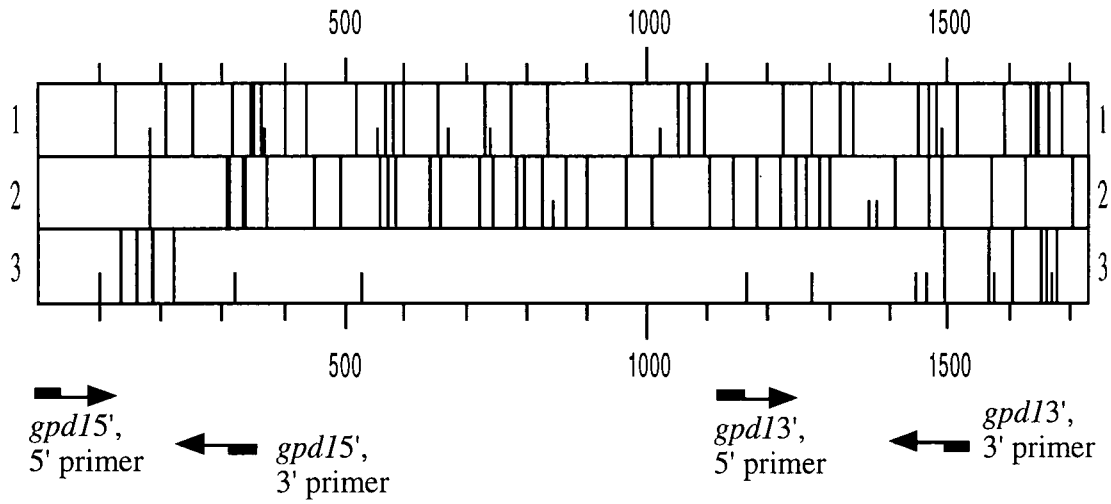

Figure 4.3. The Open Reading Frame Map of *GPD1* and Flanking Sequences

Figure 4.3 shows the reading frame map with start (half line) and stop (full line) codons for *GPD1* and flanking sequences as generated by the sequencing programme DNA Strider. The PCR primers used to generate 5' and 3' fragments are shown as bold lines and the arrows indicate the direction of synthesis.

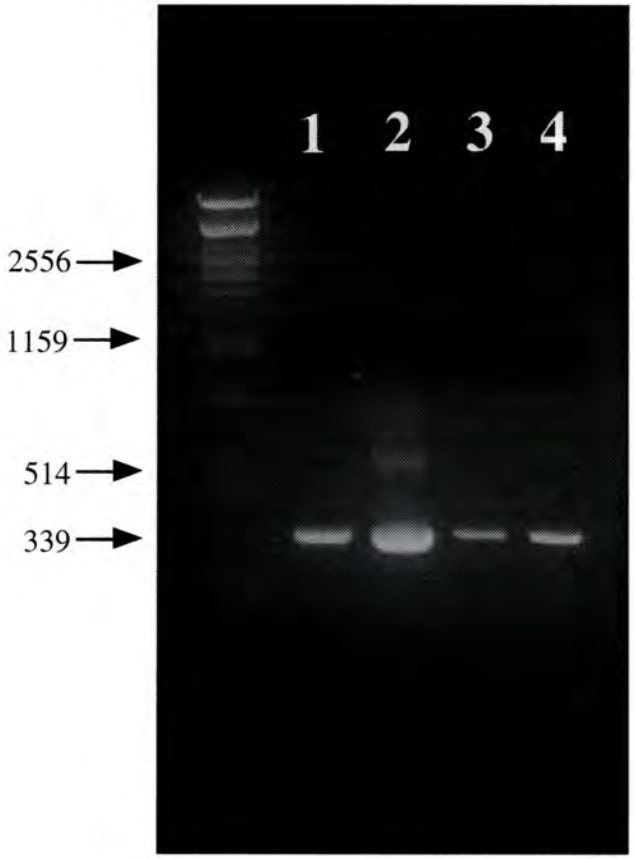

Figure 4.4. PCR Reactions of *gpd1* 5'.

Figure 4.4 shows a photograph of gel electrophoresis of λPstI size markers run alongside PCR reactions. The lanes contained DNA as follows:

Lane	PCR Template	[$MgCl_2$] in PCR reaction
1	genomic DNA	2mM
2	genomic DNA	4mM
3	yeast colony	2mM
4	yeast colony	4mM

4.2.3. Sub-cloning into pUC19

The fragment-isolated PCR product was cloned into pUC19 by blunt-end ligation. The PCR product ends were filled in using Klenow enzyme and dNTPs in ligation buffer by incubating for 30min at room temperature and then heat-inactivating the enzyme at 70°C. For the ligation, *Hinc*II- restricted pUC19 was added so that the vector:insert ratio was 1:8. The DNA was ligated as described in chapter 2 and then transformed into competent DH5α. Transformants were selected on L-Amp plates pre-spread with 40µl of X-Gal (20mg/ml in DMF). If pUC19 re-ligates to itself the transformants appear blue because of the colour change caused by β-galactosidase activity on X-Gal. Ligation of an insert into the multiple cloning site of pUC19 disrupts β-galactosidase activity, transformants do not cause a colour change on X-Gal and appear as white colonies. White colonies were picked and DNA prepared using the method described in section 2.5.3. The DNA was analysed by restriction digests and gel electrophoresis to confirm the correct size of the plasmid containing insert. High purity DNA was then prepared and automatically sequenced as described in section 2.9.1 using M13 forward and reverse primers (from the Applied Biosystems PRISM™ Ready Reaction Dye Primer Cycle Sequencing Kit) to confirm the identity and presence of the insert. The plasmid with the correct *GPD1* 5′ insert in pUC19 was termed pEH10.

4.2.4. Cloning the 5′ promoter region of *GPD1* into pFA6a

The 5′ region of *GPD1* (as amplified by PCR) was excised from pEH10 using the restriction enzymes *Pst*I and *BamH*I and purified by fragment isolation. pFA6a was also digested with *Pst*I and *BamH*I and the small fragment released was removed using a Promega Wizard Clean-up kit according to the manufacturer's instructions. The *GPD1* 5′ fragment was ligated into restricted pFA6a in a reaction which used an excess of insert to vector and then transformed into DH5α. Blue/white colour selection was not possible with this plasmid and therefore several transformants were picked for rapid screening as described in section 2.5.5. In the first 24 colonies screened one appeared to run slightly slower on an agarose gel (i.e. was slightly larger) and this was selected as possibly having the correct insert. DNA was prepared according to section 2.5.3. and analysed with restriction digests as shown in figure 4.5. The plasmid was linearised with either *BamH*I or *Pst*I and a fragment of approximately 0.34kb was released in a double digest of these two enzymes. It was therefore concluded that this plasmid contained the *GPD1* 5′ insert. Correct orientation of the insert in pFA6a was subsequently confirmed by DNA sequencing using the T7 primer which reads from the 3′ end of the multiple cloning site. This plasmid was termed pEH20 and was used in subsequent cloning stages.

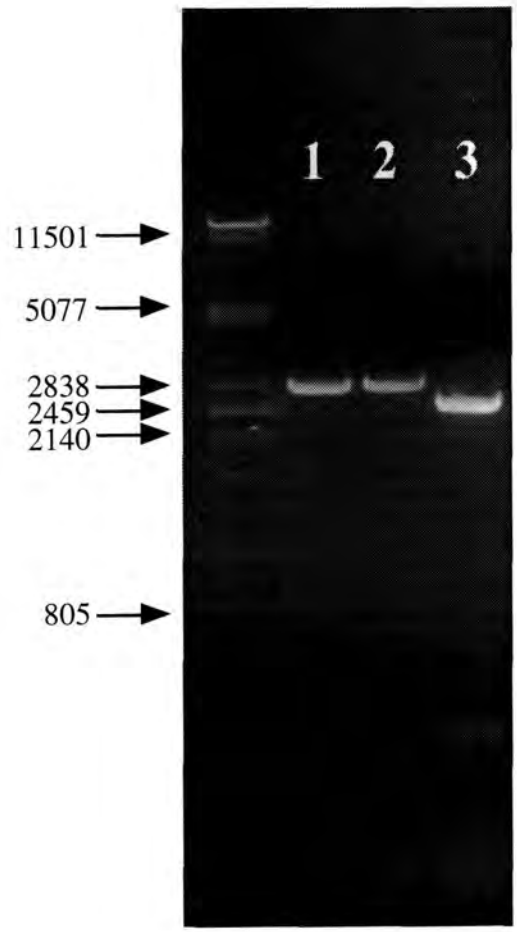

Figure 4.5. Restriction digests of plasmid pEH20.

Figure 4.5. shows a photograph of gel electrophoresis of λ*Pst*I size markers electrophoresed alongside restriction digests which were performed to confirm the presence of the *GPD1* 5' fragment in the plasmid pEH20.

Lane	Restriction enzyme	Predicted fragment size(s)
1	*BamH*I	2846
2	*Pst*I	2846
3	*BamH*I, *Pst*I	2501, 345

4.3. Cloning the 3′ Downstream Region of *GPD1*

4.3.1. Primer design

Primers were designed to amplify the 3′ downstream region of *GPD1* from *S. cerevisiae* genomic DNA by PCR. The position of the PCR primers in relation to start and stop codons in the genomic DNA open reading frame map is shown in figure 4.3. Restriction sites were incorporated into the sequence to ease subsequent cloning steps for correct insertion into pEH20. The sequence for the 5′ primer was as follows:

5′> GGG AAT TCT GCT GCC ATC CAA AGA G
*EcoR*I site

The sequence for the 3′ primer was as follows:

5′> GGG ATA TCG CCT CGA AAA AAG TGG GGG
*EcoR*V site

The region amplified by these primers includes the stop codon of *GPD1* but the reading frame for this is not significant to the cloning strategy as the *lacZ* and Kan^R genes have their own termination sequences. The 3′ region of *GPD1* is only of basic importance to provide homology for insertion of the disruption cassette into the yeast genome.

4.3.2. PCR conditions

Four PCR reactions were carried out using the same conditions as for the amplification of the promoter region described in section 4.2.2. The primers described above were expected to give a product of 449 base pairs. In this case the PCR was significantly more efficient in reaction mixture 2 (gel photo not shown) and DNA was isolated, by fragment isolation, from that tube only.

4.3.3. Sub-cloning into pUC19

Fragment-isolated *GPD1* 3′ PCR product was blunt-ended by incubation with T4 DNA polymerase and dNTPs at 37°C for 5 minutes. The enzyme was heat-inactivated at 65°C and then removed with the dNTPs from the DNA using a Promega Wizard DNA Clean-up kit. The blunt-ended PCR product was ligated into *Hinc*II-digested pUC19 and then transformed into DH5α. The transformants were selected on L-Amp plates pre-spread with X-Gal and white colonies were picked for plasmid DNA preparation.

Plasmid preparations were analysed with restriction digests and gel electrophoresis (see figure 4.6). High purity DNA was prepared from one of the transformants with the correct insert and sequenced, which confirmed the identity of the *GPD1* 3′ region. This plasmid was termed pEH21.

4.3.4. Cloning the 3′ downstream region of *GPD1* into pEH20

GPD1 3′ region was cloned into the same plasmid as the *GPD1* promoter so that the *lacZ* and Kan^R genes could be inserted as a unit between the two *GPD1* regions. *GPD1* was excised from pUC19 using the restriction enzymes *EcoR*I and *EcoR*V which cut in the primer ends of the PCR product and then purified by fragment isolation. pEH20 (pFA6a containing *GPD1* 5′) was also restricted with *EcoR*I and *EcoR*V and the DNA purified with the Promega Wizard DNA Clean-up kit. *GPD1* 3′ was ligated into restricted pEH20 and then transformed into DH5α. Several colonies were picked for rapid screening and those containing plasmids that were apparently larger were selected for plasmid DNA preparation. The plasmids were analysed by restriction digests and gel electrophoresis and one was selected which appeared to have both the 5′ promoter and 3′ the downstream regions of *GPD1* (see figure 4.7). High purity DNA was prepared and the plasmid was termed pEH22. Presence of the *GPD1* 3′ fragment was then confirmed by sequencing (as described in section 2) from the 3′ end of the multiple cloning site using the T7 primer.

4.4. The *gpd1* Disruption Cassette

4.4.1. Cloning *lacZ* and Kan^R into pEH22

pFA6a-lacZMT-kanMX3 was prepared using the Promega Wizard Miniprep method to obtain high purity DNA. It was then digested with *Sma*I and *EcoR*I to excise *lacZ* and Kan^R. The *lacZMT-kanMX3* fragmentwas isolated and used in a ligation with purified *Sma*I-, *EcoR*I-restricted pEH22. The ligation mixture was used to transform DH5α and transformants were selected on L-Agar plates containing 50μg/ml kanamycin which only allows growth of transformants with the kan^R insert. Plasmid DNA was prepared from transformants selected in this way and analysed by restriction digests and gel electrophoresis. Figure 4.8 shows the fragments of DNA obtained with certain confirmatory restriction digests. This plasmid was termed pEH23. Figure 4.9 shows the plasmid map for pEH23 with relevant restriction sites marked.

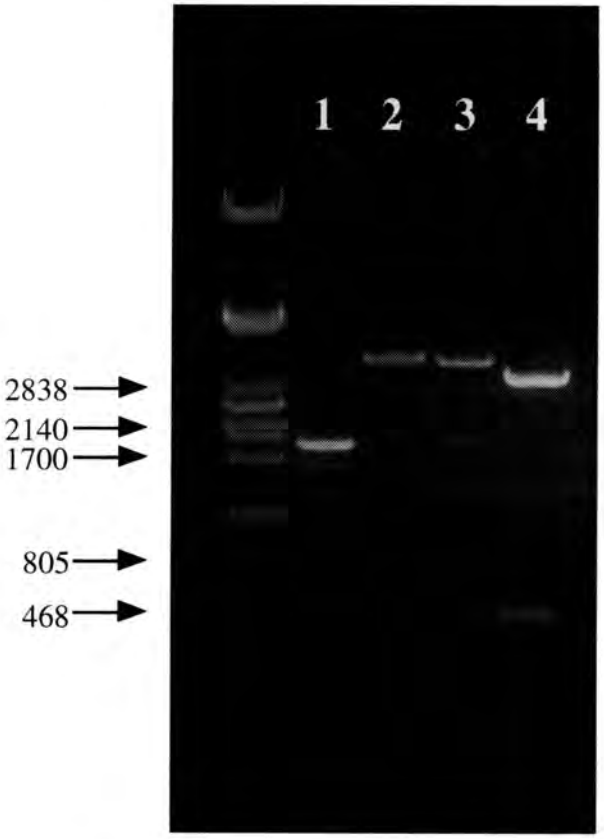

Figure 4.6. Restriction digests of plasmid pEH21.

Figure 4.6. shows a photograph of gel electrophoresis of λ*Pst*I size markers run alongside restriction digests which were performed to confirm the presence of the *GPD1* 3' fragment in pUC19 to create the plasmid pEH21.

Lane	Restriction enzyme	Predicted fragment sizes(s)
1	none	(none predicted)
2	*Bgl*II	3139
3	*BamH*I	3139
4	*EcoR*I, *EcoR*V	2700, 439

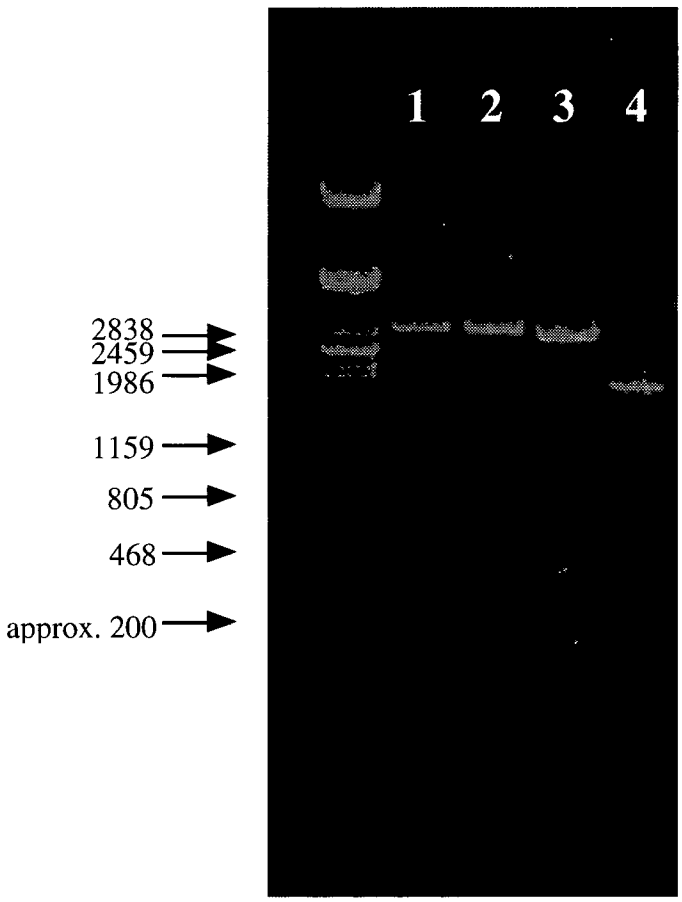

Figure 4.7. Restriction digests of plasmid pEH22.

Figure 4.7 shows a photograph of gel electrophoresis of λ*Pst*I size markers run alongside restriction digests which were performed to confirm the presence of the *GPD1* 3' fragment in pEH20 to create the plasmid pEH22.

Lane	Restriction enzyme(s)	Predicted Size(s)
1	*Bgl*II	2887, 386
2	*Pst*I, *EcoR*I	2881, 392
3	*BamH*I, *EcoR*V	2787, 486
(4	digest from different experiment)	

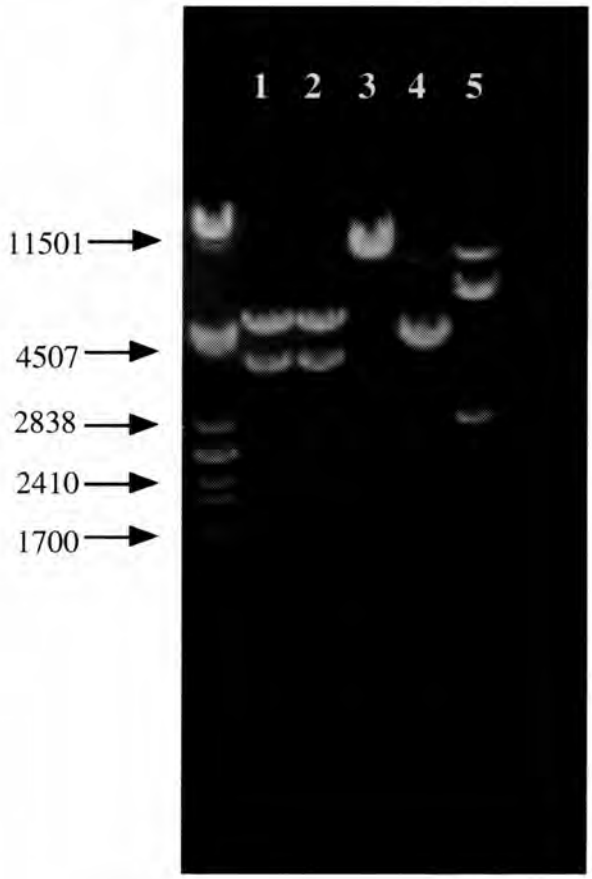

Figure 4.8. Restriction digests of plasmid pEH23.

Figure 4.8 shows a photograph of gel electrophoresis of λ*Pst*I size markers run alongside restriction digests which were performed to confirm the presence of the *lacZMT-kanMX3* cassette in pEH23.

Lane	Restriction enzyme	Predicted fragment sizes (kb)
1	*Eco*RV	5.07, 3.93
2	*Hin*dIII	5.05, 3.95
3	*Eco*RI	9.00
4	*Pst*I	4.65, 4.35
5	*Bgl*II	6.27, 2.73

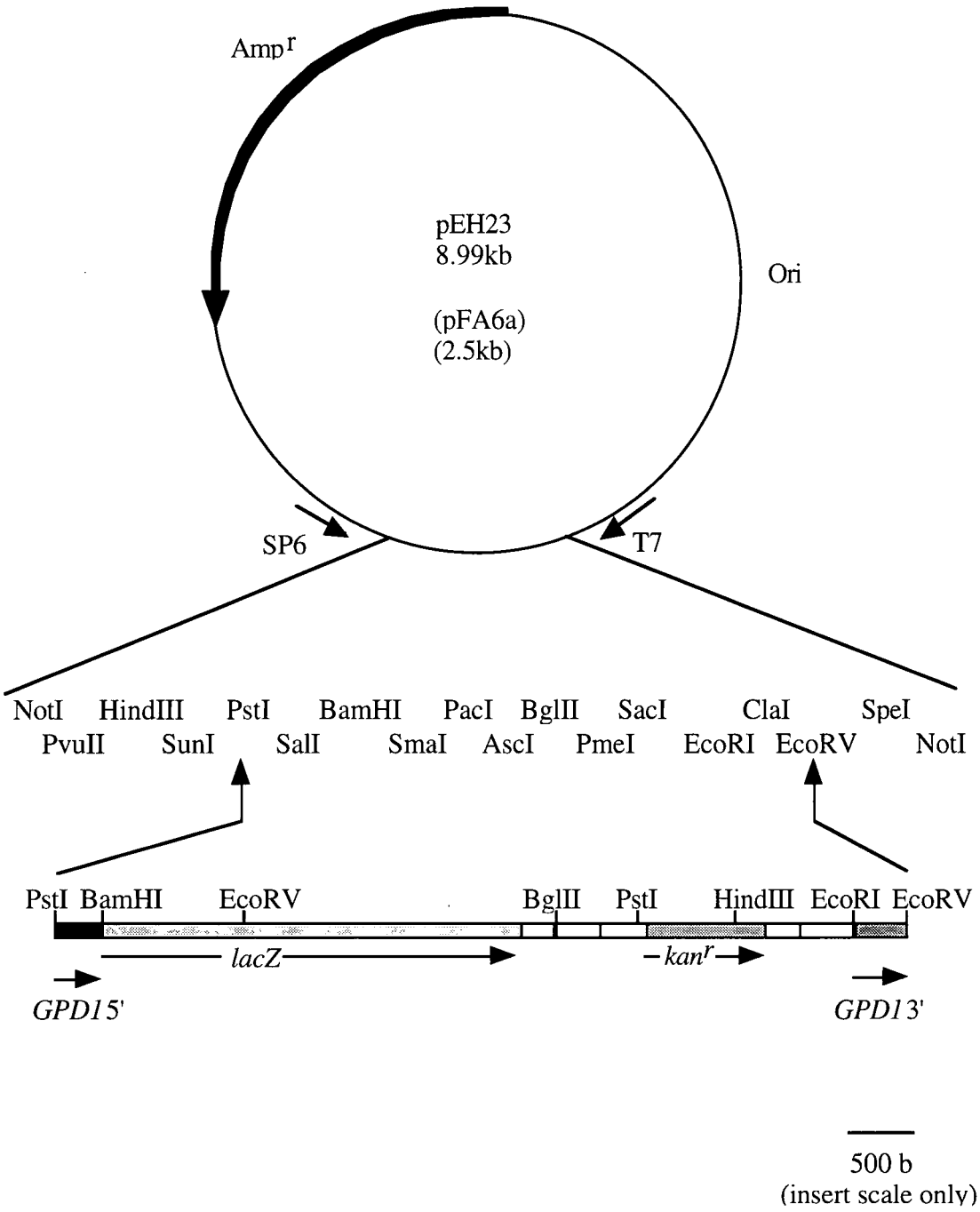

Figure 4.9. Map of plasmid pEH23. (The linear insert is drawn to scale, otherwise the map is not to scale).

4.4.2. Transformations of *S. cerevisiae* with *gpd1Δ::lacZMT-kanMX3*

pEH23 was restricted with *Not*I in a large-scale digest and electrophoresed through an agarose gel to isolate the *gpd1Δ::lacZMT-kanMX3* disruption cassette from the remaining plasmid DNA. The purified disruption cassette was used in transformations of *S. cerevisiae.* The electroporation method described in section 2.4.2. was used except that after the electroporation the cells were not plated out immediately but were incubated in 1ml of YPDA at 30°C for 3 hours to allow expression of the geneticin resistance gene (Webster and Dickson, 1983). The transformants were then plated out onto YPDA plates containing 200μg/ml geneticin for selection and incubated for 3 days.

The following strains were transformed in this way: SEY6210, MLY0145, MLY0419, MLY0803, MLY0905, MLY1143, MLY1176, MLY1218, MLY1510, YPH499, JBY10 (*Δhog1*) and JBY40 (*Δpbs2*). The number of transformants obtained seemed to be largely strain-dependent. Transformants selected on geneticin plates were restreaked for purification onto fresh YPDA plates and then the phenotype of geneticin resistance was confirmed by testing again on YPDA + 200μg/ml geneticin plates. Only a proportion of transformants (approximately half) maintained geneticin resistance after purification.

4.5. Identification of Homologous Recombinants Containing the Disruption Cassette

4.5.1. Analysis by PCR

Transformants which were able to grow on geneticin plates were analysed by PCR of genomic DNA to give a relatively quick indication of the presence of the disruption cassette. The PCR primers for the 5′ end of the promoter region and the 3′ end of the downstream region (described in sections 4.2.1. and 4.3.1. respectively) were used to amplify *GPD1* from genomic DNA isolated from the strains to be tested. In the undisrupted strains these primers should amplify a band of 1.54 kb but in the disrupted strains the primers should be approximately 6.5kb apart. PCR was carried out as described before but with an increased extension time to 2 minutes. This will not allow complete amplification of the large band in the disrupted cells and the screening is therefore for absence of amplification of the 1.54kb band indicating disruption of *GPD1*.

Unfortunately this procedure was tried with several transformed strains but the 1.54kb band corresponding to intact *GPD1* was amplified in all showing that the disruption

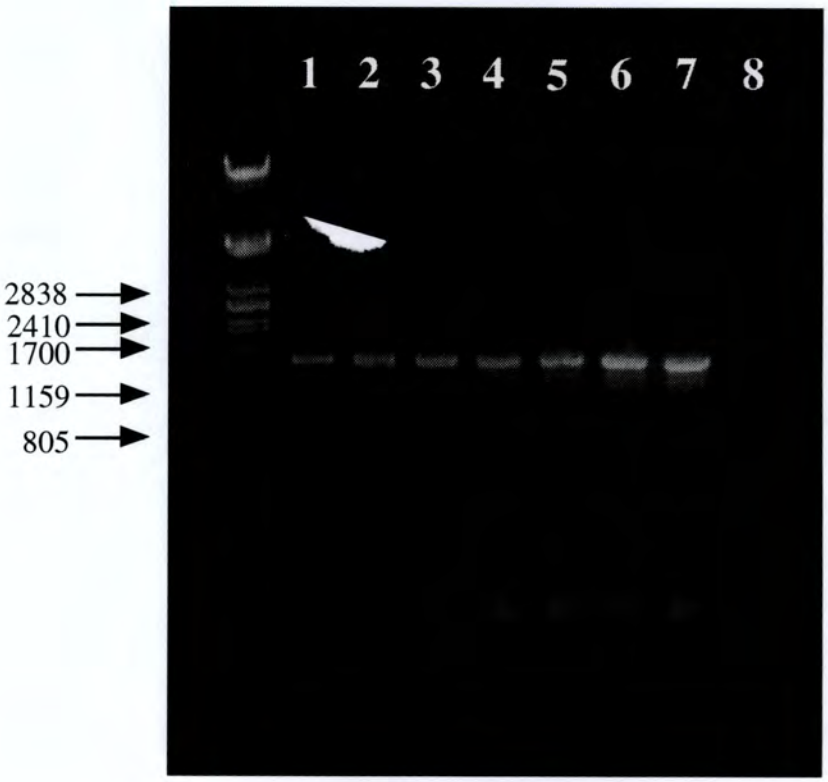

Figure 4.10. PCR reactions of DNA isolated from cells transformed with the *gpd1*Δ::lacZMT-kanMX3.
Figure 4.10 shows DNA amplified from transformants using the 5' and 3' primers of *GPD1*. The lanes contained DNA from strains as follows:

Lane	Strain
1	MLY0905-Δ1
2	MLY1218-Δ1
3	MLY1218-Δ2
4	MLY0712-Δ1
5	MLY0712-Δ2
6	MLY0712-Δ3
7	SEY6210 (untransformed; positive control)
8	no DNA; negative PCR control

4.5.2. Southern blotting of *GPD1*.

The PCR analysis of transformants showed that the genomic DNA still contained an intact copy of *GPD1* and thus they were not homologous recombinants. However, it would perhaps be possible to use these recombinants for promoter analysis if the whole construct was inserted at some other site in the genome. The genomic DNA from the geneticin resistant transformants was therefore analysed by Southern blotting.

Genomic DNA was isolated and parallel digests with *EcoR*I and *Pst*I were performed. The digests were electrophoresed through a large agarose gel for several hours to get good separation of the DNA fragments and then the DNA was transferred to nitrocellulose using the Southern Blot procedures described in section 2.6. The probe used was PCR-amplified *GPD1*. The DNA from an untransformed parental strain was also included as a control.

Figure 4.11 shows the developed blot from a gel of transformed SEY6210, YPH499, JBY10 and the control, untransformed SEY6210. The hybridising bands are clearly the same in the transformed cells as in the control. If heterologous recombination had occurred, the transformed cells would have the same bands as the parental strain, corresponding to the genomic copy of *GPD1*, but in addition they would be expected to have bands hybridising to the 5′ and 3′ ends of the disruption cassette. The *Pst*I digest on this gel appears to have been partial because three hybridising bands are observed where only one would have been expected. As this is the case in all the *Pst*I lanes, it is not significant to the analysis.

The results obtained in the Southern Blot analyses all showed identical hybridisation patterns for the transformed and non-transformed strains. This suggests that some unpredicted transformation event occurred. It would appear some part of the disruption cassette inserted into the genome to confer geneticin resistance but the *GPD1* fragments were lost. It is possible that the selection was inappropriate for this particular gene or perhaps the construct was very unstable. The evidence for this is the high numbers of transformants that were selected on geneticin and then were unable to maintain geneticin resistance upon restreaking. A slightly different selection criterion was therefore adopted.

Figure 4.11. Southern Blot of DNA from cells transformed with *gpd1*Δ::*lacZMT-kanMX3*.

The next page shows a photograph of the Southern Blot of genomic DNA from strains transformed with *gpd1*Δ::*lacZMT-kanMX3* probed with DIG-labelled *GPD1* PCR product. The approximate sizes of the bands (in kb) are marked in the right hand column. The lanes contained DNA from strains restricted with either *Eco*RI or *Pst*I as follows:

Lane	Strain	Restriction enzyme
1	SEY6210-*gpd1*Δ::*lacZMT-kanMX3*	*Eco*RI
2	SEY6210-*gpd1*Δ::*lacZMT-kanMX3*	*Pst*I
3	YPH499-*gpd1*Δ::*lacZMT-kanMX3*	*Eco*RI
4	YPH499-*gpd1*Δ::*lacZMT-kanMX3*	*Pst*I
5	JBY10-*gpd1*Δ::*lacZMT-kanMX3*	*Eco*RI
6	JBY10-*gpd1*Δ::*lacZMT-kanMX3*	*Pst*I
7	SEY6210 (control)	*Eco*RI
8	SEY6210	*Pst*I

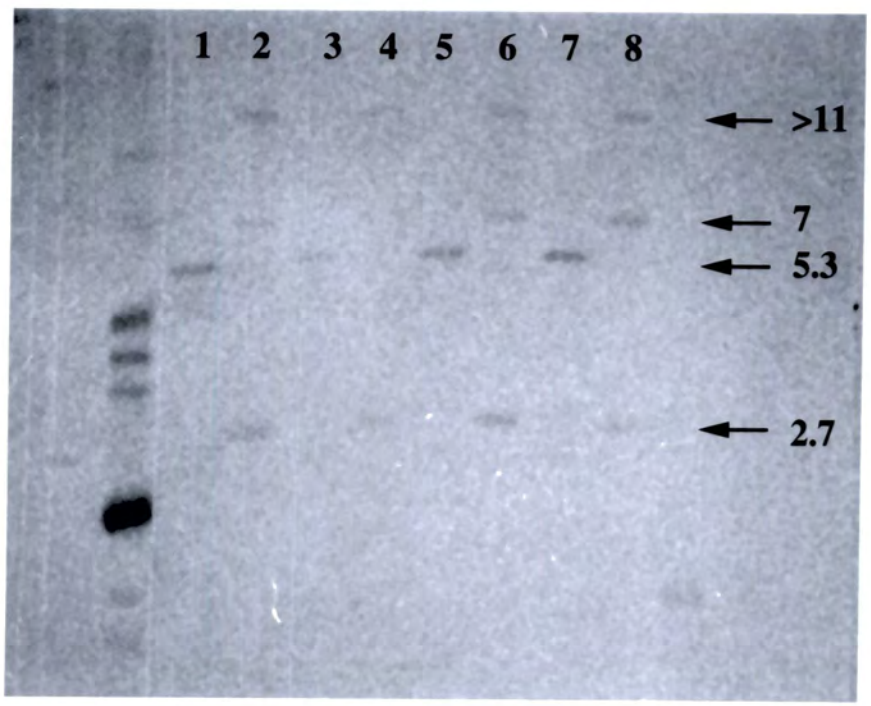
1 2 3 4 5 6 7 8
>11
7
5.3
2.7

4.6. Using the *LEU2* Gene as a Selectable Marker in *gpd1*Δ

4.6.1. Alternative cloning strategy

Using a nutritional marker in gene disruptions is a well-established technique in the laboratory and nutritional selection was therefore substituted for geneticin resistance in the *gpd1* disruptions. The laboratory strains of yeast contain the mutation *leu*2-3 and are unable to grow in the absence of leucine unless complemented by the *LEU2* gene on a plasmid or by recombination. As the construct of the *GPD1* promoter inframe with the *lacZ* gene was already available in pEH23, Kan^R was substituted with *LEU2* from plasmid pL2 directly. Figure 4.12 shows the plasmid map for pL2 and the strategy for substituting Kan^R with *LEU2* is shown in figure 4.13.

The *LEU2* gene was isolated from the plasmid pL2 by restriction digest with *Bgl*II and subsequent fragment isolation. *Bgl*II was also used to excise the Kan^R gene from plasmid pEH23. *Bgl*II cuts directly between *lacZMT* and *KanMX3* and then in the 3´ region of *GPD1*. Although this decreases the extent of the 3´ homology for recombination to 67 bases, Wach *et al.* (1994) reported successful integrations with only 35 bases homology to each target site. *LEU2* was then ligated into the *Bgl*II-cut pEH23 and transformed into DH5α. As blue/white selection was not possible, plasmids with inserts were identified by the rapid screening procedure. Plasmid DNA that appeared to be the correct size was prepared by the alkaline lysis method and the presence of the *LEU2* insert was confirmed by restriction digests. This new plasmid (pEH24) had the *GPD1* promoter region linked to *lacZMT*, followed by the selectable marker *LEU2* and then the 3´ region of *GPD1*. Figure 4.14 shows confirmatory restriction digest reactions for pEH24. The *gpd1*Δ::*lacZMT-LEU2* cassette was removed from the vector DNA in the same way as previously by excision with *Not*I.

4.6.2. Transformations with *gpd1*Δ::*lacZMT-LEU2*

The *Not*I-digested, fragment-isolated *gpd1*Δ::*lacZMT-LEU2* disruption cassette was used to transform several strains of *S. cerevisiae* by the electroporation method. Yeast minimal medium plates with amino acid supplements but with no added leucine (YMM-leu) were used for the selection of transformants containing the disruption cassette. The transformation efficiency was low for all strains, with single figure transformants or no transformants obtained throughout. Transformants were purified by restreaking on fresh YMM-leu plates and, unlike transformants obtained in selection with geneticin, all transformants maintained their ability to grow in the absence of leucine when restreaked.

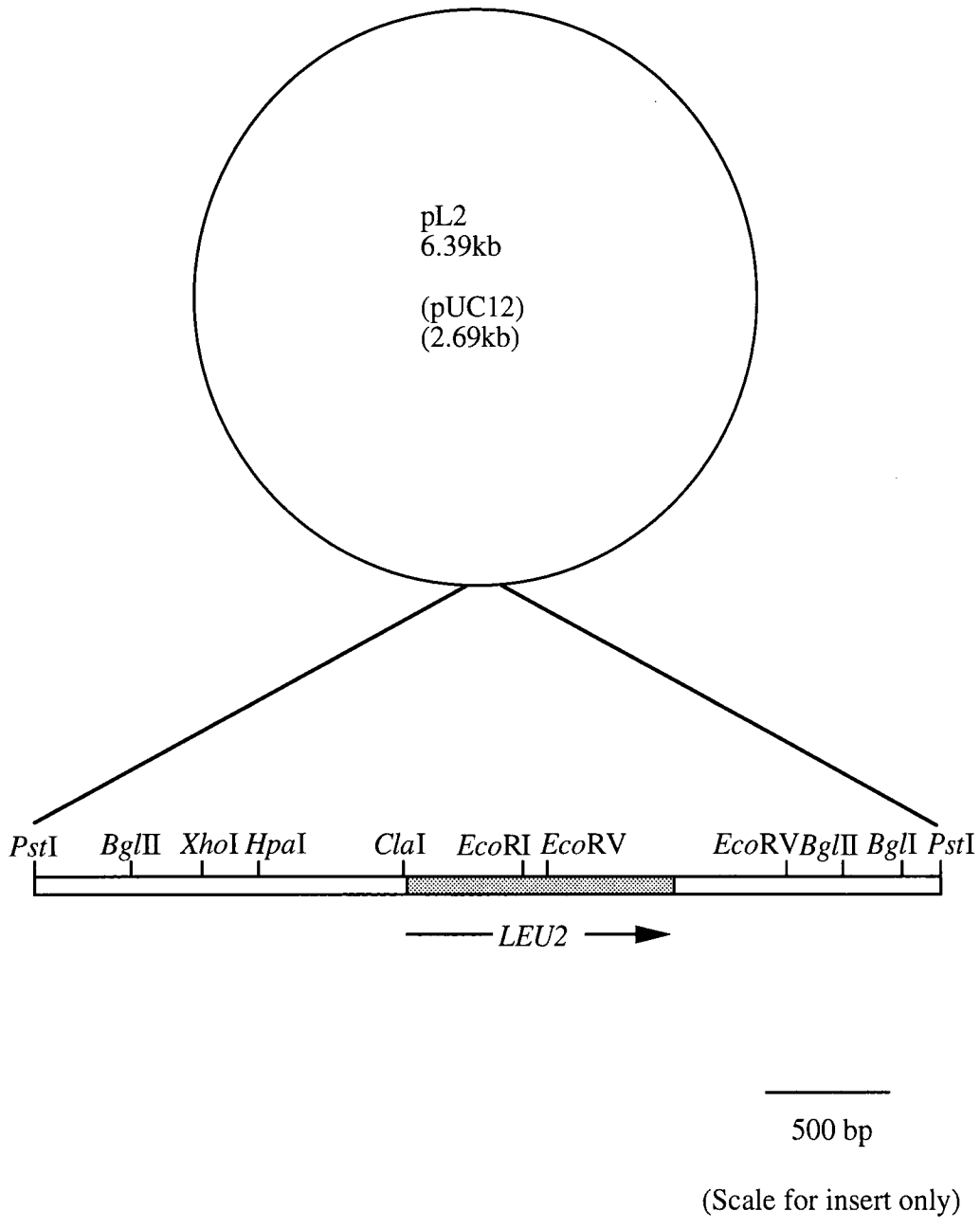

Figure 4.12. Map of plasmid pL2

Figure 4.13. Cloning strategy for creating *gpd1Δ*::lacZMT-*LEU2*.

Figure 4.13 shows the stages for cloning *LEU2* into pEH23 to make the *gpd1Δ*::lacZMT-*LEU2* disruption cassette.

1. Plasmid pEH23 is digested with *Bgl*II (indicated Bg in the figure) and the gene for kanamycin/geneticin resistance removed along with a portion of the *GPD1 3′* fragment. The *LEU2* gene cassette is isolated from pL2 also using the restriction enzyme *Bgl*II.
2. The *LEU2* cassette is ligated into the digested pEH23 making plasmid pEH24.
3. The *gpd1Δ*::lacZMT-*LEU2* disruption cassette is isolated from plasmid DNA by restriction with *Nco*I (indicated N in the figure) and then transformed into yeast for homologous recombination into the yeast genome.

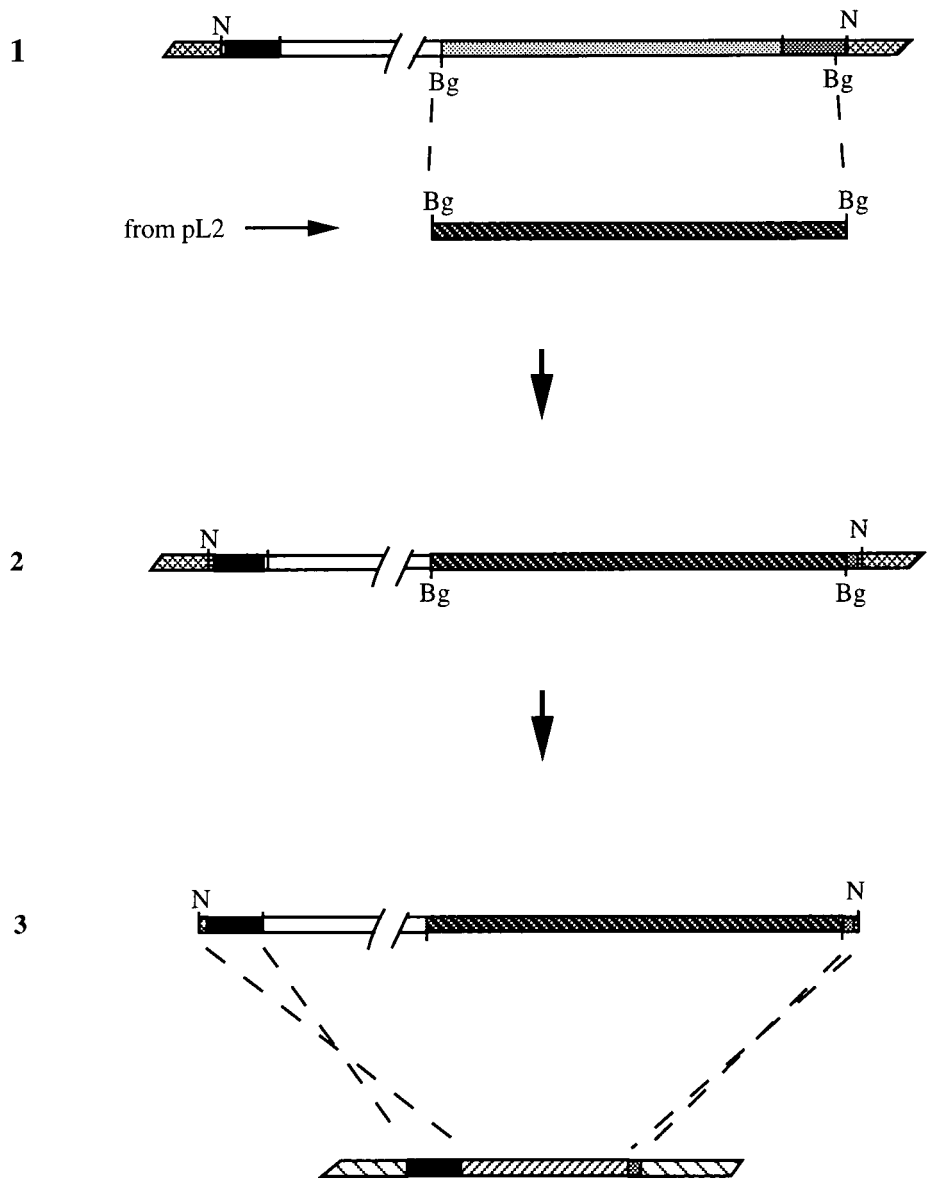
1
N
N
Bg
Bg
Bg
Bg
from pL2
2
N
N
Bg
Bg
3
N
N
GPD1 5′
GPD1 3′
pFA6a
lacZMT
kanMX3
genomic GPD1
genomic DNA (flanking GPD1)
LEU2
500 bases

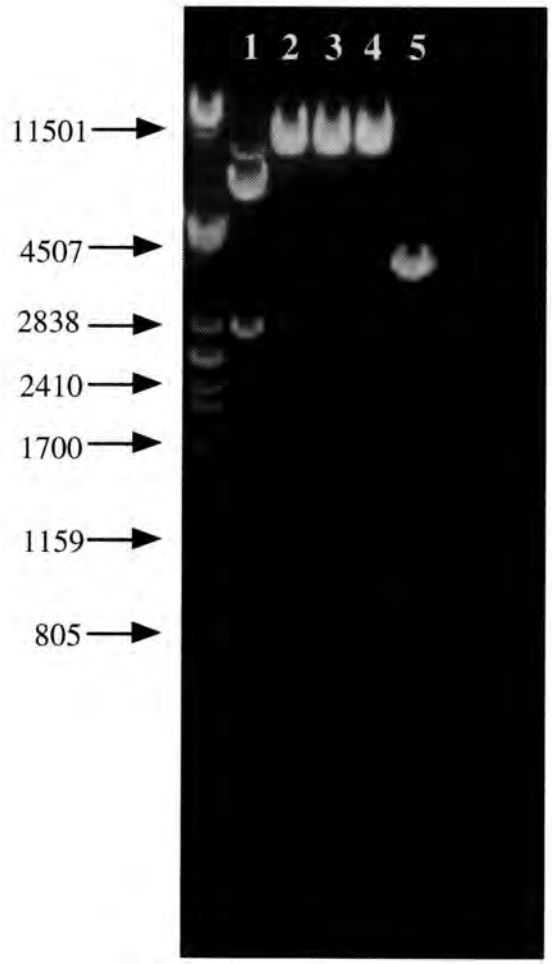

Figure 4.14. Restriction digests of plasmid pEH24

Figure 4.14. shows a photograph of gel electrophoresis of λ*Pst*I size markers run alongside restriction digests which were performed to confirm the presence of the *LEU2* cassette in the plasmid pEH24.

Lane	Restriction enzyme	Predicted fragment sizes (kb)
1	*Bgl*II	6.27, 2.88
2	*Pst*I	9.15
3	*Eco*RI	9.15
4	*Hin*dIII	9.15
5	*Eco*RV	3.97, 3.93, 0.96, 0.29

4.6.3. Analysis of transformants by PCR

Transformants containing *LEU2* were analysed by PCR (as in section 4.5.1.) to determine if the genomic copy of *GPD1* had been disrupted by homologous recombination.

Genomic DNA was isolated from the transformants and used as a template in PCR reactions. The PCR primers for the 5′ end of the promoter region and the 3′ end of the downstream region (described in sections 4.2.1 and 4.3.1 respectively) were used to amplify *GPD1*. Again the screening was for lack of amplification of the 1.54kb band as an extension time of 2 minutes was used.

Several transformants were tested in this way and the gel photograph in figure 4.15 is typical. A 1.54kb band was amplified in all of the PCR reactions which in this case were two transformants each of SEY6210, SEY6211, MLY0803, one transformant of JBY40 and one of untransformed SEY6210 which served as a positive control. Again it appeared that non-homologous recombination had occurred because the PCR reactions showed the presence of an intact copy of *GPD1*.

4.6.4. Analysis of transformants by Southern blotting

As with the geneticin-resistant transformants it would perhaps be possible to use the *LEU2* recombinants for promoter analysis if the whole *gpd1* disruption construct was inserted at some other site in the genome. The genomic DNA previously used in the PCR reactions was therefore analysed by Southern Blotting.

Genomic DNA was isolated from SEY6210 and SEY6211 which had been transformed with the *gpd1*Δ::*lacZMT-LEU2* disruption cassette and from untransformed SEY6210 as a control. The genomic DNA was restricted overnight with *EcoR*I and *Pst*I and the digested DNA was separated by gel electrophoresis. The DNA was transferred onto a nylon filter by Southern blotting and then probed with DIG-labelled *GPD1* PCR product. The developed blot, shown in figure 4.16, showed hybridising bands at the equivalent position for both disrupted and undisrupted strains confirming that *GPD1* remained intact in the cell. However, there were also very faint bands present in the transformed strains which suggested that non-specific recombination might have occurred.

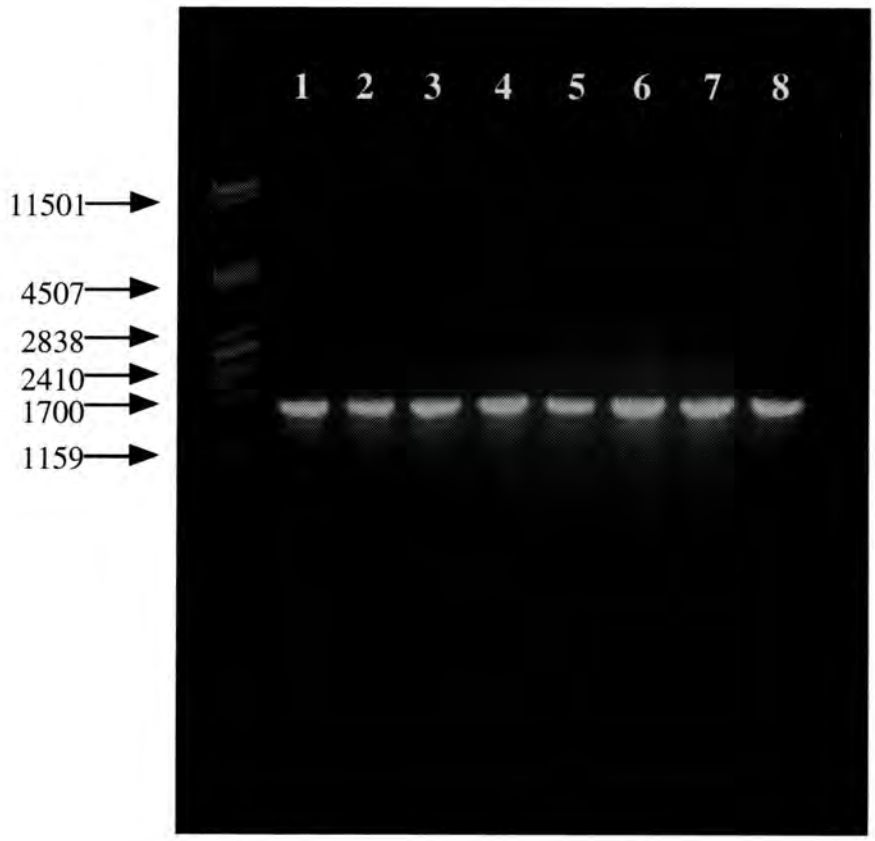

Figure 4.15. PCR reactions of DNA isolated from strains transformed with the *GPD1*Δ::*lacZMT-LEU2* disruption cassette.
Figure 4.15 shows a photograph of gel electrophoresis of DNA amplified from transformants using the 5' and 3' primers of *GPD1*. The lanes contained DNA from strains as follows:

Lane	**Strain**
1	SEY6210-Δ1
2	SEY6210-Δ2
3	SEY6211-Δ1
4	SEY6211-Δ2
5	MLY0803-Δ1
6	MLY0803-Δ2
7	JBY10-Δ1
8	SEY6210 (untransformed; positive PCR control)

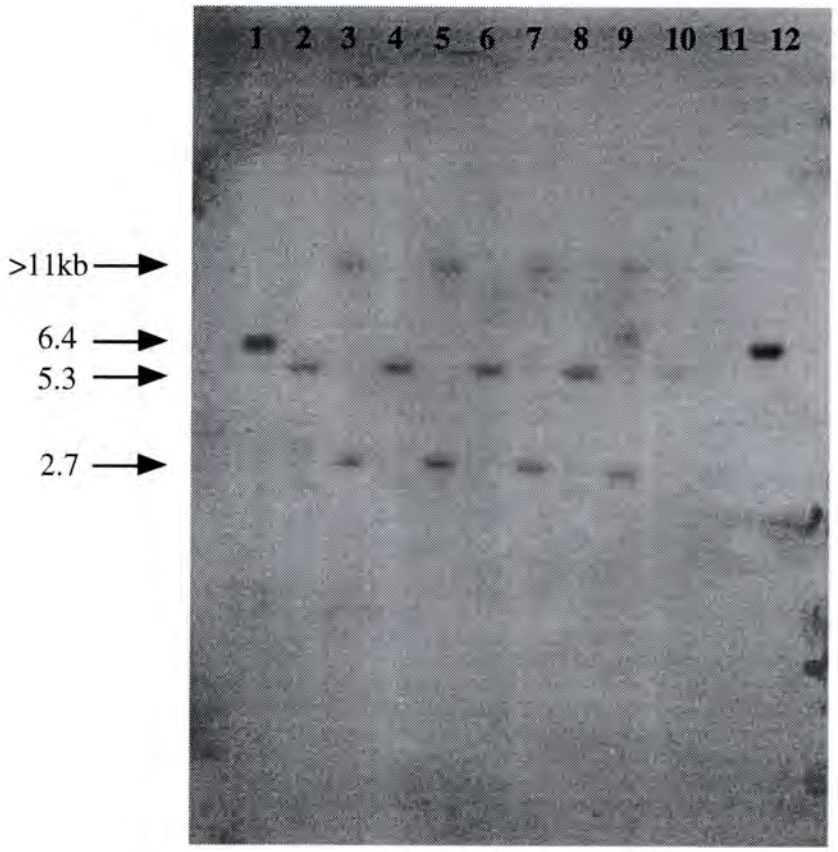

Figure 4.16. Southern Blot of Genomic DNA from Strains Transformed with *gpd1Δ::lac-ZMT-LEU2*

Figure 4.16 shows the photograph of a Southern Blot of genomic DNA from strains transformed with *gpd1Δ::lacZMT-LEU2* probed with DIG-labelled *GPD1* PCR product.The approximate sizes of the bands (in kb) shown were estimated using the size markers on the original gel. The lanes were as follows:

Lane	Strain	Restriction enzyme
1	*gpd1Δ::lacZMT-LEU2* cassette	(unrestricted)
2	SEY6210- *gpd1Δ::lacZMT-LEU2* (1)	*Eco*RI
3	SEY6210- *gpd1Δ::lacZMT-LEU2* (1)	*Pst*I
4	SEY6210- *gpd1Δ::lacZMT-LEU2* (2)	*Eco*RI
5	SEY6210- *gpd1Δ::lacZMT-LEU2* (2)	*Pst*I
6	SEY6211- *gpd1Δ::lacZMT-LEU2* (1)	*Eco*RI
7	SEY6211- *gpd1Δ::lacZMT-LEU2* (1)	*Pst*I
8	SEY6211- *gpd1Δ::lacZMT-LEU2* (2)	*Eco*RI
9	SEY6211- *gpd1Δ::lacZMT-LEU2* (2)	*Pst*I
10	SEY6210 (control)	*Eco*RI
11	SEY6210	*Pst*I
12	*gpd1Δ::lacZMT-LEU2* cassette	(unrestricted)

The blot was then stripped (according to the kit manufacturer's instructions) and re-probed with DIG-labelled *lacZMT* to look for labelling at the same sites as the *GPD1* label. Unfortunately, however, *lacZMT* was found to bind only to the positive control, i.e. the purified *gpd1*Δ::*lacZMT-LEU2* disruption cassette (data not shown). Therefore, although there was evidence for *LEU2* integration into the chromosome (by growth of transformants on YMM-leu), the *lacZMT* portion of the construct appeared to have been lost from the integrating DNA.

The attempts to create Δ*gpd1* strains were unsuccessful for reasons unknown. It appeared that the cassette which contained *kanMX3* was unstable for geneticin resistance but replacing this portion of the cassette with *LEU2* did not solve the problem even though growth of the transformants was more consistent. The lack of correct integration was not investigated further because of the relative value of such information amidst time constraints. Also time prevented a repeat attempt to create the *gpd1* disruption by any other means.

4.7. The *CTT1-lacZ* Gene Reporter

4.7.1. Introduction to the *CTT-lacZ* gene reporter

As it had not proved possible to create a *GPD1-lacZ* gene reporter, a small study was conducted to monitor the promoter activity of another salt-stress inducible gene: *CTT1*, which encodes cytoplasmic catalase T.

Cytoplasmic catalase T activity is enhanced by a variety of stress conditions; heat shock, nitrogen starvation, oxidative stress and osmotic stress (Belazzi *et al.*, 1991; Marchler *et al.*, 1993). Belazzi *et al.* (1991) created a plasmid AW1N which inserted the stress responsive element from the *CTT1* gene into the *LEU2* gene promoter which was linked to the *lacZ* reporter gene. The plasmid AW1N also contains the *URA3* gene allowing selection of the plasmid in ura$^-$ yeast.

The AW1N plasmid was very kindly donated to the laboratory by Belazzi. The basic restriction map for AW1N is shown in figure 4.17. Linearisation of the plasmid at the *Nco*I site in the *URA3* gene creates homologous ends which will allow integration of AW1N into the *ura3* locus when transformed into yeast.

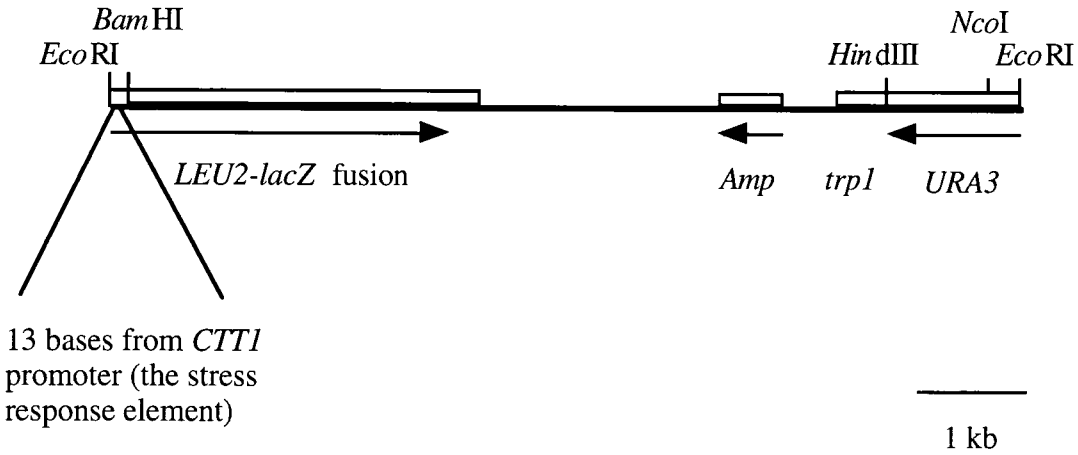

Figure 4.17 Plasmid map of AW1N (linear)

4.7.2. Transformation with AW1N

The AW1N plasmid was restricted with *Nco*I in a large scale digest and then isolated by electrophoresis through an agarose gel followed by fragment isolation. Attempts to transform SEY6210 with restricted AW1N using the electroporation method of transformation were unsuccessful, so a set of transformations were performed using the heat shock method of transformation, with DNA concentrations from 0.1μg to 5μg. Transformants were selected on minimal media with amino acid supplements but with no added uracil (YMM-ura). Transformations using the lower DNA concentrations were also unsuccessful but a few (15-30) transformants were obtained using DNA concentrations of 3-5μg per transformation. Transformants were purified by restreaking on YMM-ura. SEY6211 was also transformed with *Nco*I-restricted AW1N using the heat shock method of transformation.

4.7.3. Salt-sensitive strains containing the *CTT1-lacZ* reporter

It has previously been observed in the laboratory (unpublished results) that many of the salt-sensitive strains have a lower transformation efficiency than the parental strains SEY6210 and SEY6211. The salt-sensitive strains were therefore not used in the transformations with AW1N where very few transformants were obtained even with high concentrations of plasmid. Instead, *CTT1-lacZ* gene reporter was inserted into the salt-sensitive strains by mating and subsequent spore dissection.

The strains MLY0145, MLY0803 and MLY0905 were mated with AW1N-transformed SEY6211 and the strains MLY1164, MLY1176 and MLY1218 were mated with AW1N-transformed SEY6210. The diploids from these mating crosses were sporulated as described in section 2.7.1 and the resulting spores were tested for amino acid deficiencies and salt-sensitivity. An unlinked 2:2 segregation pattern was observed for both salt-sensitivity and ura$^+$ which also confirmed that the *URA3* gene was integrated into the chromosome of the parental strain. Mating crosses were also performed with the strains MLY0419 and MLY1143 but unfortunately very few tetrads were formed and there were no resulting spores which were both ura$^+$ and salt-sensitive.

4.7.4 β-Galactosidase assays

The activity of the *CTT1* stress response element in the salt-sensitive strains was measured by assaying β-galactosidase activity. Spores which were both salt-sensitive and ura$^+$ (i.e. contained the integrated AW1N plasmid) and AW1N-transformed SEY6210 were grown overnight in duplicate cultures of 10ml YPDA at 30^{o}C. To one of the duplicate cultures 10ml of fresh YPDA were added whilst the other duplicate was

salt-stressed by the addition of 10ml YPDA+0.9M NaCl. The cultures were grown for a further 2 hours and then the cells were harvested by centrifugation for 5 minutes at 3000g. The cells were transferred into 1.5ml microfuge tubes before being washed twice in dH_2O for the unstressed cells and once in 0.4M NaCl followed by once in dH_2O for the stressed cells. The cell pellets were resuspended in 0.5ml dH_2O and then 0.2g acid-washed glass beads were added. The tubes were vortexed for 2x 5 minutes to extract the protein. The tubes were spun for 1 minute and the supernatants were transferred into fresh microfuge tubes. The supernatants were then centrifuged for 25 minutes at 4°C to remove the cell debris. The supernatants were again transferred into fresh tubes and stored on ice before testing the protein concentration by the Bio-Rad method described in section 2.8.2. Protein concentrations for extracts isolated in this way were in the range of 15-25μg/ml.

β-galactosidase assays were then performed on all the strains to be tested using the method described in section 2.8.3. Cell extracts described in the method were in fact diluted cell extracts so that each reaction contained a standard amount of protein, 0.2mg. β-galactosidase activity can therefore be expressed as change in absorbance at 420nm per mg of protein (Amg^{-1}).

Table 4.1 and figure 4.18 show the data from the β-galactosidase assays. The activities in extracts from strain MLY0905 were similar to those of the parental strain SEY6210 but levels of activity in the other strains showed an interesting variation. For example, the unstressed and stressed cultures of MLY0145 showed very similar levels of β-galactosidase activity which were at a similar level to the stressed culture of SEY6210. MLY0803, MLY1164 and MLY1218 showed a pronounced increase in β-galactosidase activity that was much greater than the parental strain. MLY1176 was also of interest because of the very high activity observed in both unstressed and stressed cultures.

4.8. Discussion

The original aim of the experiments described in this chapter was to show the promoter activity of *GPD1* in the collection of salt-sensitive strains. This would demonstrate that the high GPDH activities observed in chapter 3 correlate with high promoter activity and not reduced turnover of the enzyme or some other means of elevated activity. Unfortunately, the attempts to create a gene reporter system were unsuccessful. There seemed to be a problem with the geneticin selection of the first construct made but selection was apparently not the problem when geneticin resistance was replaced with the *LEU2* gene in the second construct. While the *LEU2* gene had evidently integrated into the chromosome, the recombination was clearly not homologous. As this occurred

Strain	β-galactosidase activity (Amg^{-1})	
	unstressed	stressed
SEY6210	1.50	3.80
MLY0145	3.10	3.30
MLY0803	3.00	5.30
MLY0905	1.30	3.30
MLY1164	3.05	6.80
MLY1176	8.0	8.0
MLY1218	1.45	5.85

Table 4.1. β-galactosidase activities (expressed as absorbance units per mg of protein) of extracts from strains transformed with the *CTT1-lacZ* gene reporter construct. The figures shown represent the averages of duplicate samples tested for both unstressed and stressed cultures.

Figure 4.18. β-Galactosidase activities of strains transformed with the *CTT1-lacZ* gene reporter.

β-galactosidase activities were measured in protein extracts from stressed and unstressed cultures of strains transformed with *CTT1-lacZ*. Each strain was tested in duplicate.

Figure 4.18 β-galactosidase activities of strains transformed with the *CTT1-lacZ* gene reporter

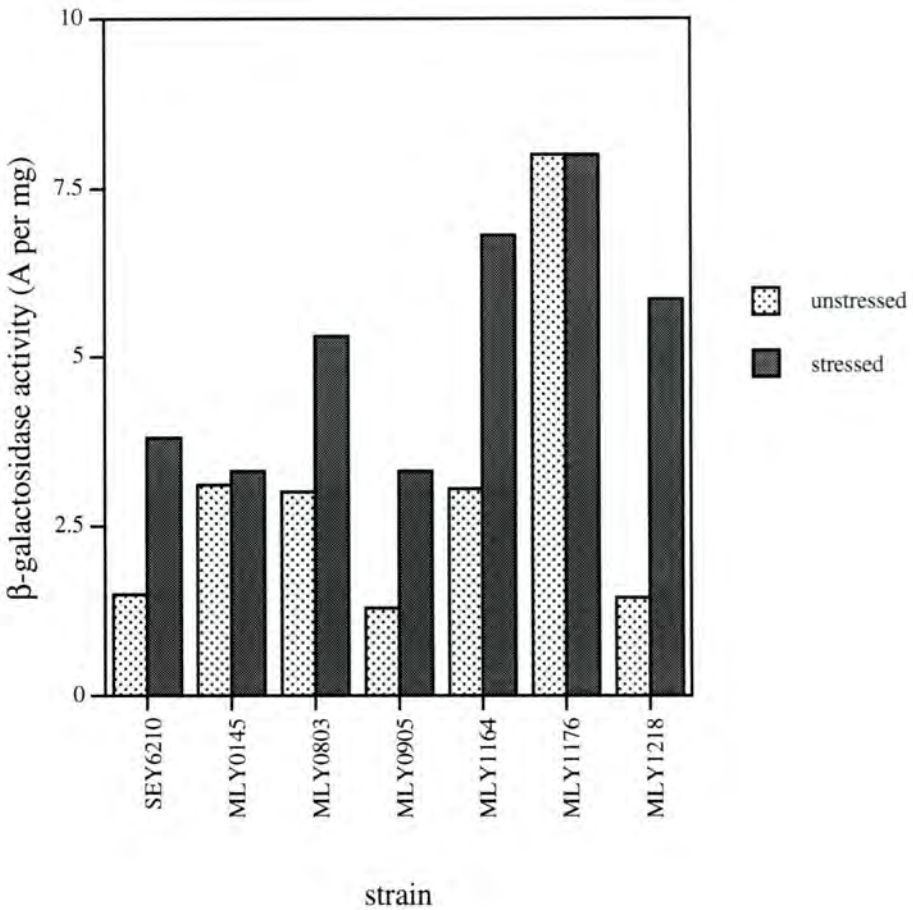

in all the cases tested, there was no reason to continue transformations with this construct and it was decided to make use of a plasmid already available to measure the activity of an alternative stress-responsive gene, *CTT1*. *CTT1* is not only under the influence salt stress through the HOG signal transduction pathway but is also responsive to heat stress, oxidative stress and nitrogen starvation (Belazzi *et al.*, 1991; Marchler *et al.*, 1993). The promoter region of *CTT1* contains a short sequence which is required for response to signalling by these stresses termed the stress response element.

The plasmid AW1N links the stress response element of *CTT1* to *lacZ*. The plasmid also contains the *URA3* gene within which there is a unique *Nco*I site. Linearisation of the plasmid at the *Nco*I site and then transformation into yeast allows integration of the plasmid at the *URA3* gene locus. The activity of the stress response element of the *CTT1* gene can then be represented by measuring β-galactosidase activity.

A selection of the salt-sensitive strains which were previously tested for GPDH activity as described in chapter 3 were mated with parental strains which contained the *CTT1-lacZ* gene reporter construct. A comparison of GPDH enzyme activity with *CTT1* promoter activity (as represented by β-galactosidase activity) for the strains tested is shown in figure 4.19. As the activity of *CTT1* is under the influence of several stresses, a study of *CTT1* induction cannot substitute a study of *GPD1* promoter activity. However these results add another dimension to the GPDH activity studies described in chapter 3. The strains apparently behave in the following ways:

MLY0145 has a relatively high level of background expression from the *CTT1* promoter but does not respond greatly to the salt stress. This is in contrast to the GPDH activities observed which show a strong elevation in response to salt stress. This strain accumulates relatively low concentrations of glycerol in response to salt stress. As mentioned in chapter 3, glycerol concentrations are expressed as μg per cell number. Therefore one explanation for the severity of the glycerol accumulation defect with respect to the observed GPDH and *CTT1* activities could be if the volume of cells was small giving a misleading value for glycerol concentration. This strain does appear to have a defect at some level of control, probably in a HOG-independent pathway as *CTT1* has a reduced salt responsiveness whereas GPDH has an elevated response to salt.

Figure 4.19. Comparison of GPDH activity and *CTT1* promoter activity.
Figure 4.19 shows a comparison of GPDH activity (as measured in chapter 3) with *CTT1* promoter activity (as demonstrated by β-galactosidase activity) for stressed and unstressed strains.

Figure 4.19 Comparison of GPDH activity and *CTT1* promoter activity

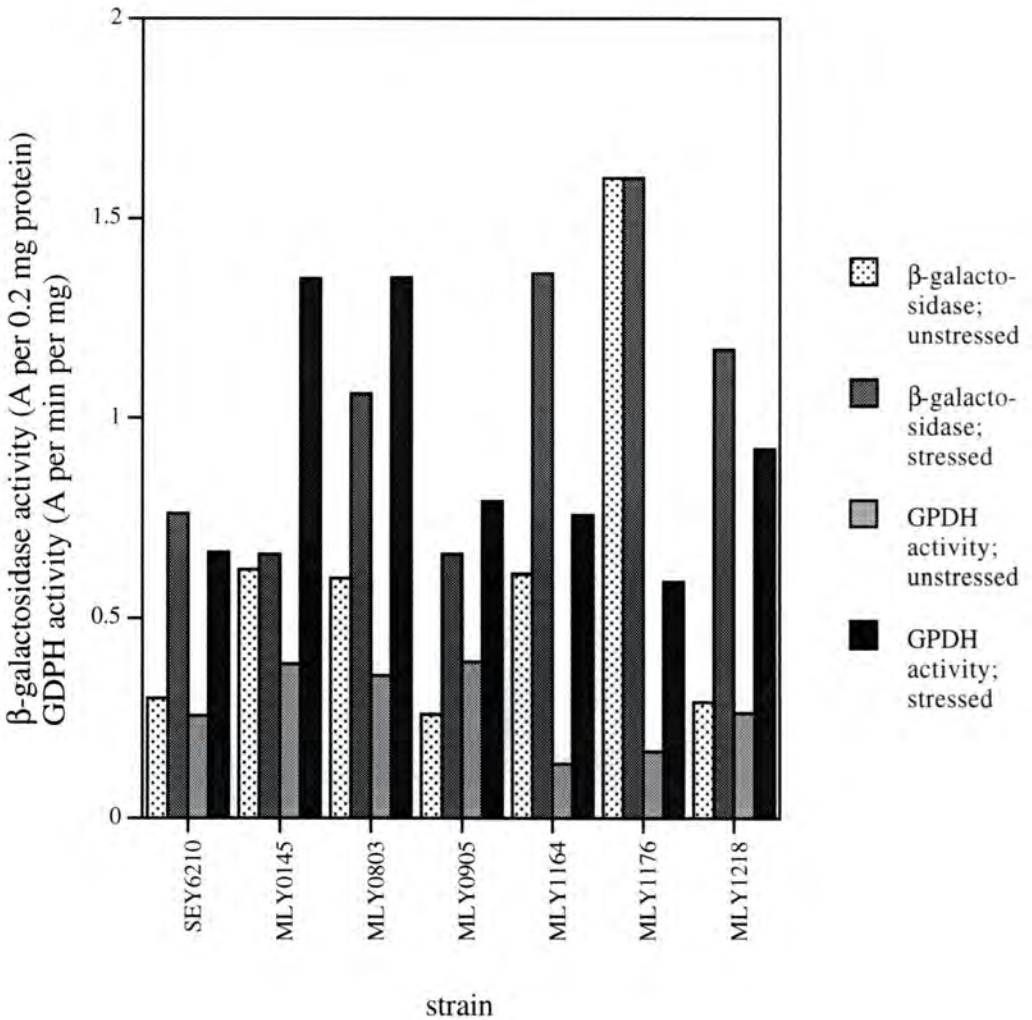

MLY0803 has a similar pattern of enhanced activities for GPDH and the *CTT1* promoter. Both GPDH activity and *CTT1* promoter activity are elevated above the level of the 'wild-type' strain although glycerol accumulation is low. The high activities of these stress-responsive genes could be accounted for if the strain had a hyperactive osmostress response. The glycerol accumulation defect could be related to a metabolic imbalance created by abnormal signalling of this type. Although a hyperactive osmostress response may be expected to improve the osmotolerance of a strain perhaps the altered metabolism is energetically too expensive.

MLY0905 behaves in a similar way to the SEY6210 parental strain for both GPDH enzyme and *CTT1* promoter activity. As discussed in chapter 3 it is possible that this strain suffers from a metabolic defect as the strain is unable to accumulate high levels of glycerol in response to salt stress but has apparently has 'normal' levels of GPDH activity.

MLY1164 is interesting for its relatively high *CTT1* promoter activity in response to salt-stress when GPDH activity is equivalent to the parental strain. This suggests that while there is apparently no abnormality in the link between the HOG signalling pathway and GPDH, there is a defect in one of the several pathways that signal through the *CTT1* promoter (which could include a metabolic signal). The glycerol accumulation of this strain is low. Again this could be related to the metabolic balance of the cell or to the cell volume.

MLY1176 is unusual for the high level of *CTT1* promoter activity in both stressed and unstressed cells, especially as the GPDH activity does not display any abnormalities. In chapter 3 it was suggested that this strain could have a defect in the sequestration of glycerol, facilitated by Fps1p (Luyten *et al.*, 1995). This would now appear to be unlikely as this would probably not cause such an unusual effect on *CTT1* promoter activity. The glycerol accumulation of this strain is extremely low, making this strain of interest for the further study of stress responses.

MLY1218 has slightly elevated activities in response to salt-stress for both GPDH and *CTT1* activity. The glycerol accumulation is very low for this strain. Therefore although it is unlikely that the strain has a defect in osmosensing signal transduction there may be a metabolic defect or inhibition of GPDH *in vivo*. It should be noted that this strain has class B fragmented vacuoles which may somehow interfere with GPDH activity.

In this small selection of stains few conclusions can be drawn and few trends observed. GPDH activity does not necessarily correlate with *CTT1* promoter activity which would

be expected if there was a signalling defect through the HOG signal transduction pathway. As the study of three different outcomes of osmosensing signal transduction for a given strain can give a wide variance in results, no single measurement can be taken as an effective screen for a signalling defect. Certainly it is clear that the study of *CTT1* promoter activity cannot substitute for the study of *GPD1* promoter activity, although it may give additional insight into the nature of a defect. For example in strain MLY1176 *CTT1* appears to be constitutively active whereas GPDH activity is equivalent to the parental strain.

CHAPTER 5

CHARACTERISATION OF A GENE INVOLVED IN VACUOLAR FUNCTION

5.1. Introduction

Vacuole inheritance in the yeast *Saccharomyces cerevisiae* is initiated early in the cell division cycle. Material from the maternal vacuole is targeted into the emerging bud by vesicles streaming along segregation structures. The vesicles then fuse to form the daughter vacuole as the bud continues to grow (Conradt *et al.*, 1992). *vac* mutants have been described in which there are frequently no apparent vacuoles in the daughter buds and no segregation structures formed. One mutation, *vac1-1*, also results in the missorting of vacuolar proteins from the Golgi body (Weisman and Wickner, 1992) while the *vac2-1* mutation has little or no effect on protein sorting and appears to be more specifically involved with the formation of segregation structures (Shaw and Wickner, 1991). Vacuole biogenesis was discussed more fully in Chapter 1.

It has been shown that one of the salt-sensitive strains created in the laboratory, *ssv17-101* (for salt-sensitive vacuolar mutation), has a novel vacuole inheritance defect (Hartley, 1995; Latterich, 1992). Although these cells are capable of forming buds containing maternally inherited vacuoles, there is clearly some breakdown in the regulation of this process as a proportion of the cells are observed without any apparent vacuole. Budding is not prevented by the absence of a coherent vacuolar structure as mutant cells have been observed in which both the maternal cells and the daughter buds lack vacuoles. *ssv17-101* cells also display a pronounced protein sorting defect. The *SSV17* gene has not yet been identified and as the transformation efficiency of the *ssv17-101* strain is extremely low, complementation with a DNA library is not a feasible strategy for cloning the gene. Attempts to map the gene located it to chromosome XIV (Hartley, 1995).

With the sequencing of the yeast genome, many Open Reading Frames (ORFs) with unknown identities and functions have been revealed. A homologue to the *VAC1* gene was identified on chromosome XIV and sequenced as part of the EC yeast genome sequencing project (Genbank: X77395, Swiss-Prot: P40343). At the time this project was started the sequence was not published but it was known that the sequence homology to *VAC1* was approximately 20%. This ORF was investigated as a potential candidate for *SSV17* because of its appropriate location in the genome and because of the sequence homology to the functionally similar gene (*VAC1*).

This chapter describes attempts to complement *ssv*17-101 cells with the ORF, (referred to as *VAC1*-Homologue or *VAC1H*) and the demonstration of a role for the *VAC1H* gene in vacuolar protein sorting.

5.2. Testing the Ability of *VAC1H* to Complement the *ssv17-101* Mutation

5.2.1. Creating a yeast vector containing the *VAC1H* gene

Although the sequence for *VAC1H* was not available at the initiation of this project, a full restriction map was released for this part of chromosome XIV and sequence data was available for small regions of sequence on either side of the ORF. From the sequence available, PCR primers were designed to allow amplification of *VAC1H* from yeast genomic DNA. PCR product of the predicted size (2.77 kb) was fragment isolated and cloned into pUC19. The resultant plasmid, termed pCH40, was analysed with restriction digests and these were correct as predicted from the available map. This work was carried out by C.A. Hartley (Hartley, 1995). Figure 5.1 shows the restriction map of pCH40.

The next stage of the project was to excise the *VAC1H* PCR product and clone it into a yeast vector. The restriction sites used for this were *Bam*HI and *Sph*I which are in the multiple cloning site of pUC19 on either side of the *Hinc*II site into which the PCR product had been cloned. However, *VAC1H* is very difficult to distinguish on a gel from pUC19 because of their similar sizes. A third cut (for example with *Sca*I) within the pUC19 backbone is a useful way to separate the two.

pCH40 was digested sequentially with *Bam*HI followed by *Sph*I because *Sph*I requires the supplement BSA for maximal activity but this may have an inhibitory effect on *Bam*HI. Attempts were then made to purify the DNA using a Wizard DNA Clean-up kit (according to the manufacturer's instructions) and digest with *Sca*I. However, problems were encountered with incomplete digests at all stages or with losing too much DNA at the purification stage. Therefore, pCH40 was cut with *Bam*HI followed by *Sph*I only and purified by fragment isolation. The yeast shuttle vector YCp50 was digested in the same way and also purified by fragment isolation. The *VAC1H* PCR product/pUC19 mix was ligated into YCp50, transformed into DH5α and transformants were selected on L-Amp plates. Plasmid DNA of several transformants was prepared by alkaline lysis and analysed with restriction digests. It was at this stage that clones containing pUC19 were separated from those containing *VAC1H* PCR product.

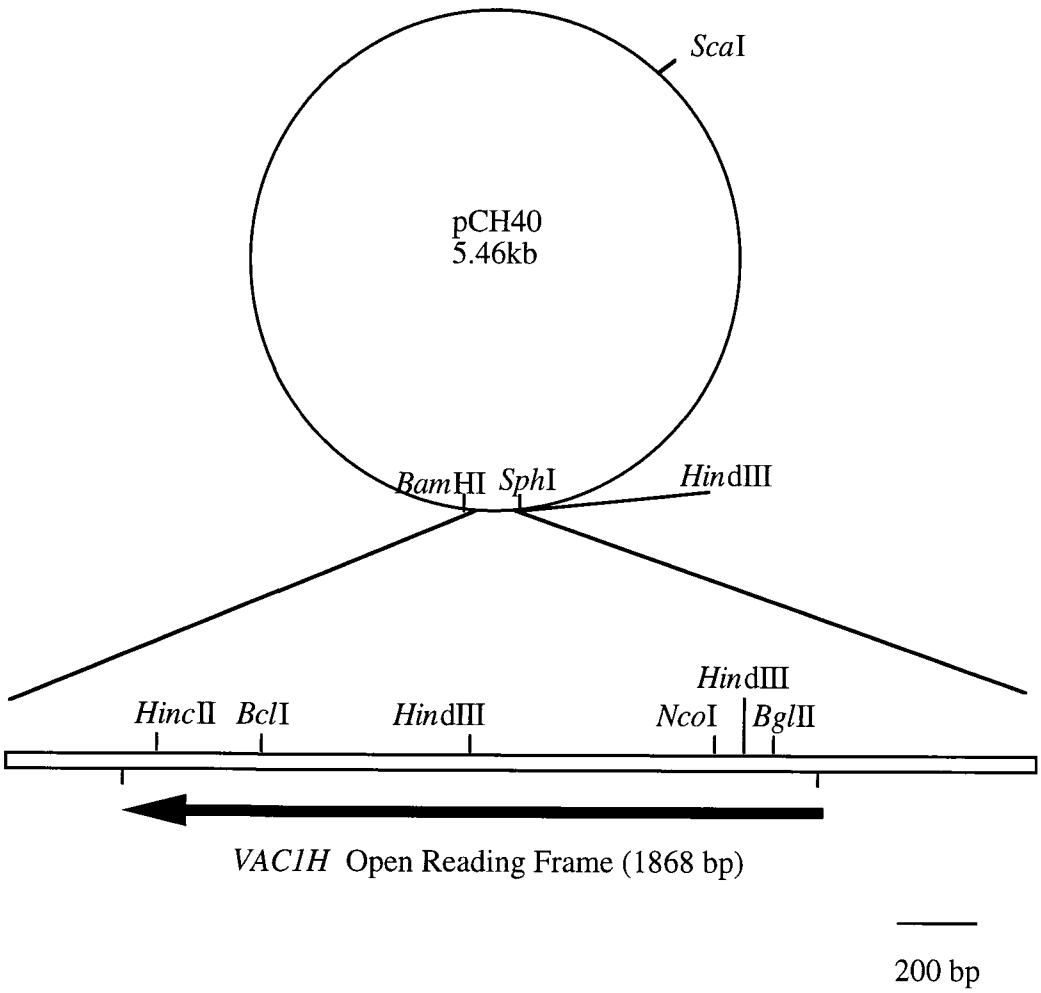

Figure 5.1. Restriction map of plasmid pCH40

The box represents the PCR-amplified genomic DNA surrounding *VAC1H* and is drawn to the scale shown. The circle represents plasmid DNA from pUC19 and is not drawn to scale.

High purity DNA was prepared from one of the plasmids containing the correct *VAC1H* insert and this was termed pEHY11. Figure 5.2 shows confirmatory restriction digests of pEHY11 and figure 5.3 shows the pEHY11 restriction map.

5.2.2. Transformation of *ssv17-101* cells with *VAC1H*

The electroporation method of yeast transformation was used to transform pEHY11 into the strain MLY0508. MLY0508 contains the *ssv17-101* and *ura3-Δ52* mutations and as YCp50 contains the *URA3* gene, transformants were selected on yeast minimal medium plates with amino acid supplements but with no added uracil (YMM-ura). Ten transformants were obtained by this method which was not unexpected for this strain which has a low frequency of transformation. The transformants were purified by re-streaking onto fresh YMM-ura plates before phenotypic analysis.

MLY0508 cells transformed with pEHY11 were tested for growth on salt to indicate whether the *VAC1H* gene could complement the *ssv17-101* mutation. Transformants were re-streaked onto YPDA+1.5M NaCl plates and incubated at 30°C for ten days but there was no apparent growth after this time. Growth of the parental, non-salt-sensitive strain SEY6211 would be apparent after 3-4 days of incubation under these conditions. It was therefore concluded that pEHY11 was unable to complement the salt-sensitivity of MLY0508 and that *VAC1H* may not be the same as *SSV17*. However, there were other possibilities for the lack of complementation which could not be ruled out at this stage. For example, there may have been a PCR error in the duplication of *VAC1H* which could have rendered it non-functional or there may have been important sequences controlling the transcription of *VAC1H* further upstream than the region amplified by PCR. To investigate these possibilities and to generally gain more information about the *VAC1H* gene a dual approach was adopted: to sequence parts of the *VAC1H* PCR product (described in the next section) and to create a *VAC1H* gene disruption (described in section 5.4).

5.3. Sequencing *VAC1H*

5.3.1. Sub-cloning portions of pCH40 for sequencing

It was useful to sequence the *VAC1H* at this stage to confirm the open reading frame for the gene and to analyse the sequence for recognised motifs for further clues to the function of the gene. pCH40 was used as a source of the PCR product for sub-cloning steps.

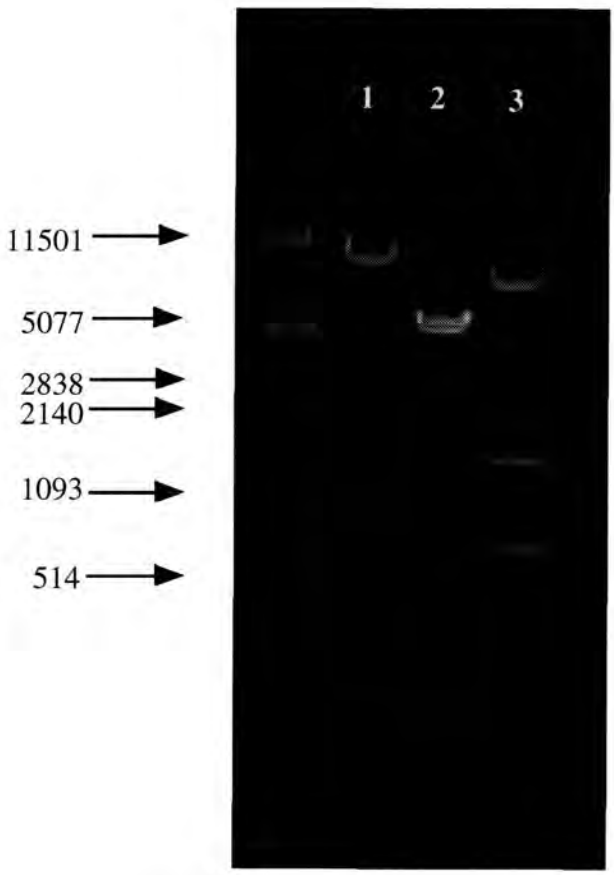

Figure 5.2. Restriction digests of plasmid pEHY11.

Figure 5.2 shows a photograph of an electrophoresis gel of λ*Pst*I size markers run alongside restriction digests of pEHY11 as follows:

Lane	Restriction enzyme	Predicted band size (kb)
1	*Bam*HI	10.54
2	*Bgl*II	5.55, 4.99
3	*Hin*dIII	8.23, 1.58, 0.73

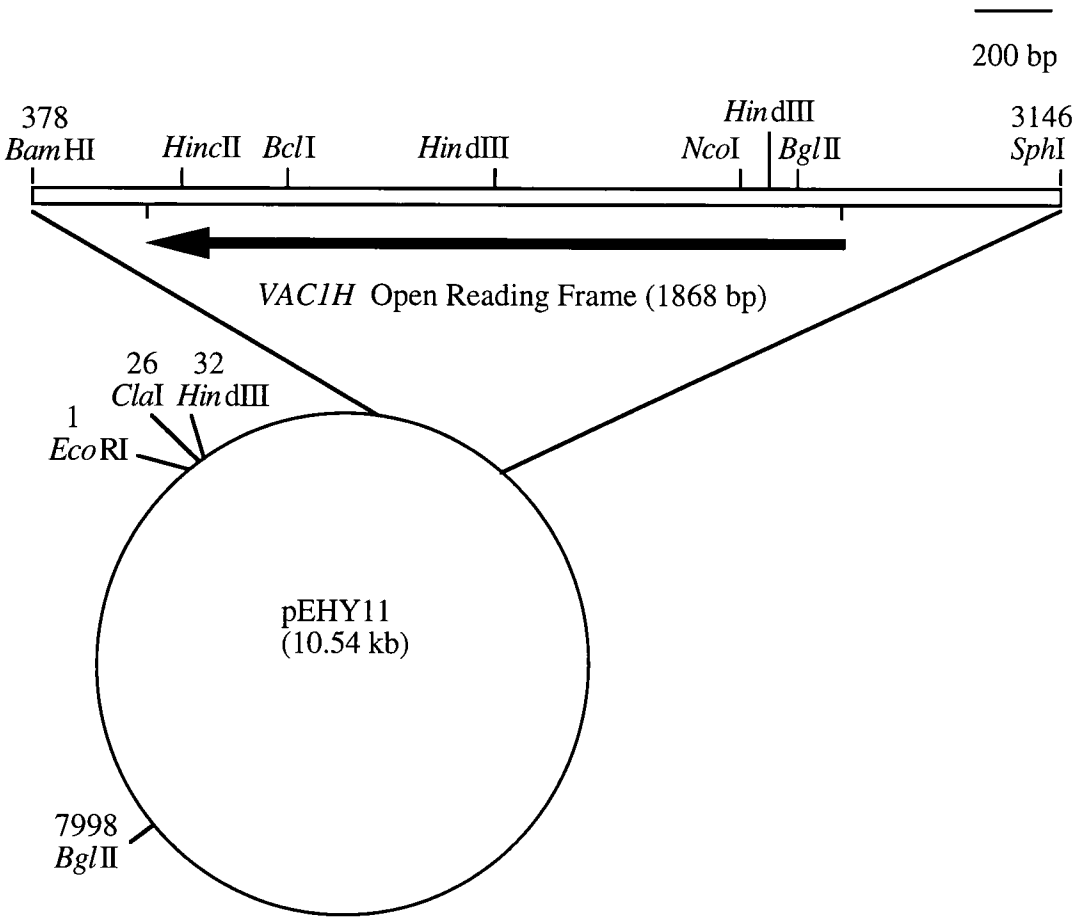

Figure 5.3. Restriction map of plasmid pEHY11

The box represents the PCR-amplified genomic DNA surrounding *VAC1H* and is drawn to the scale shown. The circle represents plasmid DNA from YCp50 and is not drawn to scale.

The 5′ region and the middle region of the PCR product were excised by restriction with *Hin*dIII which releases fragments of 0.725, 0.81, and 3.925kb. The 5′ region (with respect to the open reading frame) is the 810 b fragment and the region between the two internal *Hin*dIII sites in the ORF is the 725 b fragment. A large scale digest of pCH40 was performed and run slowly on a 1% agarose gel for good separation of the 725 b and 810 b fragments which run closely together (see figure 5.4). The 725 b and 810 b bands were carefully cut out from the gel with a sterile blade and placed in separate tubes for fragment isolation of the DNA. pUC19 was also restricted with *Hin*dIII and purified by fragment isolation.

The 5′ region of the *VAC1H* PCR product was ligated into *Hin*dIII-cut pUC19 and transformed into DH5α. Transformants were selected on L-Amp plates which had been pre-spread with 40µl of 20mg/ml X-Gal and white colonies were picked and re-streaked for purification (colonies of pUC19 re-ligated to itself will appear blue on X-Gal). Plasmid DNA was prepared by alkaline lysis and analysed with restriction digests. High purity DNA was prepared of one of the plasmids with the correct digest pattern. The concentration of the DNA was calculated spectrophotometrically and diluted to 0.25mg/ml for automatic sequencing using M13 forward and reverse primers. This plasmid was termed pEH12.

The middle region of the *VAC1H* PCR product was ligated into *Hin*dIII-cut pUC19 and selected as described above. High purity DNA was prepared of the plasmid containing the correct insert and prepared for sequencing. This plasmid was termed pEH14.

The 3′ region of the *VAC1H* PCR product was excised from pCH40 with the restriction enzymes *Hin*dIII and *Bam*HI. pCH40 and pUC19 were restricted in separate double digests with *Hin*dIII and *Bam*HI and run on an agarose gel. pUC19 and the fragment of 1.24 kb (which corresponded to the 3′ region of the *VAC1H* PCR product) were purified by fragment isolation. The 3′ region was ligated into the cut pUC19 and the ligation mixture was transformed into DH5α. Transformants were selected on L-Amp plates which were pre-spread with 40µl X-Gal (20mg/ml in DMF). White colonies were picked for plasmid DNA preparation by alkaline lysis and plasmid DNA was analysed with restriction digests. High purity DNA was prepared of the plasmid containing the correct insert and prepared for sequencing as above. This plasmid was termed pEH13. Figure 5.5 shows restriction digests of pEH13.

All three plasmids, pEH12, pEH13 and pEH14 were sequenced in both directions from the M13 forward and reverse primer sites contained in pUC19.

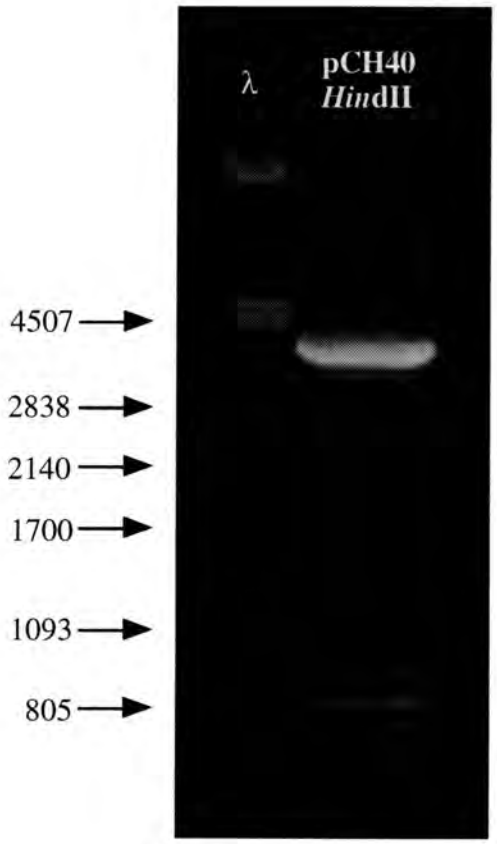

Figure 5.4. Plasmid pCH40 restricted with *Hin*dIII

Figure 5.4 shows the photograph of an electrophoresis gel of λ*Pst*I size markers run alongside pCH40 restricted with *Hin*dIII. Band sizes of 725, 810 and 3925 base pairs are expected with *Hin*dIII-restricted pCH40.

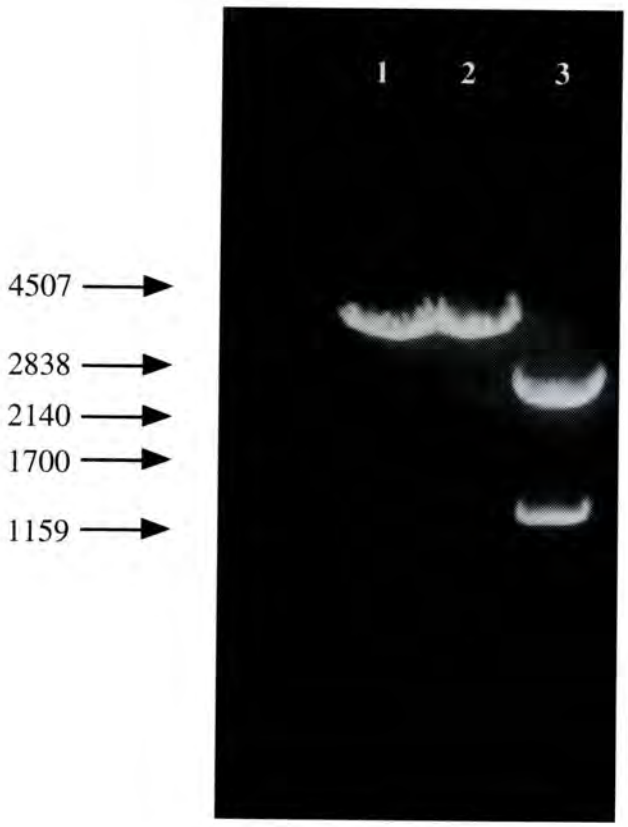

Figure 5.5. Restriction digests of plasmid pEH13.

Figure 5.5 shows the photograph of an electrophoresis gel of λ*Pst*I size markers run alongside pEH13 restricted as follows

Lane	Restriction enzyme	Predicted band size (kb)
1	*Hin*dIII	3.83
2	*Bam*HI	3.83
3	*Hin*dIII, *Bam*HI	1.24, 2.69

5.3.2. Sequence analysis of the *VAC1H* PCR product

The *VAC1H* PCR fragments in pEH12, pEH13 and pEH14 were sequenced from both ends using the M13 forward and reverse primers as described in section 2.9. The sequence data was then analysed using the computer programmes DNA Strider and Sequencher. Figure 5.6 shows open reading frames and the regions of overlap for segments where good quality sequence was obtained in both directions. Although the region of the *VAC1H* ORF was not completely sequenced in both directions, there was no apparent error that could cause a frame shift mutation or a chain termination when expressed in the cell. From this data it would seem unlikely that the lack of complementation of *SSV17-101* by *VAC1H* could be due to a PCR error, but the data is not absolutely conclusive because parts of the strand were only sequenced in one direction with no overlap.

The sequence obtained from the 3 fragments was pieced together and analysed with motif and homology searches available on the World Wide Web. A BLAST search was performed which showed that the sequence contained a zinc-finger binding motif and that the homology with *VAC1* is particularly strong in that region (as shown in figure 5.7). It was shortly after the initial search with this sequence that a repeat search revealed identity between *VAC1H* and the vacuolar protein sorting gene *VPS27*. Confirmation of the identity of *VAC1H* with *VPS27* made use of the Δ*vac1h* strain and is therefore discussed in section 5.5.

5.4. Creating a *VAC1H* Gene Disruption

5.4.1. Cloning strategy

The strategy for creating a *VAC1H* gene disruption is shown diagrammatically in figure 5.8. Part of the coding region of *VAC1H* is excised and replaced with the *LEU2* gene. *LEU2* provides a selectable marker for the disruption and the remaining sequence on either side provides the homology for recombination of the disruption into the genome.

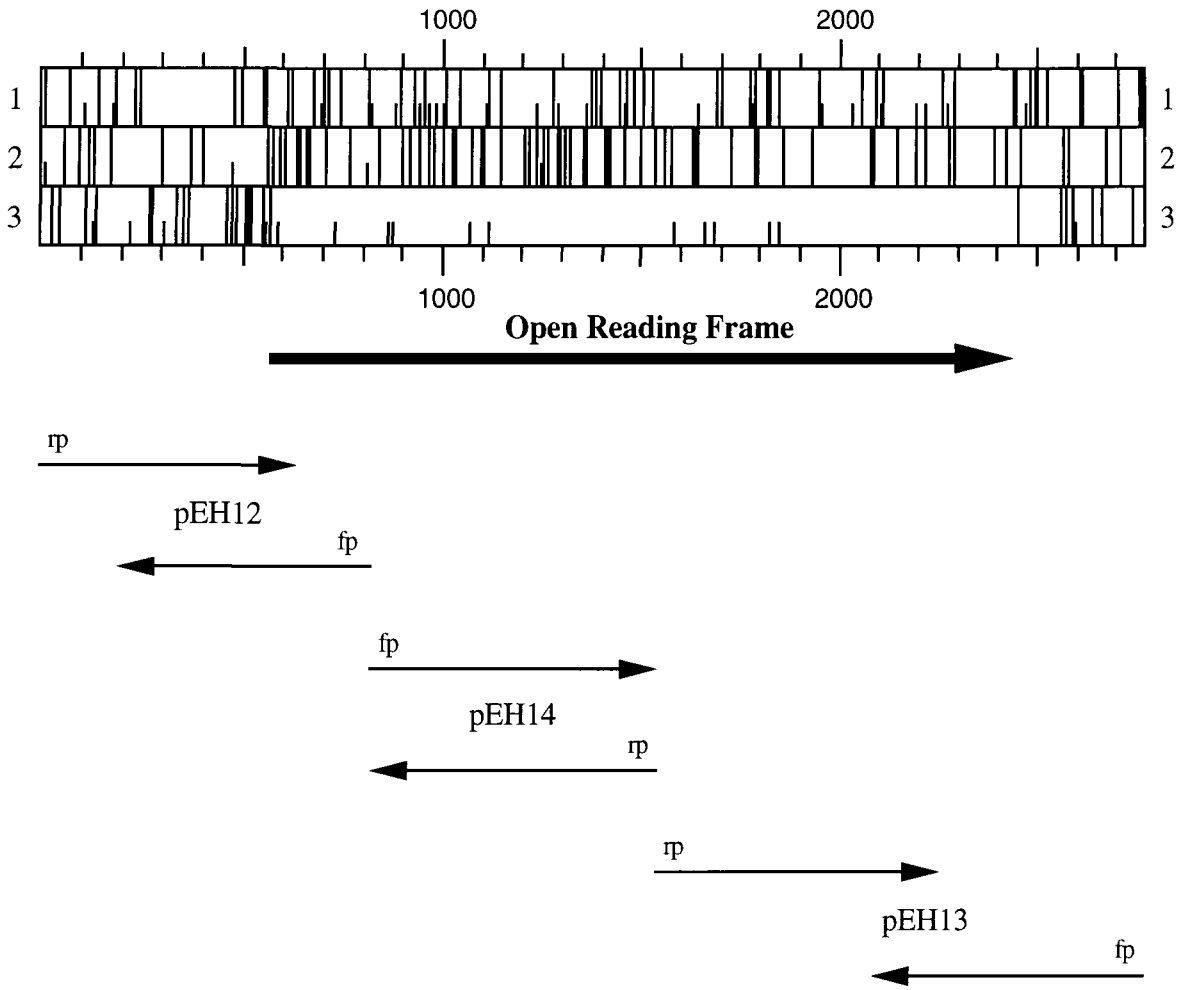

Figure 5.6. Sequencing fragments and open reading frame map of *VAC1H*

Fragments of the *VAC1H* PCR product in pEH12, pEH13 and pEH14 were sequenced in both directions using either the forward (fp) or reverse primer (rp) with regions of overlap as shown.

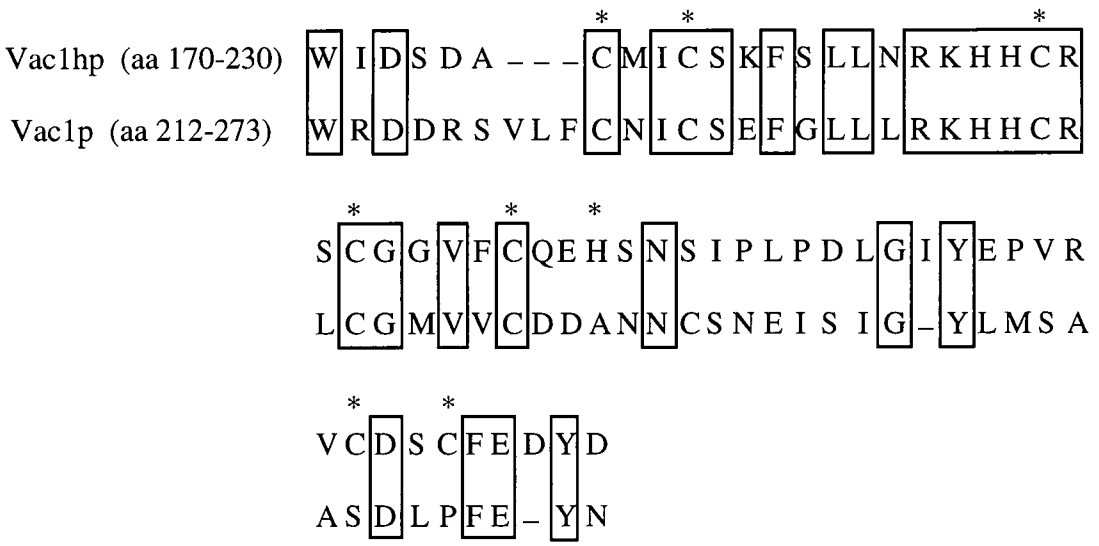

Figure 5.7. Sequence comparison of Vac1hp with Vac1p in the putative Zinc finger domain

Figure 5.7. shows the putative Zinc finger region with matching amino acids boxed. The Cys/His residues which may co-ordinate the binding of Zn are marked with an asterisk.

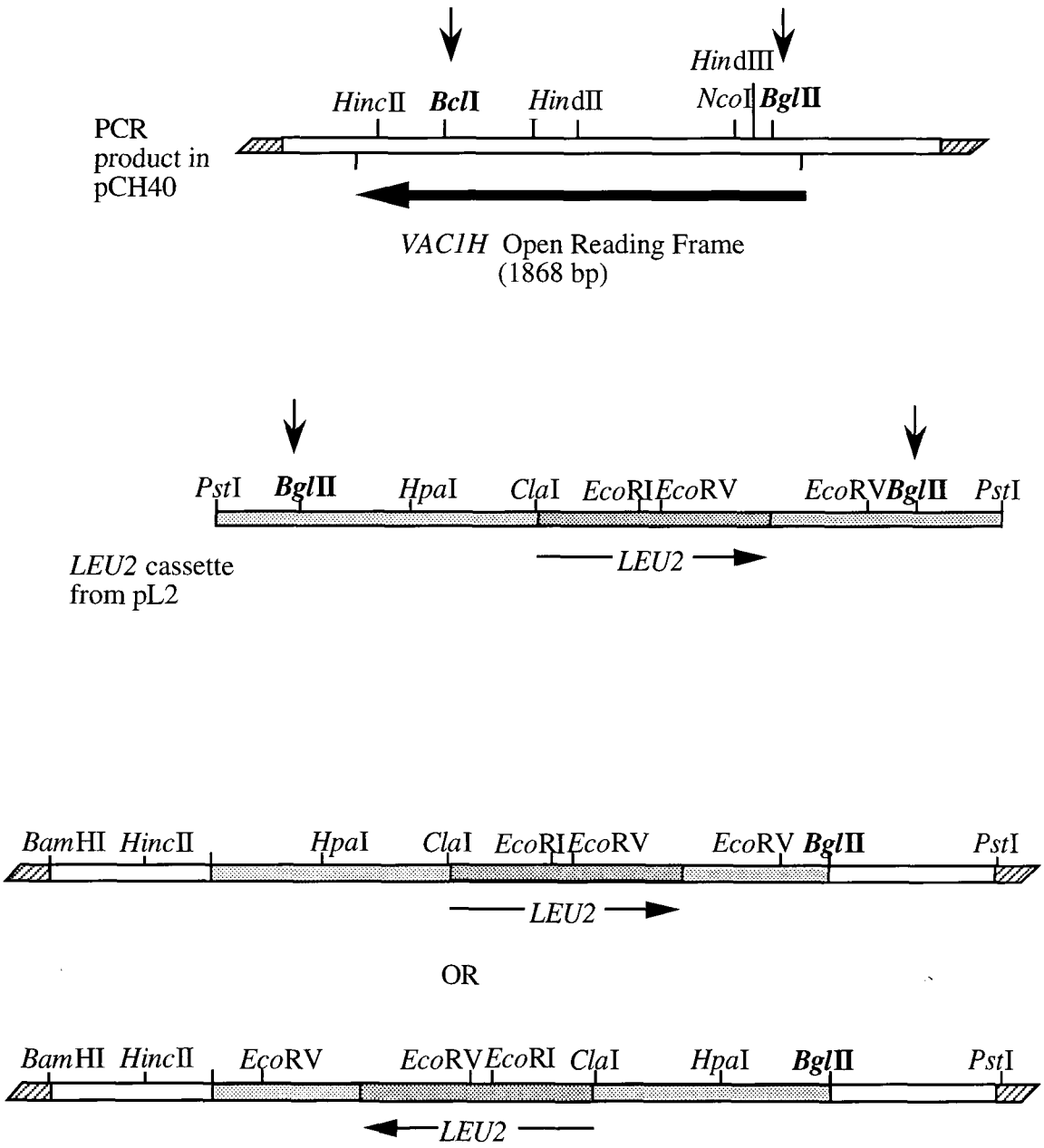

Figure 5.8. Strategy for creating a *vac1h* disruption cassette

A portion is removed from *VAC1H* (PCR product in pCH40) by excision with *Bgl*II and *Bcl*I marked above with arrows and bold type. The removed portion is replaced with the *LEU2* cassette excised from plasmid pL2 with *Bgl*II (also indicated with arrows and bold type). The *Bgl*II site is compatible with the *Bcl*I site and the *LEU2* cassette can therefore insert in either direction. The *vac1h*Δ::*LEU2* disruption cassette can then be isolated from the plasmid DNA with the restriction enzymes *Pst*I and *Bam*HI and transformed into yeast to create a Δ*vac1h* strain.

5.4.2. Creating the disruption cassette

The restriction sites *Bgl*II and *Bcl*I which are contained within the coding region of *VAC1H* were used to remove the central portion of the gene into which the *LEU2* gene could be inserted. The enzyme *Bcl*I is sensitive to DAM-methylation so before any cloning steps were performed, pCH40 was transformed into the strain GM119 which is *dam*$^-$. High purity plasmid DNA was prepared from this strain for subsequent cloning steps. *Bgl*II and *Bcl*I can be used in the same buffer but have maximal activities at different temperatures. pCH40 was therefore digested first with *Bgl*II at 37°C for 2 hours and then with *Bcl*I at 50°C for two hours. The restriction digest mix was then separated by gel electrophoresis allowing fragment isolation of pCH40 with part of the coding region of *VAC1H* removed.

The plasmid pL2 (see previous chapter, figure 4.12) was digested with *Bgl*II to excise the *LEU2* gene cassette which was then purified by fragment isolation. Restriction digests with *Bgl*II and *Bcl*I leave compatible ends for ligation and the *Bgl*II-cut *LEU2* cassette was ligated directly into the *Bgl*II and *Bcl*I sites left by pCH40 restriction. This should leave one intact *Bgl*II site whilst the *Bgl*II-*Bcl*I ligation will no longer be cut by either enzyme. The ligation mix was transformed into DH5α and transformants were selected on L-Amp plates. Blue/white selection was not possible with this construct and transformants were therefore screened using the rapid screen described in section 2.5.5. The apparently larger plasmids were then prepared by alkaline lysis for analysis by restriction digests.

High purity DNA was prepared of one of the plasmids which contained the *VAC1H* disrupted by the *LEU2* gene and this plasmid was named pEH15. The *vac1h*Δ::*LEU2* disruption cassette was isolated from the plasmid DNA by restriction with *Bam*HI and *Hin*dIII in a double digest (the internal *Hin*dIII sites were lost when the *Bgl*II-*Bcl*I fragment was removed). The *vac1h*Δ::*LEU2* cassette could then be used in transformations.

5.4.3. Creating a *vac1h*Δ::*LEU2* strain of *S. cerevisiae*

The *vac1h*Δ::*LEU2* gene cassette was transformed into the diploid strain SEY6210.5 (created from the mating of SEY6210 (MATα) with SEY6211 (MATa)). Diploids were used in the transformation because at this stage it was not known whether the *vac1h* disruption was lethal. Diploids allow the transformation to occur by leaving one copy of the gene intact and the lethality of the gene can be determined by the survival of spores

after sporulation and tetrad dissection. The electroporation method was used for the transformation and transformants were selected for their ability to grow in the absence of leucine.

Twelve transformants were obtained of which eight were purified by re-streaking on fresh YMM-leu plates. These transformed diploids were then sporulated as described in section 2.7.1. Three of the diploids (numbers 1, 2 and 8) appeared to produce a higher number of tetrads and these were selected for spore dissection. Dissection resulted in the isolation of spores showing a 2:2 segregation pattern for growth in the absence of leucine.

Homologous recombination of the disruption cassette into the chromosome allows expression of *LEU2* but not *VAC1H* and it was concluded that (assuming homologous recombination has occurred) the *VAC1H* gene disruption is a non-lethal mutation.

5.4.4. Confirming homologous recombination of *vac1hΔ::LEU2*

Homologous recombination of the *vac1hΔ::LEU2* disruption into the chromosome was confirmed by Southern blotting. Genomic DNA was isolated from four spores (originating from the same tetrad) as described in section 2.5.11. Two sets of large-scale restriction digests of the DNA from each spore were performed; one with *Hin*dIII and one with *Eco*RI. Control digests of the DNA from SEY6210.5 were also included. These digests were run on a large electrophoresis gel alongside a plasmid control and the DNA was then transferred onto a nitrocellulose membrane by Southern blotting as described in section 2.6.2.

pCH40 was digested with *Eco*RI, *Pst*I and *Sca*I in a large-scale triple digest overnight to ensure complete digestion. The fragment of approximately 2.8kb, which corresponded to the *VAC1H* PCR product, was purified by fragment isolation and labelled as a probe with the Boehringer Mannheim DIG DNA Labelling and Detection Kit (see section 2.6.1). The probe was hybridised to the Southern blot and the signal developed (as described in section 2.6.4). Figure 5.9 shows a photograph of the developed blot. In the non-disrupted yeast, hybridising bands were expected at 3.4kb in the *Eco*RI digest and at 0.73, 3.82 and 8.4kb in the *Hin*dIII digest; in the disrupted yeast hybridising bands were expected at 2.25 and 2.68, or 2.55 and 2.38kb in the *Eco*RI digest and 11.45kb in the *Hin*dIII digest. Spores a, b, c and d all came from the same tetrad; a and c were leu^+, and b and d were leu^-. As can be seen from figure 5.9, b and d had the same hybridisation pattern as SEY6210.5, whereas the pattern for the leu+ spores a and c was

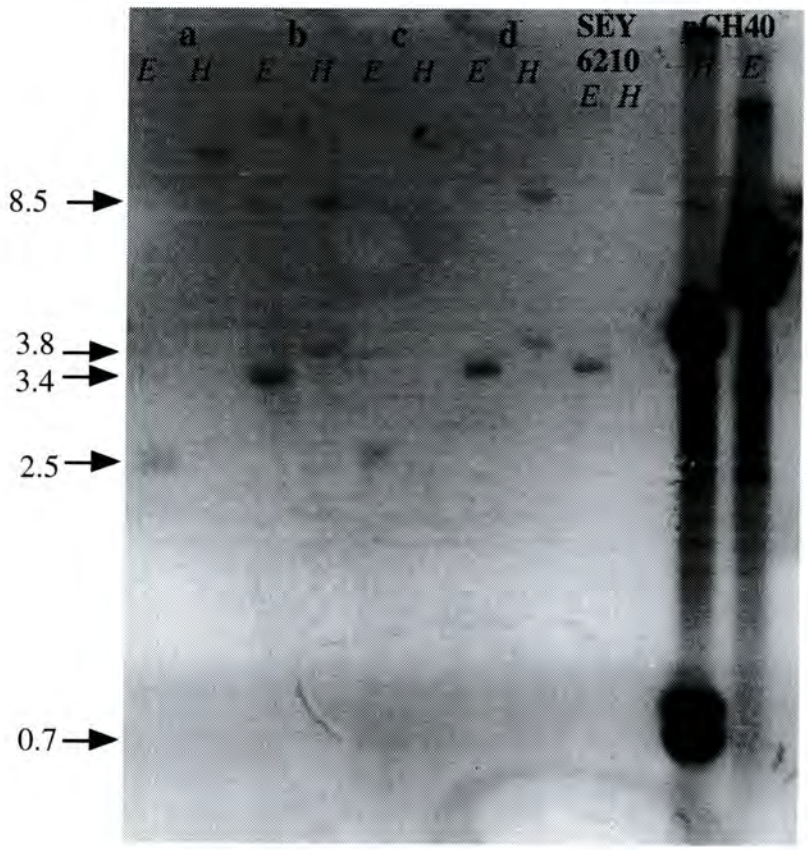

Figure 5.9. Southern Blot of genomic DNA from the *vac1h*Δ::*LEU2* spore dissection.

Genomic DNA from spores a, b, c and d, which originated from the same tetrad, was digested in separate digests with *Eco*RI (*E*) and *Hin*dIII (*H*) before running on an agarose gel. The DNA was transferred onto nitrocellulose and probed with DIG-labelled *VAC1H* PCR product. The developed blot shows that a and c share the same hybridisation pattern as each other, and b and d share a different pattern. DNA from SEY6210 was run alongside for comparison and this shows that it is very likely that spores a and c contain the *vac1h*Δ::*LEU2* disruption cassette. Also shown on the blot is plasmid DNA from pCH40, used as a positive binding control. The sizes marked (on the left in kb) have been estimated from measurements of the original gel photograph.

clearly different. Although the smallest predicted band of the *Hin*dIII digest was not visible these results are consistent with homologous recombination of *vac1hΔ::LEU2* into the chromosome of spores a and c.

5.4.5. Phenotypic analysis of *vac1hΔ::LEU2* yeast

vac1hΔ::LEU2 spores were tested for growth under a variety of conditions. Growth was not significantly impaired at 25°C, 30°C and 37°C indicating the *vac1hΔ::LEU2* spores are not temperature sensitive. Spores could grow on YPDA+1.5M NaCl plates and are therefore not salt-sensitive, re-affirming the result that *VAC1H* is unlikely to be *SSV17*. Some of the salt-sensitive vacuolar mutants created by M. Latterich, including *ssv17-101* cells, also have the pet$^-$ phenotype on glycerol plates (1% yeast extract, 2% peptone, 3% glycerol). *vac1hΔ::LEU2* cells were able to grow normally on glycerol plates and are therefore pet$^+$, again a different phenotype from *ssv17-101*.

Although *VAC1H* was no longer considered to be a candidate for the *SSV17* gene and is not of vital importance to the cell, there could still be a role for it in vacuolar function. The *vac1hΔ::LEU2* cells were therefore investigated for missorting of vacuolar proteins by immunoblotting with anti-CPY antibodies as described in section 2.7.3.

Figure 5.10 shows the photograph of an immunoblot with spores a, b, c and d described above with other leu$^+$ and leu$^-$ spores obtained in the spore dissection, with controls; *SSV17-101* cells to show positive secretion and SEY6210.5 to show background anti-CPY antibody absorption. Anti-CPY antibodies are only able to bind when the CPY has been missorted and is no longer intracellular. Patches from spores a and c give a high signal with anti-CPY suggesting a pronounced vacuolar protein sorting defect. This sorting defect can be corrected by transformation with the plasmid pEHY11, see later and also figure 5.11. The master plate used in the immunoblot was replica plated onto a YMM-leu plate and the photograph in figure 5.10a shows the corresponding growth on this plate. This demonstrates that all the patches able to grow on YMM-leu (and therefore containing the *vac1hΔ::LEU2* disruption) also have a vacuolar protein sorting defect. It can be concluded that the *VAC1H* gene plays a role in vacuolar protein sorting.

As stated in section 5.3.2 a search of the sequence data bases revealed that Vac1p is probably identical to Vps27p. *vps27* mutants have a vacuolar protein sorting defect and tend to have class E vacuolar morphology (Raymond *et al.*, 1992). The lack of salt and heat sensitivity and the vacuolar protein sorting defect of the *vac1hΔ::LEU2* cells are consistent with this finding.

Figure 5.10 Immunoblot of *vac1hΔ::LEU2* spores with anti-CPY antibodies. This photograph shows an immunoblot with anti-CPY antibodies. Spores a, b, c and d from one tetrad and spores from other tetrads (p, q, r, s, and w, x, y, z) were tested with *ssv17-101* cells as a control for positive secretion, and SEY6210 as a control for background antibody absorption. Secretion segregated in a 2:2 ratio in the three tetrads of spores tested.

Figure 5.10a Growth of spore patches in the absence of leucine

This photograph shows a replica plate of the master plate used for the immunoblot shown in figure 5.10. The plate is YMM-leu and it can be seen that the ability to grow in the absence of leucine (and thus presence of the *LEU2* gene) coincides with the protein sorting defect in all the spores tested.

5.5. Further characterisation of *VAC1H*

5.5.1. Demonstrating that *VAC1H* is *VPS27*

In order to demonstrate that *VAC1H* is *VPS27*, the *vac1hΔ::LEU2* strain was mated with *vps27* (donated to the laboratory by T.H. Stevens). The *vps27* strain is mating type a and contains the *TRP1* gene. As the mating types of the *vac1hΔ::LEU2* strains were not known, all *vac1hΔ::LEU2* spores available were used in the cross and crosses were selected on YMM-trp-leu plates. A successful mating cross was carried out between spore c of the tetrad described previously and the *vps27* strain. The diploid obtained was patched out in preparation for immunoblot analysis.

Another confirmatory step was taken by transforming the *vac1hΔ::LEU2* strain and the *vps27* strain with pEHY11 which contains the PCR product of the *VAC1H*. The resultant transformants were also patched for immunoblot analysis as shown in figure 5.11. This immunoblot demonstrates the ability of both the *vac1hΔ::LEU2* strain and the *vps27* strain to be complemented by the PCR copy of *VAC1H*. It also shows that the *vac1hΔ::LEU2* strain and the *vps27* strain are unable to complement each other. It concluded therefore experimentally and by sequence comparison that *VPS27* is *VAC1H*. The fact that the PCR product in pEHY11 is functional again shows that *SSV17* is extremely unlikely to be *VAC1H*.

5.5.2. Morphological analysis

Cells with the *vps27* phenotype are described as having Class E vacuoles; a densely staining vacuolar compartment can be observed as a 'blob' on the adjoining main vacuole (Raymond *et al.*, 1992). The *vac1hΔ::LEU2* strain and the *vps27* strain were stained with FM64-4 as described in section 2.7.2. Figure 5.12 shows the vacuole staining pictures of these two strains in comparison to the 'wild-type' SEY6210 (photograph a). The morphology of the *vps27* strain (photograph b) and the *vac1hΔ::LEU2* (photograph c) strain appear to be identical suggesting (with the previous results) that the disruption mutation is no more severe than the *vps27* mutant allele of the strain donated by T.H. Stevens. The densely staining compartment can be observed as a small circle adjacent to the main vacuolar compartment. It is possible that this compartment may also contain Golgi proteins and function as a pre-vacuolar compartment (Raymond *et al.*, 1992). In SEY6210 cells no such densely staining compartment is observed.

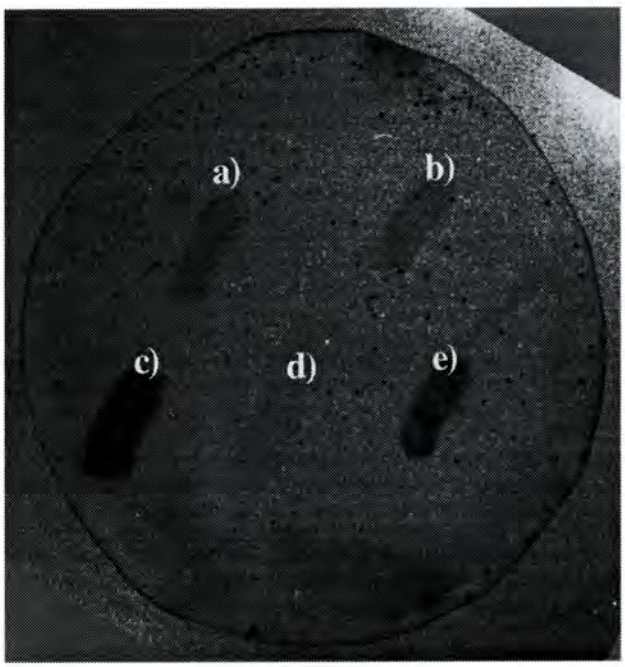

Figure 5.11. CPY immunoblot of *vps27* and *vac1hΔ::LEU2* strains transformed with pEHY11.

Figure 5.11 shows an immunoblot of the following strains with anti-CPY antibodies:

a) *vac1hΔ::LEU2* transformed with pEHY11

b) *vps27* transformed with pEHY11

c) *vac1hΔ::LEU2* crossed with *vps27*

d) SEY6210

e) *vps27* (untransformed)

Although there is some CPY secretion in the strains transformed with pEHY11, the level is greatly suppressed compared to the untransformed strains.

Figure 5.12. Vacuolar morphology

The photographs on the next page show the vacuolar morphology of strains (a) SEY6210, (b) *vps27*, (c) *vac1hΔ::LEU2*, and (d) *ssv17-101*. Cells in photographs a-c were stained with FM4-64, whereas the *ssv17-101* cells in photograph d were stained by immunofluorescence using anti-alkaline phosphatase primary antibody. *ssv17-101* staining was carried out by C.A. Hartley.

The arrows in photographs b and c indicate the class E compartment, observed as a densely staining compartment adjacent to the vacuole. The arrows in photograph d indicate the inheritance defect of *ssv17-101* cells. A mother-daughter pair can be observed where neither cell contains a coherent vacuole structure. Also indicated is a budding cell which has failed to form a segregation structure for transport of maternal vacuolar material into the emerging bud.

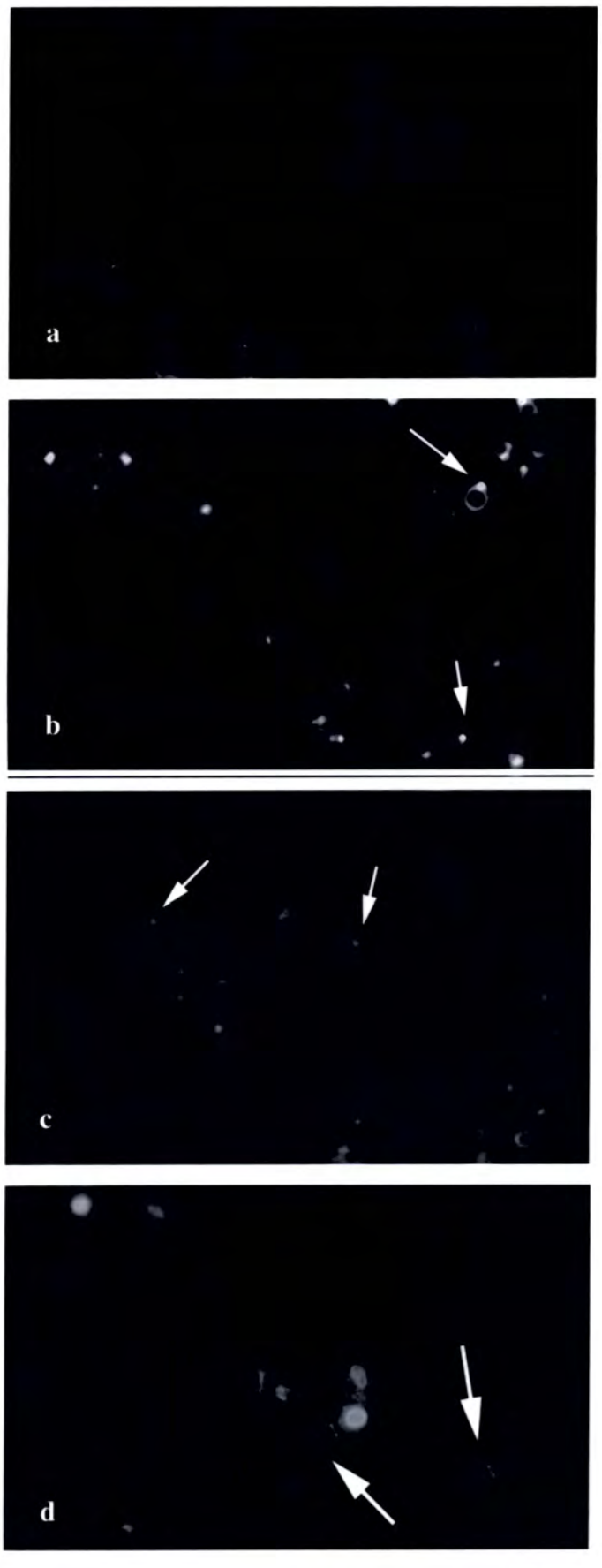
a
b
c
d

Also shown in figure 5.12 are *ssv17-101* cells (photograph d) stained by an immunofluorescence method by C.A. Hartley as part of the initial characterisation of *ssv17-101* (Hartley, 1995). In the photograph of *ssv17-101* cells the unusual vacuole segregation pattern can be observed.

5.6. Discussion

The *SSV17* gene is of interest because of its role in both osmohomeostasis and vacuole segregation. The vacuole segregation defect of *ssv17-101* could be regulatory as the timing of the segregation events appears to have become uncoupled from the cell division cycle. As can be seen in figure 5.12 photograph d, 3 types of mother and daughter buds are observed in *ssv17-101* cells: (a) both mother and daughter contain coherent vacuolar structures, (b) just the mother contains a visible vacuole that is not segregated to the bud, and (c) neither mother nor daughter contain visible vacuoles. Although only a small sub-set of the cells lack a coherent vacuole, further characterisation of *SSV17* should give insight into the mechanism of vacuole segregation and may even lead to a greater understanding of how vacuolar segregation is linked to the cell division cycle.

Of the previously described vacuolar mutants, several have an associated vacuolar protein sorting defect (Banta *et al.*, 1990; Herman and Emr, 1990; Raymond *et al.*, 1990; Weisman *et al.*, 1990). It is possible that there is a common mechanism for vesicular trafficking both from the Golgi to the vacuole and from the maternal vacuole into the emerging bud. However, *vac2* disruptions and a mutant allele of *pho80* cause segregation defects with no associated vps phenotype. These genes may play a role in regulating the formation of segregation structures from the material already involved in protein trafficking. In this scenario, Ssv17p may provide a link between the cell cycle driven vacuole segregation and the steady state vacuolar protein sorting.

Although the *VAC1H* was clearly not *SSV17*, the demonstration of a role for it in vacuole function by immunoblotting showed that it was still of interest to this project. The secretion of CPY by the *vac1hΔ::LEU2* strain showed the likelihood of *VAC1H* being one of the vps group of genes and this was shown to be the case after a sequence search showed identity between the Vac1hp and Vps27p. This finding was confirmed by experimentation showing that a *vps27* strain could be complemented by a yeast vector (pEHY11) containing the *VAC1H* PCR product. Also the *vac1hΔ::LEU2* disruption strain was unable to complement the *vps27* strain and the morphologies of the two strains were identical.

The *VPS27* gene and gene product have been further characterised by Piper *et al.*, 1995. Δ*vps27* strains have class E vacuolar morphology. They are defective for the recycling of the Vps10p CPY receptor back to the Golgi and for delivery of endocytosed α-factor receptor to the vacuole. Thus Vps27p is required for transport from the pre-vacuolar compartment. In the absence of recycling of the CPY receptor, the availability of receptor for newly-synthesised CPY is severely limited resulting in the vacuolar protein sorting defect.

VPS27 shares sequence homology with *VAC1*, with homology greatest over the region which encodes the zinc-finger binding domain. *VAC1* is required for vacuole segregation and for vacuolar protein sorting (Raymond *et al.*, 1992; Weisman and Wickner, 1992). Another gene involved in vacuole segregation and function, *FAB1*, also shares homology over the zinc-finger binding domain (Yamamoto *et al.*, 1995) suggesting this region may represent a discrete functional domain. In *fab1* mutant strains the vacuoles are abnormally large and segregation structures do not form. Thus all three genes appear to be involved in the movement of vacuolar material, be it from the prevacuole compartment to the vacuole or from the vacuole itself to the bud.

CONCLUSION

This work describes the further characterisation of the laboratory collection of salt-sensitive vacuolar mutant strains. A proportion of the *ssv* mutants were identified previously as accumulating relatively low levels of glycerol in response to salt stress. These mutants were selected for further study to attempt to demonstrate that glycerol accumulation correlates with GPDH activity. Mutants unable to increase GPDH activity in response to salt stress are of interest because they may be defective in osmosensing signal transduction.

The results of the screen of GPDH activity were surprising in that only one strain of the twelve *ssv* strains tested showed a correlation between glycerol response and enzyme activity. This strain, MLY1143, may fall into the category of genes originally screened for, i.e. those which may be involved in osmosensing signal transduction. It is unable to accumulate high levels of glycerol (B. Pöpping unpublished results) and has low enzyme activity in response to salt stress (this study). The salt-sensitivity of this strain is complemented by mating with JBY10 (Δ*hog1*) or JBY40 (Δ*pbs2*) (B. Pöpping unpublished results). Since this screen was initiated further details of the components acting upstream in the HOG pathway have emerged (Maeda *et al.*, 1995; Maeda *et al.*, 1994). It is unlikely that the salt-sensitivity of MLY1143 is caused by a mutation in one of these components because of the differences in their phenotypes. This raises the intriguing possibility that the defect may be downstream of Hog1p. The means by which Hog1p exerts control over transcription is not yet described. If the salt-sensitivity of MLY1143 could be complemented by transformation with a genomic DNA library clone this could perhaps reveal the 'missing link' between Hog1p activity and enhanced gene transcription.

Clues to the role of the vacuole in osmohomeostasis may emerge through the further characterisation of one of the strains which revealed an unusual pattern of glycerol accumulation and GPDH activity in response to salt stress. This strain, MLY0419, accumulates very low levels of glycerol and yet has very high enzyme activity when salt-stressed. MLY0419 has fragmented vacuoles and a severe vacuolar protein sorting phenotype (Latterich, 1992 and unpublished observations). Thus it would appear that the vacuolar defect interferes with glycerol production *in vivo* as high enzyme activity is observed *in vitro*. The quantification of DHAP concentration in this strain could show whether substrate is limited for GPDH activity.

The disparity in results for glycerol accumulation and GPDH activity led to a second approach to the study of the glycerol response. Attempts were made to create a *GPD1* gene reporter system to determine the promoter activity. As the construct made did not

integrate homologously into the chromosome, the promoter activity of another salt-responsive gene, *CTT1*, was studied. In some cases *CTT1* activity correlated with GPDH activity but in other cases the results were quite different. The unusually high *CTT1* activity observed in one strain, MLY1176, did not follow the same pattern of activity as GPDH. However it gave an indication that the regulation of other stress responses may be perturbed. It would be interesting to test the activity of other stress-responsive promoters in this strain to determine if there is a generally high transcription of stress responsive genes.

The glycerol accumulation assays performed previously were probably unreliable; not least because of the affect that an alteration in cell volume could have on the result which was expressed in terms of cell number. The GPDH enzyme assays gave a more useful measure of the response to salt stress but these assays were cumbersome and were qualitative rather than quantitative. The creation of a good *GPD1* gene reporter construct would have been of considerable benefit to the analysis of the salt-sensitive strains. The most useful information for the characterisation of these mutants would be to clone the corresponding genes from DNA libraries. Several attempts were made to clone the complementary genes for strains MLY0419, MLY0803 and MLY1510. Unfortunately, although tens of thousands of colonies transformed with a genomic DNA library were picked and screened, not one was a positive clone.

ssv17-101 cells have a particularly interesting vacuole inheritance defect. The characterisation of a candidate gene for *SSV17*, the *VAC1* homologue, demonstrated that although it was not in fact *SSV17* it was still involved in vacuolar function. *VAC1H* was then identified as *VPS27* which has since been described in more detail by Piper *et al.*, 1995. The identity of *SSV17* remains elusive. This gene has been mapped onto chromosome XIV (Hartley, 1995). The information obtained by the yeast genome sequencing project and the subsequent creation of clones covering known regions of the chromosome would allow a systematic approach for identifying *SSV17*.

REFERENCES

Albertyn, J., Hohmann, S., Thevelein, J. M., and Prior, B. A. (1994). *GPD1,* which encodes glycerol-3-phosphate dehydrogenase, is essential for growth under osmotic stress in *Saccharomyces cerevisiaeI,* and its expression is regulated by the high-osmolarity glycerol response pathway. Mol. Cell. Biol. *14*, 4135-4144.

Albertyn, J., Hohmann, S., Prior, B. A. (1994a). Characterization of the osmotic-stress response in *Saccharomyces cerevisiae*: osmotic stress and glucose repression regulate glycerol-3-phosphate dehydrogenase independently. Curr. Genet. *25*, 12-18.

Albertyn, J., van Tonder, A., and Prior, B. (1992). Purification and characterization of glycerol-3-phosphate dehydrogenase of *Saccharomyces cerevisiae*. FEBS Lett. *308*, 130-132.

Andre, L., Hemming, A., and Adler, L. (1991). Osmoregulation in *Saccharomyces cerevisiae*; Studies on the osmotic induction of glycerol production and glycerol 3-phosphate dehydrogenase (NAD+). FEBS Lett. *286*, 13-17.

Arnason, T., and Ellison, M. J. (1994). Stress resistance in *Saccharomyces cerevisiae* is strongly correlated with assembly of a novel type of multiubiquitin chain. Mol. Cell. Biol. *14*, 7876-7883.

Bankaitis, V. A., Johnson, L. M., and Emr, S. D. (1986). Isolation of yeast mutants defective in protein targeting to the vacuole. Proc. Natl. Acad. Sci. USA *83*, 9075-9079.

Banta, L., Robinson, J., Klionsky, D., and Emr, S. (1988). Organelle assembly in yeast: Characterisation of yeast mutants defective in vacuolar biogenesis and protein sorting. J. Cell Biol. *107*, 1369-1383.

Banta, L. M., Vida, T. S., Herman, P. K., and Emr, S. D. (1990). Characterization of yeast Vps33p, a protein required for vacuolar protein sorting and vacuole biogenesis. Mol. Cell. Biol. *10*, 4638-4649.

Belazzi, T., Wagner, A., Weiser, R., Schanz, M., Adam, G., Hartig, A., and Ruis, H. (1991). Negative regulation of transcription of the *Saccharomyces cerevisiae* catalase T (*CTT1*) gene by cAMP is mediated by a positive control element. EMBO J. *10*, 585-592.

Blomberg, A., and Adler, L. (1989). Roles of glycerol and glycerol-3-phosphate dehydrogenase (NAD+) in acquired osmotolerance of *Saccharomyces cerevisiae*. J. Bacteriol. *171*, 1087-1092.

Blomberg, and Adler (1992). Physiology of osmotolerance in fungi. Adv. Microbiol. Physiol. *33*, 145-212.

Boguslawski, G., and Polazzi, J. O. (1987). Complete nucleotide sequence of a gene conferring polymyxin B resistance on yeast: Similarity of the predicted polypeptide to protein kinases. Proc. Natl. Acad. Sci. USA *84*, 5848-5852.

Bourret, R. B., Borkovich, K. A., Simon, M. I. (1991). Signal transduction pathways involving protein phosphorylation in prokaryotes. Ann. Rev. Biochem. *60*, 401-441.

Bradford, M. (1976). A rapid and sensitive method for the quantitation of microgram quantities or protein utilising the principle of protein-dye binding. Anal. Biochem. *72*, 248.

Brewster, J. L., de Valoir, T., Dwyer, N. D., Winter, E., and Gustin, M. C. (1993). An osmosensing signal transduction pathway in yeast. Science *259*, 1760-1763.

Brewster, J. L., and Gustin, M. C. (1994). Positioning of cell growth and division after osmotic stress requires a MAP kinase pathway. Yeast *10*, 425-439.

Chen, R.-H., Sarneki, C., and Blenis, J. (1992). Nuclear localization and regulation of *erk*- and *rsk*-encoded protein kinases. Mol. Cell. Biol. *12*, 915-927.

Choi, K.-Y., Satterberg, B., Lyons, D. M., and Elion, E. A. (1994). Ste5 tethers multiple protein kinases in the MAP kinase cascade required for mating in *S. cerevisiae*. Cell *78*, 499-512.

Chowdhury, S., Smith, K. W., and Gustin, M. C. (1992). Osmotic stress and the yeast cytoskeleton: phenotype-specific suppression of an actin mutation. J. Cell Biol. *118*, 561-571.

Cohen, G. B., Ren, R., and Baltimore, D. (1995). Modular binding domains in signal transduction proteins. Cell *80*, 237-248.

Conradt, B., Shaw, J., Vida, T., Emr, S., and Wickner, W. (1992). In vitro reactions of vacuole inheritance in *Saccharomyces cerevisiae*. J. Cell Biol. *119*, 1469-1479.

Cooper, A. A., and Stevens, T. H. (1996). Vps10p cycles between the late Golgi and prevacuolar compartments in its function as the sorting receptor for multiple yeast vacuolar hydrolases. J. Cell Biol. *133*, 529-541.

Costigan, C., Gehrung, S., and Snyder, M. (1992). A synthetic lethal screen identifies SLK1, a novel protein kinase homolog implicated in yeast cell morphogenesis and cell growth. Mol. Cell. Biol. *12*, 1162-1178.

Costigan, C., Kolodrubetz, D., and Snyder, M. (1994). *NHP6A* and *NHP6B*, which encode HMG1-like proteins, are candidates for downstream components of the yeast *SLT2* mitogen-activated protein kinase pathway. Mol. Cell. Biol. *14*, 2391-2403.

Davenport, K. R., Sohaskey, M., Kamada, Y., Levin, D. E., and Gustin, M. C. (1995). A second osmosensing signal transducion pathway in yeast. J. Biol. Chem. *270*, 30157-30161.

Edgley, M., and Brown, A. D. (1983). Yeast water relations: Physiological changes induced by solute stress in *Saccharomyces cerevisiae* and *Saccharomyces rouxii*. J. Gen. Microbiol. *129*, 3453-3463.

Elion, E. A., Grisafi, P. L., and Fink, G. (1990). *FUS3* encodes a cdc2+/CDC28-related kinase required for the transition from mitosis into conjugation. Cell *60*, 649-664.

Elion, E. A., Satterberg, B., and Krantz, J. E. (1993). FUS3 phosphorylates multiple components of the mating signal transduction cascade: Evidence for STE12 and FAR1. Mol. Biol. Cell *4*, 495-510.

Eriksson, P., Andre, L., Ansell, R., Blomberg, A., and Adler, L. (1995). Cloning and characterization of *GPD2*, a second gene encoding *sn*-glycerol 3-phosphate

dehydrogenase (NAD+) in *Saccharomyces cerevisiae*, and its comparison with *GPD1*. Mol. Microbiol. *17*, 95-107.

Errede, B., Gartner, A., Zhou, Z., Nasmyth, K., and Ammerer, G. (1993). MAP-kinase related FUS3 from *S. cerevisiae* is activated by STE7 *in vitro*. Nature *362*, 261-264.

Ferrando, A., Kron, S. J., Rios, G., Fink, G., and Serrano, R. (1995). Regulation of cation transport in *Saccharomyces cerevisiae* by the salt tolerance gene *HAL3*. Mol. Cell. Biol. *15*, 5470-5481.

Finley, D., Ozkaynak, E., and Varshavsky, A. (1987). The Yeast polyubiquitin gene is essential for resistance to high temperatures, starvation, and other stresses. Cell *48*, 1035-1046.

Galan, J. M., Moreau, V., Andre, B., Volland, C., and Haguenauer-Tsapis (1996). Ubiquitination mediated by the Npi1p/Rsp5p ubquitin-protein ligase is required for endocytosis of the uracil permease. J. Biol. Chem. *271*, 10946-10952.

Gancedo, C., Gancedo, J. M., and Sols, A. (1968). Glycerol metabolism in yeasts - Pathways of utilization and production. Eur. J. Biochem. *5*, 165-172.

Garciadeblas, B., Rubio, F., Quintero, F. J., Banuelos, M. A., Haro, R., and Rodriguez-Navarro, A. (1993). Differential expression of two genes encoding isoforms of the ATPase involved in sodium efflux in *Saccharomyces cerevisiae*. Mol. Gen. Genet. *236*, 363-368.

Gartner, A., Nasmyth, K., and Ammerer, G. (1992). Signal transduction in *Saccharomyces cerevisiae* requires tyrosine and threonine phosphorylation of FUS3 and KSS1. Genes & Dev. *6*, 1280-1292.

Gaxiola, R., Corona, M., and Zinker, S. (1996). A halotolerant mutant of *Saccharomyces cerevisiae*. J. Bacteriol. *178*, 2978-2981.

Gaxiola, R., Delarrinoa, I. F., Villalba, J. M., and Serrano, R. (1992). A novel and conserved salt-induced protein is an important determinant of salt tolerance in yeast. EMBO J *11*, 3157-3164.

Gietz, D., St. Jean, A., Woods, R. A., and Schiestl, R. H. (1992). Improved methods for high efficiency transformation of intact yeast cells. Nucl. Acids Res. *20*, 1425.

Glaser, H.-U., Thomas, D., Gaxiola, R., Montrichard, F., Surdin-Kerjan, Y., and Serrano, R. (1993). Salt tolerance and methionine biosynthesis in *Saccharomyces cerevisiae* involve a putative phosphatase gene. EMBO J. *12*, 3105-3110.

Guthrie, and Wickner, W. (1988). Yeast vacuoles fragment when microtubules are disrupted. J. Cell Biol. *107*, 115-120.

Haas, A., Conradt, B., and Wickner, W. (1994). G-protein ligands inhibit in vitro reactions of vacuole inheritance. J. Cell Biol. *126*, 87-97.

Haro, R., Banuelos, M. A., Quintero, F. J., Rubio, F., and Rodriguez-Navarro, A. (1993). Genetic basis of sodium exclusion and sodium tolerance in yeast. A model for plants. Physiol. Plant. *89*, 868-874.

Haro, R., Garciadeblas, B., and Rodriguez-Navarro, A. (1991). A novel P-type ATPase from yeast involved in sodium transport. FEBS Lett. *291*, 189-191.

Hartley, C. A. (1995). Cloning and characterisation of *SSV* genes from *Saccharomyces cerevisiae*. MSc. Thesis, University of Durham.

Hasson, M. S., Blinder, D., Thorner, J., and Jeness, D. D. (1994). Mutational activation of the *STE5* gene product bypasses the requirement for G protein β and γ subunits in the yeast pheromone response pathway. Mol. Cell. Biol. *14*, 1054-1065.

Herman, P. K., and Emr, S. D. (1990). Characterization of *VPS34*, a gene required for vacuolar protein sorting and vacuole segregation in *Saccharomyces cerevisiae*. Mol.Cell.Biol. *10*, 6742-6754.

Herskowitz, I. (1995). MAP kinase pathways in yeast: for mating and more. Cell *80*, 187-197.

Hill, J., Donald, K. A. I. G., and Griffiths, D. E. (1991). DMSO-enhanced whole cell yeast transformation. Nucl. Acids Res. *19*, 5791.

Hilt, W., and Wolf, D. H. (1992). Stress-induced proteolysis in yeast. Mol. Microbiol. *6*, 2437-2442.

Hirayama, T., Maeda, T., Saito, H., and Shinozaki, K. (1995). Cloning and characterization of seven cDNAs for hyperosmolarity-responsive (*HOR*) genes *Saccharomyces cerevisiae*. Mol. Gen. Genet. *249*, 127-138.

Hughes, V., Muller, A., Stark, M. J. R., and Cohen, P. T. W. (1993). Both isoforms of protein phosphatase Z are essential for the maintenance of cell size and integrity in *Saccharomyces cerevisiae* in response to osmotic stress. Eur. J. Biochem., 269-279.

Irie, K., Takase, M., Lee, K. S., Levin, D. E., Araki, H., Matsumoto, K., and Oshima, Y. (1993). *MKK1* and *MKK2*, which encode *Saccharomyces cerevisiae* mitogen-activated protein kinase-kinase homologs, function in the pathway mediated by protein kinase C. Mol. Cell. Biol. *13*, 3076-3083.

Klionsky, D. J., and Emr, S. D. (1989). Membrane protein sorting: biosynthesis, transport and processing of yeast vacuolar alkaline phosphatase. EMBO J. *8*, 2241-2250.

Krems, B., Charizanis, C., and Entian, K.-D. (1995). Mutants of *Saccharomyces cerevisiae* sensitive to oxidative and osmotic stress. Curr. Genet. *27*, 427-434.

Latterich, M. (1992). Osmohomeostasis and vacuole biogenesis genes in the yeast *Saccharomyces cerevisiae*. Ph.D. Thesis, Durham University.

Latterich, M., Hartley, C. A., and Watson, M. D. (1993). Plasticity of vacuole biogenesis in the yeast *Saccharomyces cerevisiae*. J. Exp. Bot. *44*, 307-313.

Lee, K. S., Hines, L. K., and Levin, D. E. (1993). A pair of functionally redundant yeast genes (*PPZ1* and *PPZ2*) encoding type-1 related protein phosphatases function within the *PKC1*-mediated pathway. Mol. Cell. Biol. *13*, 5843-5853.

Lee, K. S., Irie, K., Gotoh, Y., Watanabe, Y., Araki, H., Nishida, E., Matsumoto, K., and Levin, D. E. (1993). A yeast mitogen-activated protein kinase homolog (Mpk1p) mediates signalling by protein kinase C. Mol. Cell. Biol. *13*, 3067-3075.

Lee, K. S., and Levin, D. E. (1992). Dominant mutations in a gene encoding a putative protein kinase (*BCK1*) bypass the requirement for a *Saccharomyces cerevisiae* protein kinase C homolog. Mol. Cell. Biol. *12*, 172-182.

Levin, D. E., and Bartlett-Heubusch, E. (1992). Mutants in the *S. cerevisiae PKC1* gene display a cell cycle-specific osmotic stability defect. J. Cell Biol. *116*, 1221-1229.

Lowry, O., Rosebrough, N., Farr, A., and R., R. (1951). Protein measurement with the Folin phenol reagent. J. Biol. Chem. *193*, 265-275.

Luyten, K., Albertyn, J., Skibbe, W. F., Prior, B. A., Ramos, J., Thevelein, J. M., and Hohmann, S. (1995). Fps1, a yeast member of the MIP family of channel proteins, is a facilitator for glycerol uptake and efflux and is inactive under osmotic stress. EMBO J. *14*, 1360-1371.

Maeda, T., Takekawa, M., and Saito, H. (1995). Activation of yeast PBS2 MAPKK by MAPKKKs or by binding of an SH3-containing osmosensor. Science *269*, 554-558.

Maeda, T., Wurgler-Murphy, S., and Saito, H. (1994). A two-component system that regulates an osmosensing MAP kinase cascade in yeast. Nature *369*, 242-245.

Mandel, M., and Higa, A. (1970). Calcium-dependent bacteriophage DNA infection. J. Mol. Biol. *53*, 159-162.

Mager, W. H., and Varela, J. C. S. (1993). Osmostress response of the yeast *Saccharomyces*. Mol. Microbiol. *10*, 253-258.

Marchler, G., Schuller, C., Adam, G., and Ruis, H. (1993). A *Saccharomyces cerevisiae* UAS element controlled by protein kinase A activates transcription in response to a variety of stress conditions. EMBO J. *12*, 1997-2003.

Marcus, S., Polverino, A., Barr, M., and Wigler, M. (1994). Complexes between STE5 and components of the pheromone-responsive mitogen-activated protein kinase module. Proc. Natl. Acad. Sci. USA *91*, 7762-7766.

Marcusson, E. G., Horazdovsky, B. F., Cereghino, J. L., Gharakhanian, E., and Emr, S. D. (1994). The sorting receptor for yeast vacuolar carboxypeptidase Y is encoded by the *VPS10* Gene. Cell *77*, 579-586.

Marquez, J. A., and Serrano, R. (1996). Multiple transduction pathways regulate the sodium-extrusion gene *PMR2/ENA1* during salt stress in yeast. FEBS Lett. *382*, 89-92.

Mazzoni, C., Zarzov, P., Rambourg, A., and Mann, C. (1993). The *SLT2* (*MPK1*) MAP kinase homolog is involved in polarized cell growth in *Saccharomyces cerevisiae*. J. Cell Biol. *123*, 1821-1833.

Meikle, A. J., Reed, R. H., and Gadd, G. M. (1991). The osmotic responses of *Saccharomyces cerevisiae* in K+-depleted medium. FEMS Microbiol. Lett. *78*, 89-94.

Neiman, A. M., and Herskowitz, I. (1994). Reconstitution of a yeast protein kinase cascade *in vitro*: Activation of the yeast MEK homologue STE7 by STE11. Proc. Natl. Acad. Sci. USA *91*, 3398-3402.

Nicolson, T. A., Weisman, L. S., Payne, G. S., and Wickner, W. T. (1995). A truncated form of the Pho80 Cyclin redirects the Pho85 kinase to disrupt vacuole inheritance in *S. cerevisiae*. J. Cell Biol. *130*, 835-845.

Nilsson, A., and Adler, L. (1990). Purification and characterization of glycerol-3-phosphate dehydrogenase (NAD+) in the salt-tolerant yeast *Debaryomyces hansenii*. Biochim. Biophys. Acta *1034*, 180-185.

Norbeck, J., Pahlman, A.-K., Akhtar, N., Blomberg, A., and Adler, L. (1996). Purification and characterization of two isoenzymes of DL-glycerol-3-phosphatase from *Saccharomyces cerevisiae*. J. Biol. Chem. *271*, 13875-13881.

Nothwehr, S. F., Roberts, C. J., and Stevens, T. H. (1993). Membrane retention in the yeast Golgi apparatus: Dipeptidyl aminopeptidase A is retained by a cytoplasmic signal containing aromatic residues. J. Cell Biol. *121*, 1197-1209.

Novick, P., and Botstein, D. (1985). Phenotypic analysis of temperature sensitive yeast actin mutants. Cell *40*, 405-416.

Novick, P., Ferro, S., and Schekman, R. (1981). Order of events in the yeast secretory pathway. Cell *25*, 461-469.

Ota, I. M., and Varshavsky, A. (1992). A gene encoding a putative tyrosine phosphatase suppresses the lethality of an N-end rule-dependent mutant. Proc. Natl. Acad. Sci. USA *89*, 2355-2359.

Ota, I. M., and Varshavsky, A. (1993). A yeast protein similar to bacterial two-component regulators. Science *262*, 566-569.

Papa, F. R., and Hochstrasser, M. (1993). The yeast *DOA4* gene encodes a deubiquitinating enzyme related to a product of the human *tre-2* oncogene. Nature, 313-319.

Paravicini, G., Cooper, M., Friedli, L., Smith, D. J., Carpenter, J.-L., Klig, L. S., and Payton, M. A. (1992). The osmotic integrity of the yeast cell requires a functional *PKC1* gene product. Mol. Cell. Biol. *12*, 4896-4905.

Piper, R. C., Cooper, A.A., Yang, H., and Stevens, T. H. (1995). *VPS27* controls vacuolar and endocytic traffic through a prevacuolar compartment in *Saccharomyces cerevisiae*. J. Cell Biol. *131*, 603-617.

Posas, F., Camps, M., and Ario, J. (1995). The PPZ protein phosphatases are important determinants of salt tolerance in yeast cells. J. Biol. Chem. *270*, 13036-13041.

Printen, J. A., and Sprague, G. F. (1994). Protein-protein interactions in the yeast pheromone response pathway: Ste5p interacts with all members of the MAP kinase cascade. Genetics *138*, 609-619.

Raymond, C. K., Howald-Stevenson, I., Vater, C. A., and Stevens, T. H. (1992). Morphological classification of the yeast vacuolar protein sorting mutants: evidence for a prevacuolar compartment in class E *vps* mutants. Mol. Biol. Cell *3*, 1389-1402.

Raymond, C. K., O'Hara, P. J., Eichinger, G., Rothman, J. H., and Stevens, T. H. (1990). Molecular analysis of the yeast VPS3 gene and the role of its product in vacuolar protein sorting and vacuolar segregation during the cell cycle. J. Cell Biol. *111*, 877-892.

Roberts, C. J., Raymond, C. K., Yamashiro, C. T., and Stevens, T. H. (1991). Methods for studying the yeast vacuole. Methods Enzymol. *194*, 644-661.

Roberts, C. J., Nothwehr, S. F., and Stevens, T. H. (1992). Membrane protein sorting in the yeast secretory pathway: evidence that the vacuole may be the default pathway. J. Cell Biol. *119*, 69-83.

Robinson, J. S., Klionsky, D. J., Banta, L. M., and Emr, S. D. (1988). Protein sorting in *Saccharomyces cerevisiae*: Isolation of mutants defective in the delivery and processing of multiple vacuolar hydrolases. Mol. Cell. Biol. *8*, 4936-4948.

Ronnow, B., and Kielland-Brandt, M. C. (1993). *GUT2*, a gene for mitochondrial glycerol 3-phosphate dehydrogenase of *Saccharomyces cerevisiae*. Yeast *9*, 1121-1130.

Rose, M. D., Novick, P., Thomas, J. H., Botstein, D., and Fink, G. R. (1987). A *Saccharomyces cerevisiae* genomic plasmid bank based on a centromere-containing shuttle vector. Gene *60*, 237-243.

Rothman, J. H., Howald, I., and Stevens, T. H. (1989). Characterisation of genes required for protein sorting and vacuolar function in the yeast *Saccharomyces cerevisiae*. EMBO J. *8*, 2057-2065.

Rothman, J. H., Hunter, C. P., Valls, L. A., and Stevens, T. H. (1986). Overproduction-induced mislocalisation of a yeast vacuolar protein allows isolation of its structural gene. Proc. Natl. Acad. Sci. USA *83*, 3248-3252.

Rothman, J. H., Raymond, C. K., Gilbert, T., O'Hara, P. J., and Stevens, T. H. (1990). A putative GTP binding protein homologous to interferon-inducible Mx proteins performs an essential function in yeast protein sorting. Cell *61*, 1063-1074.

Sambrook, J., Fritsch, E. F., and Maniatis, T. (1989). Molecular cloning: A laboratory manual. Cold Spring Harbor Laboratory Press.

Schuller, C., Brewster, J. L., Alexander, M. R., Gustin, M. C., and Ruis, H. (1994). The HOG pathway controls osmotic regulation of transcription via the stress response element of the *Saccharomyces cerevisiae CTT1* gene. EMBO J. *13*, 4382-4389.

Shaw, J. M., and Wickner, W. T. (1991). *vac2*: a yeast mutant which distinguishes vacuole segregation from Golgi-to-vacuole protein targeting. EMBO J. *10*, 1741-1748.

Shimizu, J., Yoda, K., and Yamasaki, M. (1994). The hypo-osmolarity-sensitive phenotype of the *Saccharomyces cerevisiae hpo2* mutant is due to a mutation in *PKC1*, which regulates expression of β-glucanase. Mol. Gen. Genet. *242*, 641-648.

Sikorski, R. S., and Hieter, P. (1989). A system of shuttle vectors and yeast host strains designed for efficient manipulation of DNA in *Saccharomyces cerevisiae*. Genetics *122*, 19-27.

Singer, B., and Riezman, H. (1990). Detection of an intermediate compartment involved in transport of α-factor from the plasma membrane to the vacuole in yeast. J. Cell Biol. *110*, 1911-1922.

Singer, J. D., Manning, B. M., and Formosa, T. (1996). Coordinating DNA replication to produce one copy of the genome requires genes that act in ubiquitin metabolism. Mol. Cell. Biol. *16*, 1356-1366.

Sprague, G. F., and Cronan, J. E. (1977). Isolation and characterization of *Saccharomyces cerevisiae* mutants defective in glycerol catabolism. J. Bacteriol. *129*, 1335-1342.

Stack, J. H., Dewald, D. B., Takegawa, K., and Emr, S. D. (1995). Vesicle-mediated protein-transport - regulatory interactions between Vps15 protein kinase and the Vps34 PtdIns 3-kinase essential for protein sorting to the vacuole in yeast. J. Cell Biol. *129*, 321-334.

Stack, J. H., and Emr, S. D. (1994). Vps34p required for yeast vacuolar protein sorting is a multiple specificity kinase that exhibits both protein kinase and phosphatidylinositol-specific PI 3-kinase activities. J. Biol. Chem. *269*, 31552-31562.

Stack, J. H., Herman, P. K., Schu, P. V., and Emr, S. D. (1993). A membrane-associated complex containing the Vps15 protein kinase and the Vps34 PI 3-kinase is essential for protein sorting to the yeast lysosome-like vacuole. Embo J *12*, 2195-2204.

Stevens, T. H., Rothman, J. H., Payne, G. S., and Schekman, R. (1986). Gene dosage-dependent secretion of yeast vacuolar carboxypeptidase Y. J. Cell Biol. *102*, 1551-1557.

Teague, M. A., Chaleff, D. T., and Errede, B. (1986). Nucleotide sequence of the yeast regulatory gene *STE7* predicts a protein homologous to protein kinases. Proc. Natl. Acad. Sci. USA *83*, 7371-7375.

Valls, L. A., Winther, J. R., and Stevens, T. H. (1990). Yeast carboypeptidase Y vacuolar targeting signal is defined by four propeptide amino acids. J. Cell Biol. *111*, 361-368.

Varela, J. C. S., van Beekvelt, C., Planta, R.J., Mager, W. H. (1992). Osmostress-induced changes in yeast gene expression. Mol. Microbiol. *6*, 2183-2190.

Varshavsky, A. (1992). The N-end rule. Cell *69*, 725-735.

Vater, C. A., Raymond, C. K., Ekena, K., Howald-Stevenson, I., and Stevens, T. H. (1992). The *VPS1* protein, a homolog of dynamin required for vacuolar protein sorting in *Saccharomyces cerevisiae*, is a GTPase with two functionally separable domains. J. Cell Biol. *119*, 773-786.

Vida, T. A., Huyer, G., and Emr, S. D. (1993). Yeast vacuolar proenzymes are sorted in the late Golgi complex and transported to the vacuole via a prevacuolar endosome-like compartment. J. Cell Biol. *121*, 1245-1256.

Vida, T. A., and Emr, S. D. (1995). A new vital stain for visualizing vacuolar membrane dynamics and endocytosis in yeast. J. Cell Biol. *128*, 779-792.

Wach, A., Brachat, A., Pohlmann, R., and Philippsen, P. (1994). New heterologous modules for classical or PCR-based gene disruptions in *Saccharomyces cerevisiae*. Yeast *10*, 1793-1808.

Wada, Y., Ohsumi, Y., and Anraku, Y. (1992). Genes for directing vacuolar morphogenesis in *Saccharomyces cerevisiae*. J. Biol. Chem. *267*, 18665-18670.

Watanabe, Y., Irie, K., and Matsumoto, K. (1995). Yeast *RLM1* encodes a serum response factor-like protein that may function downstream of the Mpk1 (Slt2) mitogen-activated protein kinase pathway. Mol. Cell. Biol. *15*, 5740-5749.

Webster, T. D., and Dickson, R. C. (1983). Direct selection of *Saccharomyces cerevisiae* resistant to the antibiotic G418 following transformation with a DNA vector carrying the kanamycin-resistance gene of Tn*903*. Gene *26*, 243-252.

Weisman, L. S., Emr, S. D., and Wickner, W. (1990). Mutants of *Saccharomyces cerevisiae* that block intervacuole vesicular traffic and vacuole division and segregation. Proc. Natl. Acad. Sci. USA *87*, 1076-1080.
Weisman, L. S., and Wickner, W. (1988). Intervacuole exchange in the yeast zygote: A new pathway in organelle communication. Science *241*, 589-591.

Weisman, L. S., and Wickner, W. (1992). Molecular characterization of *VAC1*, a gene required for vacuole inheritance and vacuole protein sorting. J. Biol. Chem. *267*, 618-623.

Wichmann, H., Hengst, L., and Gallwitz, D. (1992). Endocytosis in yeast: evidence for the involvement of a small GTP-binding protein (Ypt7p). Cell *71*, 1131-1142.

Wilsbach, K., and Payne, G. S. (1993). Vps1p, a member of the dynamin GTPase family, is necessary for Golgi membrane protein retention in *Saccharomyces cerevisiae*. EMBO J. *12*, 3049-3059.

Yamamoto, A., DeWald, D. B., Boronenkov, I. V., Anderson, R. A., Emr, S. D., and Koshland, D. (1995). Novel PI(4)P 5-kinase homologue, Fab1p, essential for normal vacuole function and morphology in yeast. Mol. Biol. Cell *6*, 525-539.

Yanisch-Perron, C., Vieira, J., and Messing, J. (1985). Improved M13 cloning vectors and host strains: nucleotide sequence of the M13mp18 and pUC19 vectors. Gene *33*, 103-119.

Yu, G., Deschenes, R. J., and Fassler, J. S. (1995). The essential transcription factor, Mcm1, is a downstream target of Sln1, a yeast "two-component" regulator. J. Biol. Chem. *270*, 8739-9743.

Zhou, Z., Gartner, A., Cade, R., Ammerer, G., and Errede, B. (1993). Pheromone-induced signal transduction in *Saccharomyces cerevisiae* requires the sequential function of three protein kinases. Mol. Cell. Biol. *13*, 2069-2080.